Putting a Spin on Photochemical Processes.
The Role of Electron Spin in Photophysical and Photochemical Processes

1. Introduction. Spin Chemistry.

This chapter explores the role of **electron spin** in determining the course of photophysical and photochemical processes. The approach taken to understand electron spin will be analogous to that employed for understanding the role of **electronic orbitals** in determining the course of photophysical and photochemical processes. We shall refer to those quantum mechanical principles which describe the qualitative aspects of electron spin in molecular systems. We shall then consider models which allow the visualization of the qualitative aspects of electron spin by reference to simple systems, i.e., those containing the essence of the physics and chemistry which determines the properties of spin systems that are essential to understanding photochemical and photophysical processes. With these simple **structural models**, and particularly with the **vector model of spin**, we shall employ an "Aufbau Principle" to determine the **number of possible spin states** and the **relative magnetic energies of the possible spin states**. We shall then establish a **dynamic model** to determine the "allowed" and "forbidden" (more realistically the "more probable" and the "less probable") **transitions** between spin states for both radiative and radiationless transitions. We shall also show how the characteristics of spin states can be associated with molecular structure and how measurements of spin characteristics can be employed for the determination of molecular structure of systems possessing one or two orbitally unpaired electrons. Our goal is to develop a useful paradigm for understanding the role of spin, in particular electron spin, in photophysical and photochemical processes.

We shall see that the same paradigm applies to the principles of **magnetic resonance spectroscopy**, a powerful tool for the investigation of photochemical reaction mechanisms. Electron spin resonance (ESR) or nuclear spin resonance (more popularly termed nuclear magnetic resonance, NMR) are forms of spectroscopy in which *radiative* transitions between magnetic energy levels, separated by interactions of spins with an applied static magnetic field, are induced by the magnetic component of elecromagnetic radiation. Intersystem crossings are *radiationless* transitions between magnetic energy levels which differ in spin angular momentum. **Spin chemistry** is a field which evolves from the dependence of the selection rules for intersystem crossing on the features of spin angular momentum and from the fact that the elementary steps of making and breaking of chemical bonds (or electron transfers) must preserve spin angular momentum (Wigner's Rules).

The principles of magnetic resonance, intersystem crossing and spin chemistry are all interrelated through the principles of **spin angular momentum** and the relationships between spin angular momentum and **magnetic moments**. Interactions between magnetic moments provide a clear general physical model for the magnetic energy levels and possible the transitions between magnetic energy levels. We need a model which will allow visualization of spin angular momentum and magnetic moments and which provides a basis for understanding spin chemistry and magnetic resonance spectroscopy.

Visualization of Spin Chemistry.

It is generally accepted that the most elegant, proper and effective way to do science is to do it mathematically. However, when learning a subject that is highly mathematical, it is often difficult to appreciate what is going on and the mathematics may become an intellectually sterile "black box" for getting the "correct" answer. Quantum mechanics is a subject that requires considerable mathematical sophistication for its quantitative use. It is not possible to understand molecular photochemistry without the liberal and essential use of ideas from quantum mechanics. However, the approach taken in this text, as in its predecessors, is that much of the mathematics of quantum mechanics can be reasonably visualized and interpreted in terms of pictures that capture the qualitative aspects of the phenomena under consideration. Such visualization of the mathematics of quantum mechanisms can be quite an intellectual treat as the imagination creates a "motion picture" of the choreography of structural and dynamic events imagined to occur at the microscopic level. Such visualizations, like all analogies and models, are an incomplete and imperfect representation of the "correct" mathematical representations and complete mathematics, but one must remember that chemical systems are always so complicated that the "correct" representations are rarely used. Indeed, it may safely be said that no mathematic representation of any complex chemical phenomenon is ever truly complete and the shortcuts and approximations employed to mathematically represent complex chemical phenomena are sometimes more intellectually compromising and less informative than resorting to imperfect physical pictures.

In defense of the pictorial approach, it is sometimes useful to approach the effectiveness of the language of mathematics by creating pictures which are themselves mathematical objects. For example, **the use of vectors simultaneously provides both clear and precise visualization of quantities and dynamic processes and a useful matrix of mathematical rules and procedures.** When such is the case, the power of visualization and insights that it can provide more than compensate for potential pitfalls of a qualitative mathematical treatment. Chemists, in particular, have sought visualization and verbal interpretations of quantum mechanics, features that are emphasized in this text.

Spin. Angular Momentum and Magnetic Moments

What is electronic spin? The **spin** of a fundamental microscopic particle such as an electron (or a nucleus) is associated with a quantity termed its **intrinsic spin angular momentum**. Thus, to understand and appreciate the qualitative and quantitiative aspects of spin we must appeal to the aspects of angular momentum. We therefore ask, what is angular momentum at the microscopic scale of fundamental particles of an atom? Classically, **angular momentum is a property of a macroscopic object which is in a state of rotation about an axis.** At the quantum mechanical or microscopic level, spin is a fixed characteristic of a fundamental particle, similar to the charge or mass of an electron or proton. For example, an electron possesses a fixed and characteristic spin angular momentum of 1/2\ (\, Planck's constant divided by 2π, is the fundamental quantum mechanical unit of angular momentum) whether it is a "free" electron which is not associated with any nucleus, or whether the electron is associated with a nucleus in an atom, a molecule or a radical. The spin angular momentum of an electron is the same whatever orbital the electron happens to occupy. At this point we simply note that although spin is a quantum property of electrons, **we still can profitably visualize spin by resorting to a classical analogy of a spherical object executing a spinning motion about an axis, i.e., a top or a gyroscope.**

It is important to emphasize that certain nuclei, such as a proton or a ^{13}C nucleus also possess spin, namely, 1/2 \ exactly the same amount as an electron! This equivalence of angular momentum of all "sspin 1/2 particles" will be of critical importance for understanding certain intersystem crossing processes and magnetic resonance phenomena. For example, we shall see that the spins of certain nuclei can also play an important role, especially in determining the chemical reactivity of radical pairs and biradicals. We shall also be interested in the structure and dynamics of the electron's spin and how the electron spin in a molecule or radical interacts with its own molecular structure, with molecules in its environment, with applied laboratory magnetic fields, and with applied oscillating electromagnetic radiation.

Visualization of the characteristics of electron spin will come from the development of a model which associates specific **magnetic properties**, i.e., a **magnetic moment**, with the electron's **spin angular momentum**. To visualize electron spin and its associated magnetic moment, we shall appeal to a specific model that will allow the development of a **vector representation of electron spin**. We shall then relate the properties of this model to experimental properties and various aspects of molecular structure. With the vector model we will be able to visualize and qualitatively interpret all of the key structrural and

dynamic properties involving the **number and energetic ordering of electronic spin states and radiationless and radiative transitions between spin states** that are involved in the general photophysical and photochemical paradigms.

The Spin States and Spin Transitions in the General Photochemical Paradigm.

A simplified, but general, "working" photochemical paradigm (Figure 1) for photophysics and photochemistry of reactions involving photochemical primary processes from the triplet state provides a convenient framework for a discussion of the role of electron spin in molecular photochemistry. In this paradigm, there are at least six states or structures that are typically involved in a complete photochemical process: S_0 (R), S_1(R), T_1(R), ^{3}I, ^{1}I and S_0 (P). In the photophysical paradigm, the reactive intermediate, I, is not involved since no photochemistry occurs. The orbital description of these states is given in Figure 1 (bottom), where the spins of the electrons in the triplet states are loosely shown as "**parallel**" and the spins of the electrons in the singlet states are shown as "**antiparallel** (the meaning of these terms will be defined more precisely in detail below in terms of the vector model). In this discussion we are ignoring photochemical reactions originating from a singlet state, S_1, because for such processes a change in spin is usually not a critical factor in the photochemistry and because the majority of photochemical reactions which have been examined involve the triplet state.

Each of the states in the paradigm can be classified in terms of the **electron configuration** of the two highest energy electrons of the molecules, R and P, or the excited state R* or the intermediate, I (Figure 1, bottom). The **electronic transitions** can be classified in terms of the **orbital structure of the electronic states** occurring when one state is converted to another. Thus, the number of electron states and the transitions between them are conveniently classified in terms of the orbital configuration of the two highest energy electrons. Effectively, all of the other electrons of the molecule are considered passive in this simple model. In an analogous manner, we shall attempt to classify each of the states and possible transitions in terms of the electron spin. In other words, we shall define **spin configurations** which define **spin states**, and classify **spin transitions** between the **spin states** in terms of the **spin structure of the magnetic states.** In the same way that we visualize and classify transitions between electronic states in terms of orbital jumps of electrons, we shall employ the vector model to visualize and classify transitions between magnetic states in terms of vector flips and vector rephasing. Furthermore, in the same manner that only the two highest energy electrons are considered explicitly, only the orbitally unpaired electron spins need be considered explicitly because the spins of a pair of electrons in the same orbital completely compensate each other's angular momentum and magnetic properties.

The basic interactions that determine the number and the structure of the electronic states and the transitions between them are **electrostatic** or **Coulombic** in origin (repulsions and attractions between electronic and nuclear charges), whereas the basic interactions that determine the nature of the spin states are **magnetic** in origin. These magnetic interactions may be represented as the **interactions of a magnetic moment** associated with an electron spin and some other magnetic moment imposed externally (by an applied magnetic field or electromagnetic radiation) or internally (by magnetic moments of other spins or by magnetic moments generated by the orbital motions of electrons). Since **magnetic moments are vector quantities** (i.e., they may be mathematically represented by a **magnitude** and an **orientation** in space) it is plausible to assume that a **vector representation of electron spin** will provide an effective working model for determining the number of spin states and for determining the mechanisms of transitions between spin states.

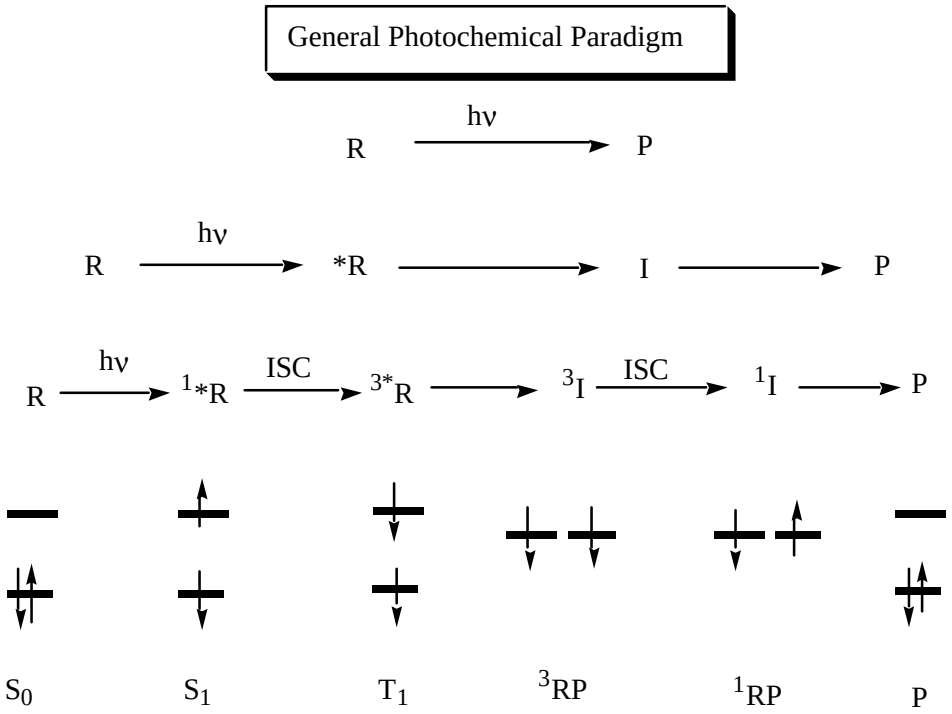

Figure 1. The general photochemical paradigm. Electron spin must be considered in the key transformation involving a spin change for two steps: (1) the molecular $S_1 \varnothing T_1$ ISC and (2) the ISC involving the reactive radical pair, RP, (or biradical) intermediate: $^3RP \varnothing {}^1RP$. In addition, the theory of electron spin allows us to obtain information on the structure of T_1 and ^3RP.

Desirable Features of the Vector Model

Before we develop the vector model, let us briefly indicate the nature of the final conceptual tool we hope to create. First we need to associate some energetic and dynamic features with a structural, i.e., visualizable, model of electron spin. A good model will allow us to enumerate and rank the relative energies of the magnetic configurations and spin states in the same way that we can enumerate and qualitatively rank the relative energy of electronic orbitals and electronic states. The connection of spin structure and energy will come about through the association of spin angular momentum with magnetic moment due to electron spin. The energy of the spin will depend on the interactions of the spin's magnetic moment and other magnetic moments to which it is coupled. These interactions **will influence both the energy of the electron spin and the dynamics of the electron spin**. A successful model will allow us to classify all of the important magnetic interactions in terms of two basic types, a so-called **dipolar interaction** and a **contact interaction** (analogous to the two basic types of electrostatic interactions involving dipolar interaction or overlap interactions) and several couplings or "mechanisms" by which the basic interactions can connect an electron spin to a magnetic moment due to some internal or external source. These mechanisms involve coupling of the magnetic moment due to spin angular momentum and other magnetic moments, which may be "internal" couplings (spin-orbit coupling and spin-spin coupling) or "external" couplings (spin-static magnetic field coupling, spin-electromagnetic field coupling, spin-lattice coupling).

2. Spin Chemistry and the Vector Model

The story of magnetic resonance spectroscopy and intersystem crossing is essentially a choreography of the twisting motion which causes reorientation or rephasing of electron spins. We can visualize this choreography wonderfully through the concept of **vectors**. Vectors are a tool for understanding spin structure, as the Lewis formulae are to understanding molecular structure. Vectors provide both a vivid and simple physical basis for visualizing the intersystem crossing processes and magnetic resonance phenomena (NMR and ESR) and in addition provide us with an economical and precise mathematic shorthand for keeping track of the structure and dynamics of spin systems. For example, the precessional motions associated with the choreography of spin in intersystem crossing are readily and elegantly handled by vector mechanics in which we will visualize transitions between spin states occurring as the result of changes in the relative precessional motions or orientations of two or more vectors representing the spins or the magnetic moments associated with spins.

We now consider some of the simple mathematical properties of vectors, after which we will relate the concept of vectors to the structure and dynamics of classical angular momentum and then to quantum mechanical spin angular momentum. After connecting vectors to spin angular momentum, we shall make a connection between spin angular momentum and magnetic moments directly associated with spin angular momentum. From knowledge of the properties of magnetic moments in a magnetic field, we shall be able to deduce qualitatively the magnetic energy diagram corresponding to the angular momentum states. We will then show how the vector model nicely depicts the precessional motion of the magnetic moment associated with spin, and how both radiative and radiationless transitions between magnetic states can be visualized as the result of coupled magnetic moments.

Vectors and Angular Momentum and Magnetic Moments.

In order to gain or renew familiarity with the properties of classical angular momentum and vectors, we shall present a brief review of some important principles involving both, by referring to a **vector model for angular momentum**. Some physical quantities are completely described by a magnitude , i.e., a single number and a unit. Such quantities are termed **scalars**. Examples of scalar quantities are energy, mass, volume, time, wavelength, temperature, and length. However, other quantities have a **directional quality** and their complete description requires both a magnitude and a direction. Examples of vector quantities are electric dipoles, angular momentum, magnetic fields and magnetic moments. Such quantities are termed **vectors**. In discussing vector quantities we must always be concerned **not only with the magnitude of the**

quantity but a direction. Scalar quantities will be represented in normal type and **vectors** will be represented in **bold face type.** For example, the magnitude of spin angular momentum is defined as a scalar, and therefore does not refer to direction and is represented by the symbol S. Similarly, the magnitude of a magnetic moment is a scalar and is represented by the symbol μ. When both magnitude and direction are condsidered, the spin angular momentum is a vector and is represented by the symbol **S**. The magnetic moment is a vector and is represented by the symbol $\boldsymbol{\mu}$.

The importance of vectors is that the characteristics of many physical quantities such as angular momentum, spin angular momentum, magnetic moments, magnetic fields, etc., can be faithfully represented by vectors. When this is the case, the powerful and simple shorthand, rules and algebra of vector mathematics can be employed to describe and to analyze the physical quantities in a completely general manner independent of the specific quantity the vectors represent. We may think of vectors as existing in a "vectorial space" that is independent of the physical space occupied by the physical object. Vector notation often clarifies the meanings of many equations whose physical and chemical bases are hidden by obscure mathematical symbolism. Thus, one motivation for using vectors is to simplify higher mathematical equations. Vectors are also closely related to the fundamental ideas of symmetry and their use can lead to valuable insights into the possible forms of fundamental scientific laws. We shall review the fundamental features of vectors and introduce a vector model of angular momentum and magnetic moments that will help to visualize the spin angular momentum states, the transitions between spin angular momentum states and the mechanisms of magnetic resonance spectroscopy, spin relaxation and spin chemistry.

Definition and Important Properties of a Vector.

There is perhaps no more natural and obvious way to represent a direction than an arrow. Similarly, a natural and obvious way to represent a **magnitude** is with the **length** of a line segment. Vectors combine these two intuitive and universal means of representation: **a vector is simply a mathematical object representing simultaneously a distance and a direction**. It is the fact that vectors are conveniently represented by an "arrow", which makes quantities represented by the vectors and the interactions between vector quantities readily visualizable. The arrowhead indicates the sense of the direction and the length of the arrow represents the magnitude of a physical quantity. In general, since direction must be specificed for all vector quantities, an axis is needed to serve as reference (Cartesian axis x, y, z) coordinate system for direction. This **reference axis**, by convention, will always be termed the **z**

axis. The orientation of the vector in space is defined in terms of the angle, θ, that the arrow or vector makes with the z-axis. Examples of vector notation for length and direction are given below in Figure 2 with spin angular momentum **S** as examples. In Figure 2 is depicted (a) an arbritrary spin vector with an undefined reference axis, **S**; (b and c) a spin vector with a specific length, S, and orientation in space, θ, relative to a reference axis; and (d) a representation of two equivalent spin vectors $\mathbf{S}_1$ and $\mathbf{S}_2$, i.e., $\mathbf{S_1}$ and $\mathbf{S_2}$ possess identical lengths, i.e., $S_1 = S_2$.

(a) An arbritrary Spin Vector is represented by the symbol , **S,** and by an arrow.

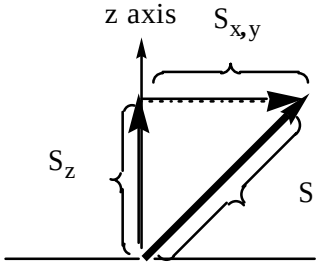

(b) Vector Length: S is the total **length** of the spin angular momentum vector **S**; S_z is the length of the component on the spin angular momentum on the z axis; $S_{x,y}$ is the length of the component on the x or y axis.

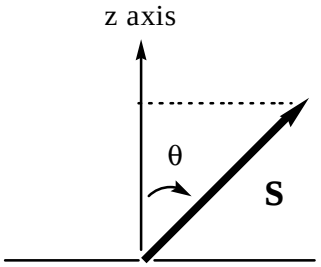

(c) Vector Direction: The **direction** of the spin angular momentum vector is given by the angle θ made by the vector with the z axis.

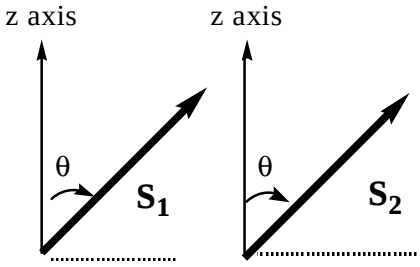

$\mathbf{S_1} = \mathbf{S_2}$

(d) Equivalent Vectors $\mathbf{S_1}$ and $\mathbf{S_2}$. The two spin vectors show are identical (congruent) in spin space because they differ only by a parallel translation. They possess the same length, S, and direction, θ.

Figure 2. Some simple properties of vectors with electron spin as an example. See text for discussion.

We must emphazise that vectors are mathematical objects and that represent physical objects. As a result, the vectors shown in Figure 2 refer not to real space, but to mathematical objects in a **spin space**. It is important not to confuse the "spin space" of vectors, with the real space of electons, nuclei and molecules. Furthermore, the lengths of the vectors represent the magnitude of spin, not distances. For example, the units of spin are angluar momentum (units, e.g., erg-s or J-s) and are not distance (units, e.g., Å or nm). We will attempt, however, to establish a relationship between the Euclidean space or molecules and radicals to the spin space of vectors when we discuss magnetic resonance and intersystem crossing.

Vector Representation of Electron Spin

Now let us consider some important properties of all vectors, again with a vector representation of spin angular momentum **S** as a particular example.

Property (1). If two spin vectors have the same length and direction they are defined as equal and equivalent vectors, **no matter where they are located in spin space**. This property is similar to that of congruence of geometric figures, except that the reference axis must remain fixed. Thus, a **parallel** translation does not change a vector and all vectors of the same length which are parallel to each other represent the same vector, i.e., they are equivalent. For example (Figure 2, d), the two **spin** vectors, $\mathbf{S}_1$ and $\mathbf{S}_2$ have the same length (S) and direction (angle θ relative to the z-axis), therefore they are completely equivalent, i.e., they represent the same vector in the same way that molecules are equivalent if they have the identical molecular structures. Put mathematically, if two vectors possess identical length and direction: $\mathbf{S}_1 = \mathbf{S}_2$.

Property (2). The length of a spin vector is termed the magnitude of its spin angular momentum. Planck's constant, *h*, possesses the units of angular momentum (J-s) and the magnitude of spin is always expressed in units of $h/2\pi$ (which is commonly abbrebriated as \). By definition the magnitude of a vector quantity is a scalar (a single number) and is always positive (the absolute value of the number). Occasionally, because the magnitude of a vector is defined as a positive quantity, the symbol representing the magnitude of a vector may also represented by vertical bars (absolute value sign, | |) or the same letter as the vector except in plain type. For example, the symbol $|\mathbf{S}_1|$ and S_1 represents the magnitude of the vector $\mathbf{S}_1$. Since $\mathbf{S}_1$ and $\mathbf{S}_2$ are equivalent vectors, their lenghts are exactly identical: $|\mathbf{S}_1| = S_1 = S_2 = |\mathbf{S}_2|$. In Figure 2, the lengths of all of the spin vectors shown are the same in all instances (equal to S or $|\mathbf{S}|$).

It is important to note that any rotation of a vector of fixed length in vector space changes the vector to a different one, even though the magnitude of the vector does not change, because the angle θ with respect to the reference axis changes upon rotation.

Property (3). The orientation of a vector in space may be unambiguously defined by an angle, θ, that the vector makes with respect to the z axis (Figure 2 c). Thus, for full characterizaiton the x and y coordintes must be specified. In refering to molecular structures, the z axis is usually taken as the molecular axis of highest symmetry (or pseudosymmetry). For example, in a linear molecule this is the internuclear axis. In a strong laboratory magnetic field the z-axis is taken as the direction of the magnetic field (north to south pole).

We now consider two important procedures involving vectors that are commonly employed in describing **couplings** of spin angular momenta:

(1) Vector addition and subtraction
(2) Resolution of vectors into components

Vector Addition and Subtraction. Resultants and Spin Space.

Two spin vectors, $\mathbf{S}_1$ and $\mathbf{S}_2$ can be added or subtracted to produce new vectors (Figure 3). The addition is symbolized by $\mathbf{S_1} + \mathbf{S_2}$, where boldface symbols emphasizing that vectors, not scalars, are being added. Each of the vectors make a definite angle with the z axis. The addition of two vectors may be accomplished by applying the parallelogram law of vector adition: **the addition or sum of two vectors, $\mathbf{S_1} + \mathbf{S_2}$ is the diagonal of the parallelogram of which $\mathbf{S_1}$ and $\mathbf{S_2}$ are the adjacent sides.** Figure 3 b shows an example of the addition of the vectors $\mathbf{S_1}$ and $\mathbf{S_2}$ according to the parallelogram law, for convenience referenced to the z axis. The new vector, **S**, representing the addition of $\mathbf{S_1}$ and $\mathbf{S_2}$ is termed the **resultant** of the addition and is shown as a heavier arrow in the Figure. An equivalent method (Figure 3 c) of adding two vectors is to place the tail of $\mathbf{S_1}$ at the head of $\mathbf{S_2}$ and draw a new vector from the tail of $\mathbf{S_1}$ to the head of $\mathbf{S_2}$. The new vector, **S**, can be seen to be identical to the resultant from the parallelogram method. Since both methods are mathematically equivalent, which representation employed will be a matter of convenience.

Two vectors, $\mathbf{S_1}$ and $\mathbf{S_2}$ can be also be subtracted to produce a new vector. The subtraction is symbolized by $\mathbf{S_1} - \mathbf{S_2}$. The vector $-\mathbf{S}_1$ is simply the vector $\mathbf{S}_1$ multiplied by -1, which in vector notation corresponds to rotating $\mathbf{S}_2$ by 180º in space. In other words, $\mathbf{S}_1$ has the same length as $-\mathbf{S}_1$, and the two vectors are colinear but are antiparallel to one another. In spin chemistry the coupling

between two spins or more generally between a spin and some other angular momentum can be characterized as a vector addition or subtraction. We shall soon see how the rules of "counting" possible spin states that result from interacting spins can be formulated in terms of vector additions and subtractions. Figure 3 d shows an example of the subtraction of the vectors $\mathbf{S_1}$ and $\mathbf{S_2}$. As in the case of vector additon, the subtraction of $\mathbf{S_1}$ from $\mathbf{S_2}$, can be achieved by placing the tail of $-\mathbf{S_1}$ at the head of $\mathbf{S_2}$ (figure 3d) or by the parallelogram method.

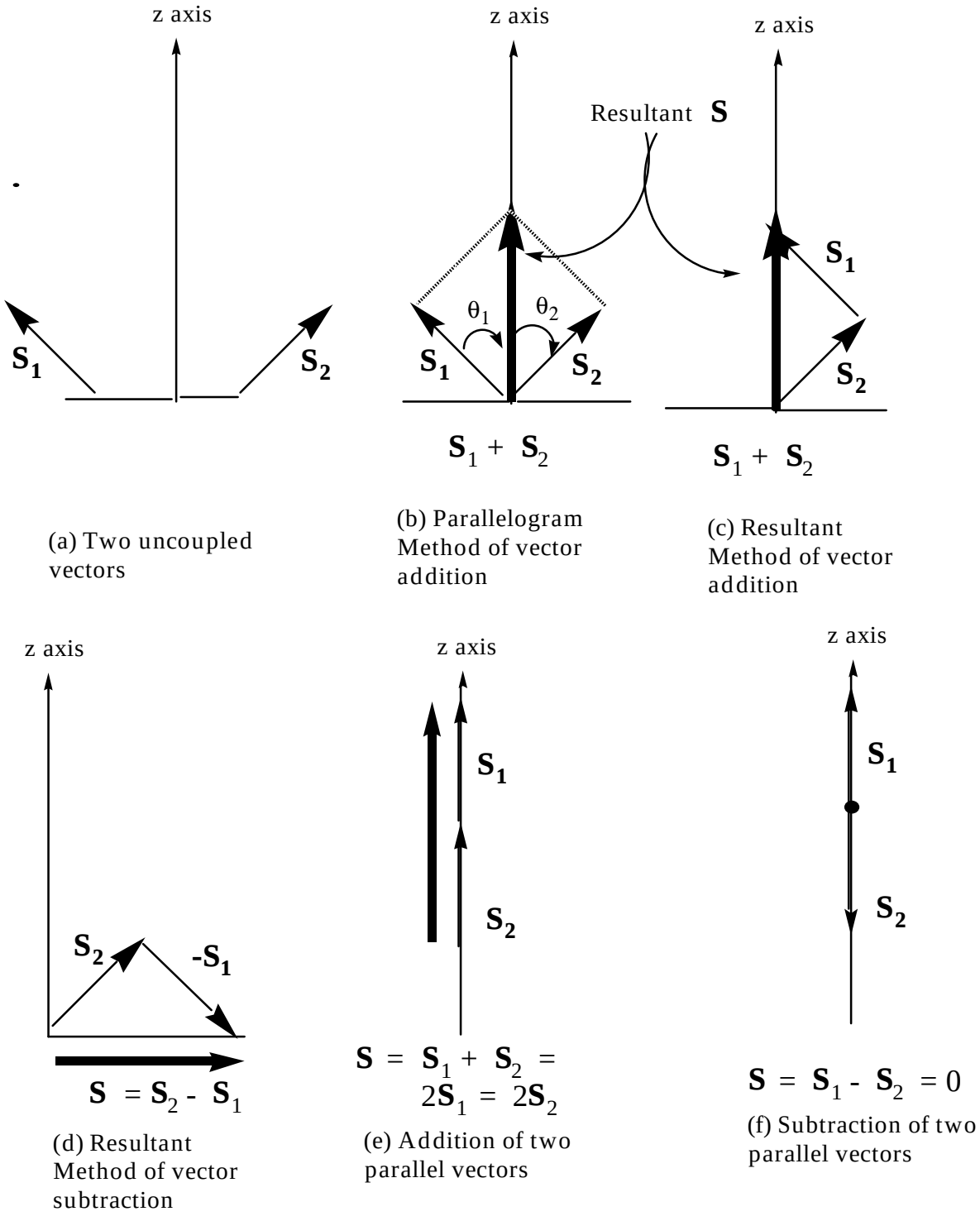

Figure 3. Examples of addition and subtraction of vectors with spin as an example.

A special case of vector addition occurs when the two vectors are parallel or antiparallel. For parallel vectors it is convenient to display the vectors as parallel or antiparallel to the z axis (Figure 3 e and f). If the vectors are parallel ($\mathbf{S_1} + \mathbf{S_2}$), the magnitude of the vector sum is simply equal to the sum of the magnitudes of the individual vectors. If the vectors are antiparallel, the magnitude of the vector addition equals the absolute value of the difference of the magnitudes of the vectors and the resultant is parallel to the component vectors. In Figure 3 e and f examples of the addition and subtraction of two parallel and antiparallel spin vectors of equal length are shown. For the case of addition, the resultant is parallel to the original components ($\theta = 0$) and twice the magnitude of an individual component. (The resultant has been displaced slightly sidewise to show it more clearly).

Vector Resolution into Components

Just as two vectors may be added together to produce a new single vector, a given vector can be considered to be the sum of two or more component vectors, each of which has a specific magnitude and direction. These component vectors are conveniently resolved as the x-, y- and z-components of the vector on the Cartesian coordinates in 3 dimensions. For example, components of a vector are defined in a Cartesian coordinate axis system such that any vector lying in the xz plane can be represented as the sum of a vector parallel to the x axis and one parallel to the z axis (Figure 2 b, $\mathbf{S_{x,y}}$ and $\mathbf{S_z}$). The magnitude of a component in the z direction is positive when the vector points in the positive z direction and the component in the z direction is negative when the vector points in the negative z direction. The component method has a very simplifying effect in calculating vector sums, because it involves the use of right triangles and well known geometric principles such as the use of trigonometric functions and the Pythagorean theorem. Its most important use will be in dealing with angular momentum and magnetic moments. The quantized nature of angular momentum of elementary particles and the Uncertainty Principle require that only one component of angular momentum (by convention the component on the z axis) can be measured accurately in any experiment. The vector model will assist in clarifying this rather non-intuitive principle of quantum mechanics.

It is important to note that although two vectors may be added or subtracted to produce a non-zero resultant, the component on one or more of the principle axes may be zero. For example, in Figure 3 d, the resultant of subtracting $\mathbf{S_2}$ from $\mathbf{S_1}$ in non-zero, but its component on the z axis is zero. This feature of a finite sized vector with a zero component on the z axis will be important when we consider the vector model of the triplet state.

Summary

In quantum mechanics, angular momenta in general and spin angular momenta in particular, behave according to the rules of vectors. The total angular momentum of a system can therefore be regarded as the *resultant vector* of contributing vectors. The vector model of spin angular momenta provides insight into the physical significance of various coupling schemes, sparks and guides the imagniation to interpret many phenomena which depend on spin mechanics and places a ring of concrete geometry on the abstract operators of angular momentum quantum mechanics.

3. Angular Momentum States.

We now employ the vector model to enumerate the possible number of spin angular momentum states for several commonly encountered situations in photochemistry. We shall give examples for the important situations involving the coupling of several electron spins, since these examples will capture the most important features of cases commonly observed in photochemical sytems. Of these the most important is the coupling of two electron spins with one another. After deducing the number of states that result from coupling of individual spins, we shall be interested in the relative energy ranking of these spin states when magnetic interactions and couplings are present. These interactions and couplings will be connected to molecular structure through the relationship of spin angular momentum and magnetic moments due to spin. The coupling of magnetic moment due to spin with other magnetic moments will be the basis for the understanding of both magnetic resonance spectroscopy and intersystem crossing. For magnetic resonance spectroscopy, the influence of an applied laboratory magnetic field on the energy levels is of particular importance. For intersystem crossing, couplings of the electron spin with other sources of angular momentum are important.

Before counting angular momentum states for the important commonly encountered cases, we shall briefly review the principles of both classical angular momentum and quantum angular momentum and relate these quantities to the vector model.

Classical Angular Momentum. The Physics of Rotational Motion.

Classical angular momentum refers to the rotation motion of of an object around a fixed point or about a fixed axis. The two most important models of angular momentum for chemistry are (1) a particle constrained to move in a circular path with a fixed radius about a point (Figure 4, left) and (2) a spherical body rotating about a fixed axis that passes through a point at the center of the sphere (Figure 4, right). These two simple models capture the essence of the origin of electron orbital angular momentum and to electron spin angular momentum.

We choose two definite physical models to visualize (1) **orbital** angular momentum in terms of **an electron of mass m_e travelling in a circular Bohr orbit or radius r with angular velocity v**, and (2) **spin** angular momentum in terms of **a spherical top or gyroscope spinning about an axis with a moment of inertia, I, and an angular velocity, v** (the moment of inertia is related to a radius of gyration, r, rotating about the center of mass). Let the orbital angular momentum be symbolized by **L** and the spin angular momentum of a single

electron be symbolized by **S**. According to classical mechanics the values of **L** and **S** are given by equations 1 and 2, respectively.

$$\mathbf{L} = m\mathbf{v}r \qquad (1)$$

$$\mathbf{S} = I\mathbf{v} \qquad (2)$$

According to classical mechanics, both the orbital and spin angular momentum of a particle undergoing circular motion (as an electron in a Bohr orbit) or a rotating top or gyroscope (as an electron spinning on its axis) may be represented as a **vector**. To visualize this vector we employ the "right hand thumb rule" which states the angular momentum vector points in the direction that a right-hand thumb points when the fingers of the right hand are turned in the same sense as the rotation. Figure 4 shows the vector representation of the orbital angular momentum of an electron, **L**, in a Bohr orbit and of the spin angular momentum, **S**, of a single electron spinning on its axis. From classical mechanics, the direction of the angular momentum vector is always perpendicular to the plane defined by the circular motion of the electron in its orbit or the rotation of the spherical electric charge. The length of the vector represents the magnitude of the angular momentum. The important features of the classical representation of angular momentum are**: (1) that angular momentum can be represented by a vector whose direction is related to the sense of the direction of rotation; (2) that the representation of the vector can be conveniently placed on the axis of rotation; and (3) that the length of the vector is proportional to the absolute magnitude of the angular momentum.** In these diagrams the vector sizes are generally schematic and not to scale.

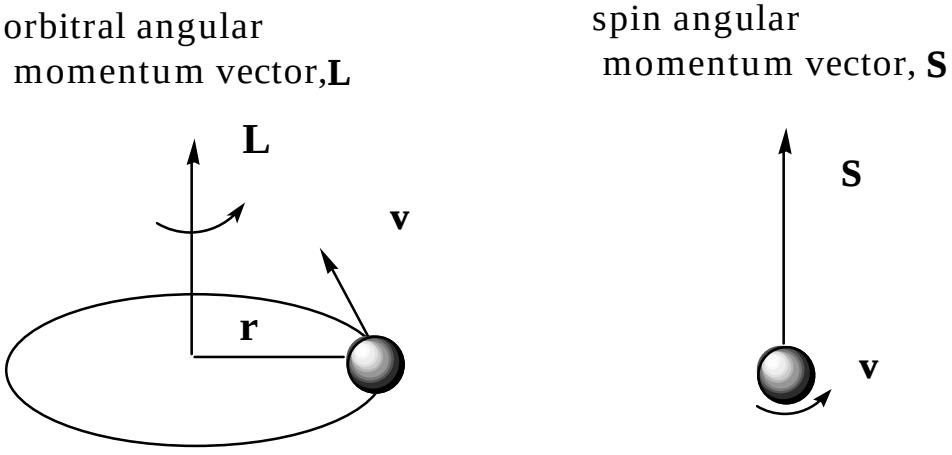

Figure 4. Classical representation of the angular momentum of an electron in a Bohr orbit (left) and of an electron spinning about an axis (right). The important features to note are the angular momentum in both cases possesses a characteristic circular motion: in one case the mass of the particle is at a distance,

r, from the axis of rotation, and in the other case the center of mass is at a distance, r, from the axis of rotation.

Quantum Electron Spin Angular Momentum

The results of classical angular momentum provide a clear physical model for representation of orbital and spin angular momentum in terms of the vector model. Let us now consider the new features that are introduced by the laws of quantum mechanics which spin angular momentum (both electronic and nuclear) must obey.

The elementary components of an atom (electrons and protons) behave as if they were spinning on an axis. The motion of the electron spin (or a nuclear spin) can be considered to be a "zero point" motion. It is eternal and cannot be stopped. The spinning electron is like a ltoy top that is simultaneously provided with a pulse of rotational energy and magically freed from friction or other means of dissipating the rotational energy. Thus, the magnitude of an electron spin is fixed and constant in time and cannot be changed. These qualities are all subsumed in the statement that an electron possesses exactly 1/2\ worth of spin angular momentum. Recall that \ is Planck's constant divided by 2π. The factor 2π is a natural consequence of the **circular** motion implicit in all forms of angular momentum. No matter where the electron resides, in bonds with a partner of opposite spin orientation, as an entity in a half occupied orbital, as a member of a cluster of spins of the same orientation, or in orbitals of different angular momentum (s, p, d, etc.), *the spin of the individual electron is always 1/2\ exactly*. We shall see that the fact that the proton, ^{13}C and other nuclei also possess exactly 1/2 \ of spin angular momentum will allow them to couple with electron spins and thereby be actively involved in magnetic resonance and intersystem crossing. This coupling will allow the conservation of angular momentum to be maintained as angular momentum is exchanged between the coupled partners. The situation will be completely analogous to maintaining conservtion of energy while energy is being exchanged between coupled partners.

According to the laws of classical mechanics the angular momentum of a rotqting body may assume any value or any direction of the angular momentum, consistent with torques applied to the body. This means that in a Cartesian coordinate system, the angular momentum of a body around each of the three perpendicular axes may take any value consistent with the magnitude of the angular momentum. Thus, if electron spin were a classical quantity, the magnitude and direction of the vector representing the spin angular momentum could assume any length, S, and any angle θ relative to the z-axis. The situation is quite different for a quantum mechanical particle, such as an electron or a proton. In the quantum case t**he amount of angular momentum is quantized**

and can achieve only certain definite values for any given value of the angular momentum. This means that only certain orientations of the angular momentum can occur in physical space. This in turn implies that only certain orientations of the spin angular momentum vector are allowed in spin space. What we mean by this is that for all measurable (stable) situations, the quantum mechanical rules must be followed. In certain, unstable, situations the rules are temporarily modified and transition between states of different spin may occur. Let us now review the rules for stable situations, i.e., the situations which will determine the measurable magnetic energy levels from which transitions between spin states can occur. Then we will investigate how a given spin state may become unstable and undergo radiative or radiationless transitions to another spin state.

Quantum Rules of Spin Angular Momentum

According to the laws of quantum mechanics, an electron or group of electrons can be characterized completely by certain quantum numbers. When we say that an electron or a proton has a spin of $1/2$ we usually are referring to the electron's **spin quantum number**, S, rather than the magnitude of the spin angular momentum. However, when we say we are dealing with any particle with spin of $1/2$ we also mean that the particle has an inherent, irremovable angular momentum of $1/2\backslash$ **which can be measured in an experiment.** (The quantum number for total spin will be represented by the plain type and care will be taken to distinguish this unitless quantity from the magnitude of the spin, which has the units of angular momentum). For electron spin there are only two pertintent quantum numbers: S, the quantum number associted with **the length of the total spin** and M_S the quantum number assoicated with the **orientation of the total spin** relative to the z axis. The relationship between the quantum number, S (unitless), and the magnitude of the total spin angular momentum **S** (in units of \) is given by eq. 3a. The pecular square root relationship of eq. 3a will be discussed below.

$$\text{Magnitude of } \mathbf{S} \text{ (units of } \backslash) = [S(S + 1)]^{1/2} \qquad (3a)$$

The possible values of S, the total electron spin angular momentum quantum number, are given by eq. 3b, where n is 0 or a positive integer.

$$\text{Possible values of S (unitless)} = n/2 \qquad (3b)$$

From eq. 3a and 3b we deduce that the total spin quantum number may be equal to 0, $1/2$, 1, $3/2$, 2, etc. and that the magnitude of the spin angular momentum may be equal to 0 \, $(3/4)^{1/2}$ \, $(2)^{1/2}$ \, $(15/4)^{1/2}$ \, $(5)^{1/2}$ \, etc. We shall see below that we need not deal with the square root quantities because the

measuarble values of the spin on the z axis will bear a simple relationship to the quantum number M_S.

According to the laws of quantum mechanics spin angular momentum is not only quantized in magnitude, but in orientation relative to the z axis in physical space. Therefore, **the vector representing spin can only assume certain orientations relative to the z axis in spin vector space**. The quantum number M_S specifies the possible orientation of a given angular momentum in space. This quantum number is analogous to the familiar quantum number for orientation of orbitals in space, e.g., a p-orbital along the x, y or z-axis. The measurable values of the possible orientations of spin angular momentum on the z axis are given the quantum numbers, M_S, where the possible values of M_S are given by eq. 4a. The values of M_S each correspond to an allowed measurable value of $\mathbf{S}_z$.

$$\text{Possible values of } M_S \text{ (unitless)} = S, (S-1),..., (-S) \qquad (4a)$$

The values of M_S (unitless) are the same as the value of the angular momentum of the spin (units of \) on the z-axis . As a result of this relationship, it is convenient to refer to the values of the spin angular momentum on the z axis rather than the total spin angular momentum (which has the peculiar square root character given in eq. 3a). For example, for $S = 1/2$, the possible values of M_S are $+1/2$ and $-1/2$ and for $S = 1$, the possible values of M_S are +1, 0 and -1, respectively. The positive sign means that the head of the vector is pointing in the positive direction of the z axis, and the negative sign means that the head of the vector is pointing in the negarive direction of the z axis. For these values of M_S the values of $\mathbf{S}_z$ are $+1/2\,\backslash$, $-1/2\,\backslash$, $+1\,\backslash$, $0\,\backslash$ and $-1\,\backslash$, respectively. These important cases will be considered in greater detail below. We shall see that nearly all cases of interest will only involve the coupling of only a few spins with each other or with an applied field and can readily be extended conceptually to more complicated cases.

From Eq. 4a we can conclude that for any given value for the total quantum number of spin, S, there are exactly 2S + 1 allowed orientations of the total spin. This important conclusion is expressed in Eq. 4b, where M is termed the **multiplicity** of a given state of angular momentum.

$$\text{Multiplicity, M, of state with quantum number S} = 2S + 1 \qquad (4b)$$

Let us consider three simple, but common examples of $S = 0, 1/2$ and 1. According to Eq. 4b, for $S = 0$, $M = 1$. Thus, when there is only one spin state when $S = 0$ and this is termed a **singlet state**. For $S = 1/2$, $M = 2$. Thus, when

there are two spin states when S = 1/2 and this is termed a **doublet state**. For S = 1, M = 3. Thus, when there are three spin states when S = 1 and this is termed a **triplet state**. In the absence of a magnetic field the two doublet states and the three triplet states have the same energy (are degenerate). However, the application of a magnetic field (internal or external) removes the degeneracy as we shall soon see.

Pythagorean Relationships and Spin Angular Momentum

The peculiar square root relationship of eq. 3a is embedded in the remarkable trigonometric features of all vectors. The triangular relationship among vectors in 2 dimensions is shown in Figure 5. From the familar Pythagorean theorem, Eqs. 5 a and 5 b provide a relationship between the **square** of the total angular momentum $\mathbf{S}^2$ and the components on the z and x (or y) axis. Note that the lengths $|S_x| = |S_y|$ because of the cylindrical symmetry of the x,y plane about the z axis. This cylindrical symmetry has a profound influence on the vector properties of spin.

$$\mathbf{S^2} = \mathbf{S_z^2} + \mathbf{S_{x,z}^2} \qquad (5a)$$

$$\mathbf{S} = (\mathbf{S_z^2} + \mathbf{S_{x,z}^2})^{1/2} \qquad (5b)$$

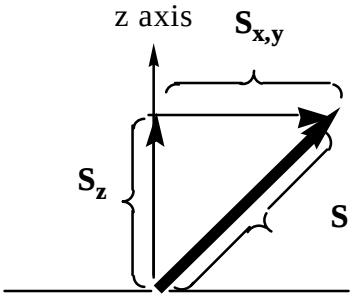

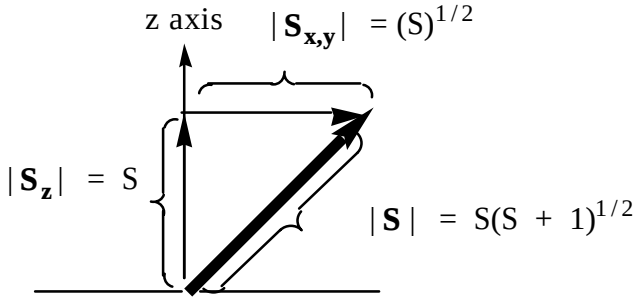

Angular Momentum (Vector Quantity):
S is the total angular momentum
$\mathbf{S_z}$ is the component on the z axis
$\mathbf{S_{x,y}}$ is the component on the x or y axis. The units are in \.

Vector Length (Scalar Quantity):
$|\mathbf{S}|$ is the total **length** of the angular momentum; $|\mathbf{S_z}|$ is the length of the component on the z axis; $|\mathbf{S_{x,y}}|$ is the length of the component on the x or y axis.

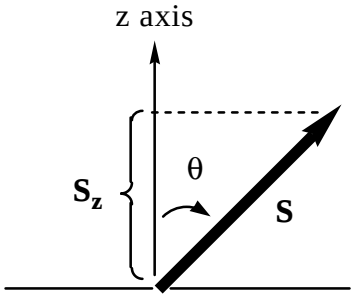

Vector Direction: The **direction** of the angular momentum vector is given by the angle θ made by the vector with the z axis. The value of θ is given by $\cos\theta = |\mathbf{S_z}| / |\mathbf{S}|$.

Figure 5. Trigonometric relationships between the angular momentum vector and the geometric axes.

By inspection of the vector diagram and use of trigonometry, if we require the value of $\mathbf{S_z}$ to follow the quantum mechanical rules then the value of **S** must also be constrained to values determined by the Pythagorean theorem through eq. 5b! Furthermore, the allowed values of the angle, θ, between **S** and $\mathbf{S_z}$, will be given by elementary trigometric relationships through eq. 6, where the magnitudes of **S** and $\mathbf{S_z}$ conform to the allowed values of θ are those for which the $|\mathbf{S_z}|$ and $|\mathbf{S}|$.

$$\cos\theta = |S_z| / |S| \qquad (6)$$

For example, for the case of S = 1/2 (Figure 6 below), the possible values of θ are: (1) for $M_S = 1/2$, $\theta = 55^o$, for $M_S = -1/2$, $\theta = 125^o$. For the case of S = 1

(Figure 7 below) , the possible values of θ are: (1) for M_S = 1, θ = 45 º, for M_S = 0, θ = 90º and for M_S = -1, θ = 135 º.

Let us now consider the vector representation of spin quantization in some detail for the two most important cases in photochemistry: a single spin and two coupled spins.

Vector Model of a Single Electron Spin

Figure 6 shows the vector model for a single electron spin. In the Figure we show the angular momentum vector pointing perpendicular to the plane of rotation of a rotating spherical electron. Since the spin quantum number, S, of a single electron is 1/2, according to eq. 3a, the value of the length of **S** for a single electron is $[S(S + 1)]^{1/2} = (3/4)^{1/2}$ (values of **S** will always be in units of \). Thus the length of a single electron spin is **independent of its orientation** and is $= (3/4)^{1/2}$. What are the possible orientations of **S** allowed by quantum mechanics? From equation 4a and 4 b, we deduce that there are two such states (a doublet state) and that the possible values of $\mathbf{S}_z$ are +1/2 \ and -1/2 \. From eq. 6 we have computed that the possible angles these two states are θ = 55º and 125º relative to the z-axis (the direction parallel to the positive direction along the z-axis is defined as 0º). Thus, from Figure 6 we can readily visualize the two possible orientations or an electron spin in terms of the vector model in **two dimensional** spin space. At this point the coordinates in the x,y plane are not specified. We shall return to this important issue when we deal below with the uncertainty principle and cones of orientation of spin vectors.

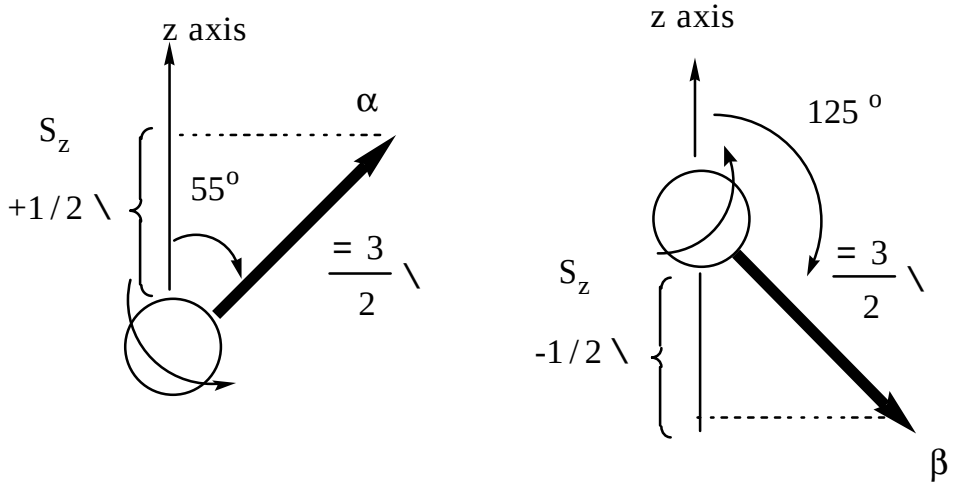

Figure 6. Vector representation of a spin 1/2 particle (an electron, a proton, a 13C nucleus). The symbol α refers to the spin wave function of a spin with M_s=

+1/2 and the symbol β refers to the spin wave function of a spin with M_s = -1/2. See text for discussion.

In quantum mechanics spin is represented by a wave function (the mathematical details of which will not concern us). The symbols α and β are employed to represent the spin wave functions corresponding to the M_S = 1/2 and -1/2 quantum numbers, respectively. Thus, the spin vector with the 55º value of θ is related to an α spin function and the spin vector with the 125º value of θ is related a β spin function. The α spin is said to be pointing "up" (relative to the z-axis) and the β spin is said to be pointing "down" relative to ther z-axis. The α and β representations of spin wave functions will be useful in describing spin states which are strongly mixed.

Vector Model of Two Coupled Electron Spins. Singlet and Triplet States.

When two particles possessing angular momentum interact or couple, how many different states of **total angular momentum** can result from the coupling? Knowledge of the rules for coupling of angular momentum is very important in photochemistry since various steps in most photochemical processes will involve the coupling of one electron spin with another or the coupling of one electron spin with some other form of angular momentum intramolecularly or intermolecularly. Evidentally, from eq. 3a and 3 b, quantum mechanics constrains the number of angular momentum states that can exist, so the number of states that can result from coupling must also be constrained! The rules for coupling of angular momentum are very simple if the vector model is employed.

Rule 1 is that the final **total** angular momentum (units of \) of a coupled system can take on only three possible types of allowed values (eq. 3b): (1) 0; (2) a positive half integer; or (3) a whole integer.

Rule 2 is that the allowed values of the spin **differ from the maximum value of the spin by one less fundamental unit of angular momentum**, \, to produce as many states as possible consistent with rule 1.

Let us apply these rules for the most important case of two electron spins coupling with one another. We start with the value of a single electron spin as 1/2 \. From the rules, we first find the **maximum** value of the coupled angular momentum on the z axis, which is simply the sum of the individual values, i.e., (1/2 + 1/2)\ = 1 \. Thus, one of the possible coupled states will have a total angular momentum of 1. All other possible states will differ from the state of maximum angular momentum by one unit of \ and must be positive or zero (rule 2). Clearly there is only one such state that follows the rules: the state for

which the total angular momentum is 0. *Any other states would possess a negative value for the total angular momentum, which is not allowed by the rules of quantum mechanics.* Thus, from these simple considerations we conclude that the only possible spin states that can result from the coupling of two individual electron spins (or coupling of two spin 1/2 particles of any kind) correspond to total spin angular momentum of 1 or 0. These states possess the spin quantum number for projection on the z axis of S = 1 and S = 0, respectively.

In Figure 7, the vector representation of the two possible state for two coupled spins is shown. In one case the two spins are antiparallel (S = 0) and so that the angular momenta exactly cancel and the resulting spin is 0. In this case the only possible value of S is equal to 0, so this is a singlet state. Notice that this spin state possesses one α spin and one β spin. When we consider electron exchange we cannot label this state as $\alpha_1\beta_2$ or $\beta_1\alpha_2$ because this would imply that we can distinguish electrton 1 and eletron 2. However, an acceptable spin function for the singlet state turns out to be $(1/2)^{1/2}(\alpha_1\beta_2 - \beta_1\alpha_2)$, i.e., a mixture of the two spin states (From this point on, we shall ignore a mathematically required "normalization" factor of $(1/2)^{1/2}$ when discussing the sin wave function of the singlet state and shall drop the labels 1 and 2 which will be implicit). We can think of the - sign in the function $\alpha\beta - \beta\alpha$ as representing the "out of phase" character of the two spin vectors which causes the spin angular momentum of the individual spin vectors to exactly cancel.

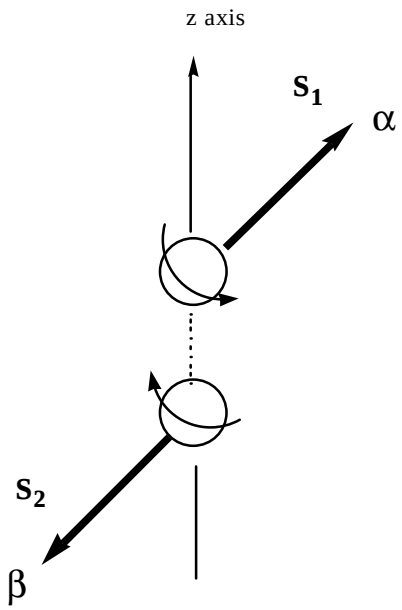

$\mathbf{S} = \mathbf{S_1} - \mathbf{S_2} = 0 \backslash$

(a)

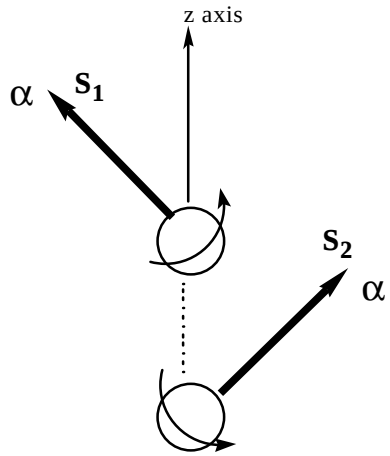

$S = \mathbf{S_1} + \mathbf{S_2} = = 2\backslash$

(b)

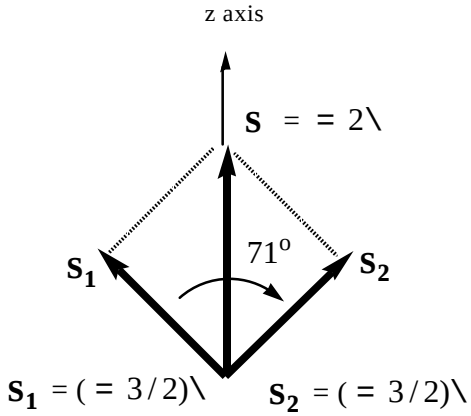

(c)

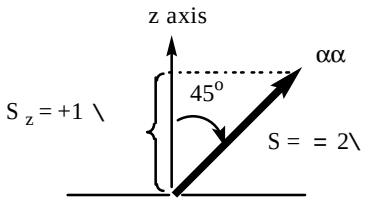

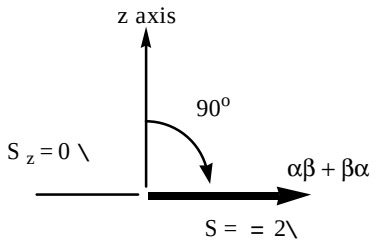

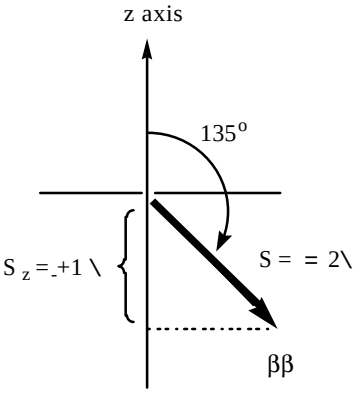

(d)

Figure 7. Subtraction and addition of two spin 1/2 particles. Upon addition, the spin vectors add up (middle) to a total length of $(2)^{1/2}$, but have a projections (right) of 1, 0 and -1 on the z axis (right). These representations apply to the coupling of an two spin 1/2 particles, electrons with electrons, electrons with nuclei and nuclei with nuclei.

The second possible state possesses S = 1 and is therefore a triplet state. The angular momentum of the state can take three possible orientations in physical space, as can the vector representing the angular momentum in spin space. The vector model of the triplet state reveals some rather interesting features which result from the rules of quantum mechanics and the rules of vector additions. In order to arrive at a resultant angular momentum corresponding to a vector length of 1 \ on the z axis (i.e., a total spin vector length of $(1/2)^{1/2}$ \ ), using individual component vectors whose lengths are $(3/4)^{1/2}$ \ , the individual vectors cannot lie at an arbitrary orientation, but must make a definite angle with one another. Have a definite angle to one another is equivalent to having a definite **phase** (angular) relationship of the two vectors. From triogonometry, if the value of the angle between the two vectors (termed the azimuthal angle) is 71º then the resultant of addition of the two vectors is the required $(1/2)^{1/2}$ \ (Figure 7c). The common, and less precise description of two 1/2 spins coupling to produce a spin 1 system is to say that the spins are "parallel", i.e. colinear. The vector model reveals that this description is not correct, although the use of the term is acceptable to make the qualitative point that there is a net spin. In the vector diagrams representing the triplet state, we shall show the vectors separated at an angle which will be understood to be that required to satisfy the phase relationship required by quantum mechanics. We shall return to this point when discussing the cones of possible orientations of electron spins.

In the case of S = 1, the vector model of the three allowed orientations of the spin vector (Figure 7 d) shows several important features: (1) the length of the vector **S** is = $(2)^{1/2}$ for each of three allowed orientations; (2) the three allowed orientations of **S** relative to the z-axis are 45 º, 90º, and 135º (Eq. 6), corresponding to the value of M_S of +1, 0 and -1, respectively (values of 1 \, 0 \ and -1 \ on the z axis). As in the case of the state for which coupling produces **S** = 0, the M_S state for S = 1 possesses an α spin and a β spin relative to the z-axis. Upon introduction of electron exchange we shall cannot label the electrons and distinguish them, so that the true state must be a mixture of the two spins, α and β, but different from the S = 0 state with no net spin. The appropriate spin function for the triplet state is $\alpha\beta + \beta\alpha$ (again the normalization constant of $(1/2)^{1/2}$ will be ignored throughout the text). We can interpret the + sign to mean that the spin vectors are in phase (with $\theta = 71^o$). For the state with $M_S = +1$,

the spin function $\alpha\alpha$ is acceptable because since both electrons possess the same orientation, we need not attempt to distinguish them. The same holds for the M_S = -1, for which the spin function $\beta\beta$ is acceptable.

It is interesting to note (compare Figures 6 and 7) that the component length of the angular momentum on the x or y axes, $S_{x,y}$, grows smaller as the value of S gets larger. At the same time, the angle θ gets smaller as the size of the vectors **S** and $\mathbf{S_z}$ approach the same value. This is a feature of the so-called correspondence principle, which states that as the angular momentum of a system increases (i.e., as the angular momentum quantum number increases) the quantum system approaches the classical limit for which it is allowed that $S = S_z$. At this limit both the magnitude (S_z) and the direction (90^o) of the vector $\mathbf{S} = \mathbf{S_z}$ would be precisely measurable.

Consequences of the Uncertainty Principle. The Cones of Possible Orientations

We have seen that according to quantum mechanics, the angular momentum vector representing a rotating particle or a spinning body can take up only a specific discrete set of orientations in space. Moreover, the Uncertainty Principle states that the length and the direction of the angular momentum vector are conjugate quantities which means that if one is measured precisely, the other cannot be measured with any precision. So far we have for simplicity considered a two dimensional representation of the spin vectors. Let us now consider the more realistic situation in three dimensional spin space. From the Uncertainty Princple, if the value of the angular momentum is precisely measured on the z axis, the x and y components in three dimensional space are completely uncertain. This means that we can measure the value of $\mathbf{S}_z$ precisely and also means that we give up all precision in the measurement of $\mathbf{S}_x$ or $\mathbf{S}_y$.

This restriction of the the Uncertainty Principle is represented in the vector description by indicating the set of possible orientations that the angular momentum vector can assume relative to the z axis, since this corresponds to the range of possible component vectors that exist in the x,y plane. **This set of possible vectors constitutes a cone such that whatever the specific position the vector takes on the cone, the angle of the vector with the z axis and the projection of the vector on the z axis are always the same; however, the x and y components or the vector are completely undetermined.** Such a cone is termed the **cone of possible orientations of the spin**.

Cone of Possible Orientations for Spin 1/2

There is one cone associated with each possible orientation of the spin angular momentum; thus, once cone exists for each value of the quantum number M_S. For example, for a single spin of 1/2, there are two such cones, one associated with $M_S = 1/2$ (α spin) and the other associated with $M_S = -1/2$ (β spin). Figure 8 (left) shows a representation of the two cones for an α spin and for a β spin. An arbitrary possible position of the spin vector in the cone is shown for each case. We emphasize that it is impossible to measure such a position within the cone, although the existence of the vector somewhere in the cone (i.e., as an α or as a β spin) can be inferred. **Thus, the vector for spin = 1/2 lies in one of two cones that represents all of the possible orientations of the angular momentum which may have a projection of +1/2 \, or -1/2 \ on the z-axis. The cones possess a side whose length is $(3/4)^{1/2}$ = 0.87 and an angle θ of either 55 ^{o} or 125 ^{o}** (units of length of the spin vector are always \).

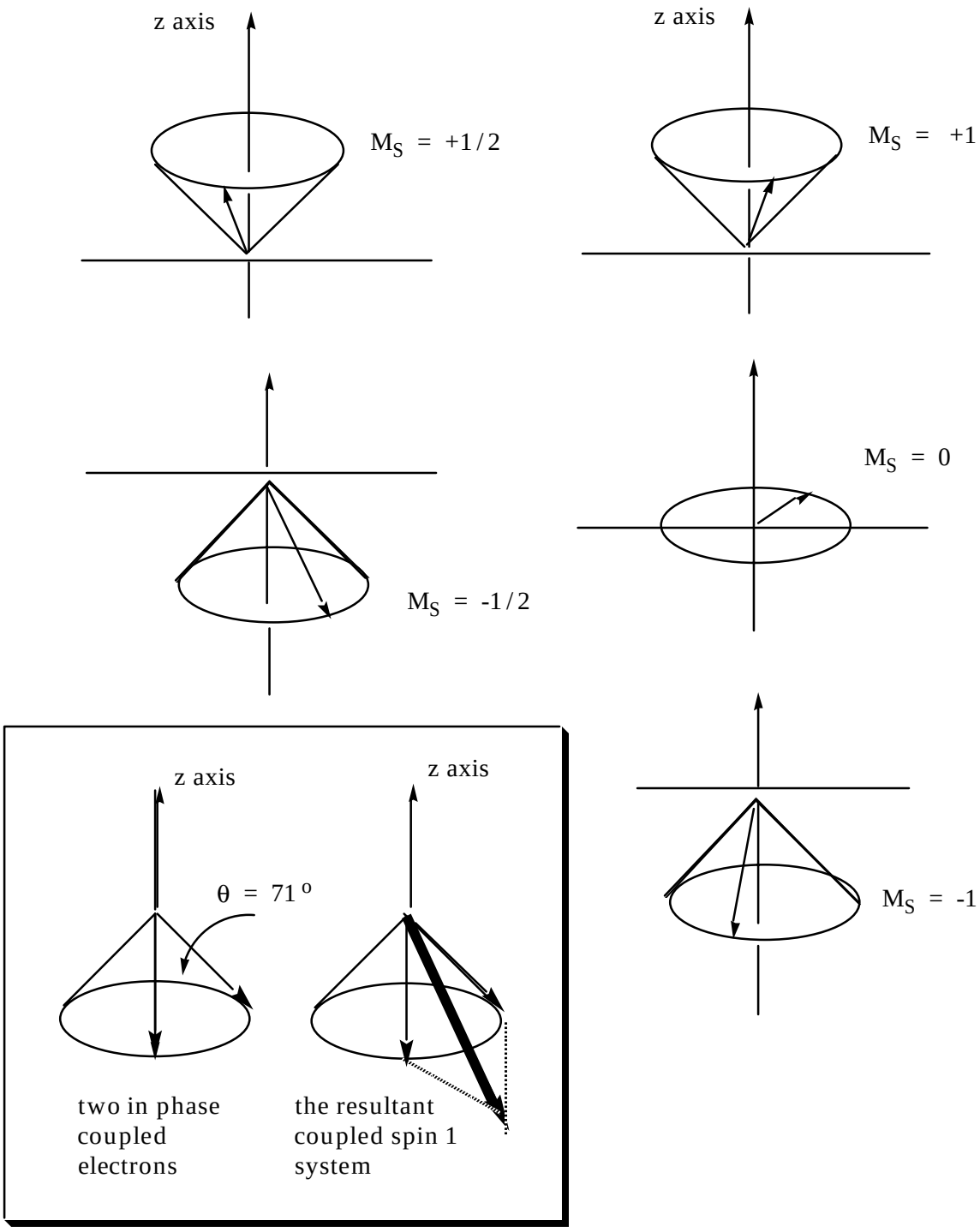

Figure 8. Cones of possible orientation for a spin 1/2 (left) and spin 1 (right) system of angular momentum. An arbitrary position of the spin vectors is shown for each of the possible cones. See text for discussion of the insert.

The above discussion shows that although we can have no knowledge of their precise position within a cone, we can determine whether a vector lies in

one or the other of the two possible cones for a spin 1/2 system, i.e., that the projection of the angular momentum on the z-axis is exactly -1/2 \ or +1/2 \. Each cone has a definite projection of M_s units of angular momentum on the z-axis and this projection represents the precise values of S_z. The S_x and S_y projections are indefinite, but the vector representing the angular momentum can be imagined as stationary and "resting" somewhere in the cone. In the absence of an external torque (magnetic field) the vector is "at rest" and does not move around in the cone. If any magnetic field is applied (as the result of a static applied laboratory field, an oscillating applied laboratory field, fields due to the magnetic moments generated by the motion of spins in the environment, etc.) the vector will begin to sweep around the cone, a motion that we shall refer to as precession. At this point, we simply consider that the spin vector is motionless and located somewhere in the cone.

Cone of Possible Orientations for Spin 1

Let us next consider the cones for the orientations of the case of S = 1 Figure 8, right). The situation is analogous to that for the spin = 1/2 case in that cones of orientation for the spin vector exist. In this case there are three cones of possible orientation for M_S = +1, 0 and -1. Thus, t**he vector for spin = 1 lies in a cone that represents all of the possible orientations of the angular momentum which may have a projection of 1 \, 0 \ or -1 \ on the z-axis. Each of the cones possess a side whose length is $(2)^{1/2} = 1.7$, but differ with respect to the angle θ that the side of the cone makes with the z axis**. An interesting feature of this case is that the projection of the spin on the z-axis is 0, even though the length of **S** is 1.7 \. It should be noted that the magnitude of the spin vectors for S = 1 are larger than those for S = 1/2, although by convention the units are not explicitly shown in the figures. We note that for the singlet state, since the value of the spin vector is zero, there is no cone of orientation since the vector length is zero.

Finally, we can employ the cone of possible orientations to represent two coupled 1/2 spins and to clarify the point mentioned above concerning the requirement that two 1/2 spins must be in phase in order to produce a triplet. In the box in the lower left of Figure 8, a representation of two β spin 1/2 vectors (M_S = 1) at the azimuthal angle (angle between vectors on the cone) of 77º are shown. Also shown is the resultant S = 1 system. The resultant length **on the cone of orientation** is exactly $[S(S + 1)]^{1/2} = 1.7$ \, the angle, θ, relative to the z axis is 45 º and the component on the z axis is -1. Upward rotation of this representation by 45 º produces the represenation of the M_S = 0 state and upward rotation of the latter representaion by another 45 º produces the representaion of the M_S = +1 state.

Summary

The angular momentum of a rotating or spinning particle is conveniently and mathematically represented by a vector. For an electron spin the vector possesses a length of $[S(S + 1)]^{1/2}$ where S is the electron spin quantum number of the system. Following the rules of quantum mechanics, the vector representing the angular momentum due to electron spin can only possess certain observablevalues and any particular value can only possess specific orientaitons in space. Sionce only one component of a spin vector (conventionally the z axis) can be observed, the aximuth of the vectro (its orientation in the xy plane) is completely unknown. However, the vector must be oriented in one of the cones of orientation allowed by quantum mechanics.

The vector model for spin angular momentum allows a clear visualization of the coupling of spins to produce different states of angular momenta. We now need to connect the vector model of angular momentum with models that allow us to deduce the magnetic energies and dynamics of transitions between magnetic states. This is done in the following sections.

4. A Physical Model for an Electron with Angular Momentum. An Electron in a Bohr Orbit. The Quantum Magnet Resulting from Orbital Motion.

We now have developed a vector model that allows the ready visualization of spin angular momentum in a three dimensional vectorial "spin space". We now need to come to grips with the problem of associating the spin angular momentum states with magnetic energies in the same way that we associate electronic states with electronic energies. Thus we need to associate some magnetic features with our vector model of electron spin. We have seen how to qualitatively rank the relative energy of **electronic orbitals and electronic states through electronic interactions**, so we shall develop an analogous model which will allow us to rank the relative energy of the **electronic spins and spin states through magnetic interactions**. We also need to develop a model that will allow us to visualize the interactions and couplings of electron spins which will lead to transitions between the magnetic energy levels corresponding to magnetic resonance spectroscopy and intersystem crossing.

The connection of spin structure and magnetic energy level diagrams will be made through the development of a relationship between spin angular momentum and the magnetic moment due to electron spin. The magnetic energy of the spin will depend on the coupling of the spin's magnetic moment with other magnetic moments. These couplings will both influence the energy of the electron spin magnetic energy levels and the dynamics of the electron spin transitons between magnetic energy levels.

All of the important **interactions** which bring about couplings may be classified in terms of two basic types, a so called **dipolar** interaction and a **contact** or **overlap** interaction (in analogy with the two basic types of electrostatic interactions). In addition, there are only a small number of couplings or "mechanisms" by which the two basic interactions can connect an electron spin to a magnetic moment due to some internal or external source.

We shall employ the intuitively appealing physical model of an electron executing circular motion about an axis in a Bohr orbit (Figure 4, left) to demonstrate the relationship between an electron's **orbital angular momentum** and the **magnetic moment** associated with **orbital motion**. We shall extend this model to a physical model of a spherical electron rotating about an axis (Figure 4, right) to deduce the relationship between an electron's **spin angular momentum** and the **magnetic moment** associated with **spin motion** (with appropriate quantum mechanical modifications).

Magnetic Moments Resulting from Orbital Motion of an Electron

The properties of classical magnets are all completely characterized by the magnetic moment of the magnet. Since the magnet moment is a vector quantity, all of the vectorial concepts that were discussed above for angular momentum will apply to magnetic moments!

From the simple model of an electron in a circular Bohr orbit, we shall proceed as follows:

(1) deduce from classical considerations the origin of the magnetic moment of an electron resulting from the electron's circular motion orbit about a nucleus, i.e., the magnetic moment, μ_L, that results from the electron's **orbital** angular momentum, **L**;
(2) extend this model to infer the origin of the magnetic moment of spherical electron that is spinning on a fixed axis of rotation, i.e., the magnetic moment, μ_S, that results from the electron's **spin** angular momentum, **S**;
(3) use the vector model for the spin structure of an electron and the vector model of the magnetic moment, to deduce the magnetic energy relationships between the spin structures (which define the energetic ordering of the magnetic states, and the radiationless and radiative transitions between these states).

The Magnetic Moment of an Electron is a Bohr Orbit

An electron in a Bohr atom is modeled as a point negative charge rotating in a circle about a fixed axis about a nucleus. By virtue of its constant circular motion and angular momentum, **L**, an orbiting Bohr electron produces a magnetic moment, μ_L, which can be represented by a vector coinsiding with the axis of rotation (Figure 9). This behavior is completely analogous to that of an electric current in a circular wire, which produces a magnetic moment perpendicular to the plane of the wire. Let us now see how this magnetic moment, μ_L, is related to the angular momentum of the electron, **L**, in a Bohr orbit. We are concerned with the factors determining the magnitude of the magnetic moment and its energy in a direction along the z-axis. i.e., its vectorial qualities.

Clasical considerations indicate that the magnitude of μ_L is proportional to the magnitude of **L**. From the model of the electron in the Bohr orbit the proportionality constant between **L** and μ_L can be shown to be -(e/2m), the ratio of the unit of electric charge to the electron's mass, so that a simple relationship exists between μ_L and **L** is given by eq. 7.

$$\boldsymbol{\mu}_L = -(e/2m)\mathbf{L} \qquad (7)$$

The proportionality constant (e/2m), reflects the relationship between the magnetic moment and angular momentum of a Bohr orbit electron and is a fundamental quantity of quantum magnetism. It is therefore given a special symbol γ_e and the name **magnetogyric ratio** of the electron and is defined as a positive quantity. Thus, eq. 7 may be expressed as eq. 8.

$$\boldsymbol{\mu}_L = -\gamma_e \mathbf{L} \qquad (8)$$

If the electron possesses one unit of angular momentum, its magnetic moment, $\boldsymbol{\mu}_L$ is equal exactly to \(e/2m). This quantity may be viewed as the **fundamental unit of quantum magnetism and is given the special name of the Bohr magneton, since it was derived from the simple analysis of a Bohr atom.** We shall give the Bohr magneton a special symbol, μ_e and note that its numerical value is 9.3×10^{-20} JG^{-1}. When we see the symbol μ_e we should think of a magnetic moment generated by an electron possesing an angular momentum of exactly 1 \.

Eqs. 7 and 8 show:

(1) the vector representing the magnetic moment, $\boldsymbol{\mu}_L$, and orbital angular momentum , **L**, are co-linear (they are equivalent through a proportionality factor);
(2) the vector that represents the magnetic moment of an electron is opposite in direction to that of the angular momentum vector (recall that a negative sign relating vectors means that the vectors possess orientations 180^o apart);
(3) the proportionality factor γ_e allows us to deduce that the magnitude of the magnetic moment due to orbital motion is directly proportional to the charge of the electron and inversely proportional to its mass.

The reason that Eqs. 7 and 8 are so important is that they allow us to visualize both the angular momentum, which must be strictly conserved in all magnetic transitions and the magnetic moment which provides the interactions which determine magentic energies and which "trigger" radiationless and radiative magnetic transitions to occur. Figure 9 presents such a vectorial description (the Figure is schematic only so that the sizes of the vectors are unitless and not to any particular scale).

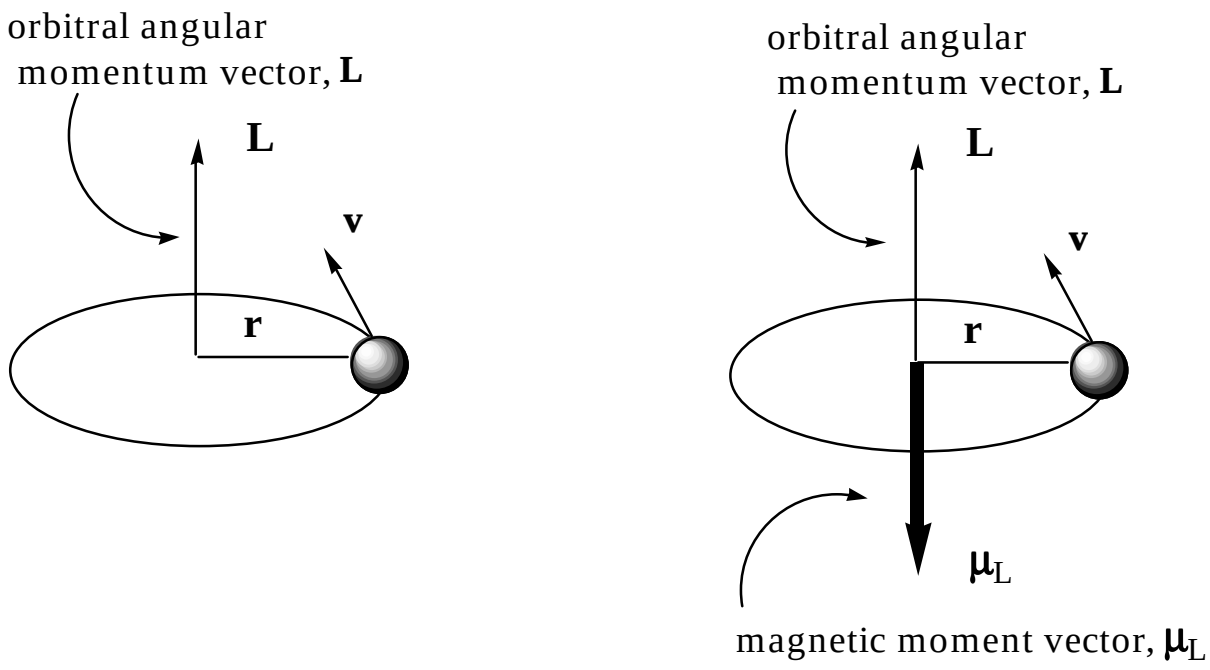

Figure 9. The vector model for the orbital angular momentum and the magnetic moment due to an electron in a Bohr orbit. The direction of the magnetic moment vector is opposite that of the direction of the angular momentum vector for an electron. The units of **L** are \ and the units of μ_L are J-G^{-1}.

We now need to proceed to deduce the magnetic moment is associated with an electron spin. We shall start with the results deduced from the electron in a Bohr orbit and transfer these ideas to the model of a rotating sphere, and determine what modifications of the model are necessary.

Electron Spin Angular Momentum and the Magnetic Moment Associated with Magnetic Moment Associated with Electron Spin

An electron in isolation possesses several simple properties: mass, electron charge, spin angular momentum, and a magnetic moment. There is no question that the electron is a quantum particle and as such will possess many properties which are quite unusual and unpredictable from observations of classical particles. Nonetheless, there is a clear visualization that is possible if we take as a model for the electron a material particle of definite size and spherical shape with a negative electric charge distributed over its surface. The properties of mass and charge are clearly articulated in this simple model. In order to understand the angular momentum of the electron resulting from its spin motion, it is intuitively natural to assume that since the mass of the electron is fixed and since its spin angular momentum is quantized and fixed, the spherical

electron must spin about an axis with a fixed velocity, **v** (Figure 10). It is also quite natural to apply the results relating the orbital angular momentum of an electron to a magnetic moment due to its orbital motion to infer the relationship of the spin angular momentum of an electron to a magnetic moment due to its spin motion.

However, we should not be too surprised if the electron spin angular momentum has some differences because **there is no simple classical analogue of electron spin**. From the model of orbital angular momentum, the concept of electron spin angular momentum was devised to explain atomic spectra and was empirical in origin. Since the electron is a charged particle, we expect that as a result of its spinning motion, it will generate a magnetic moment, μ_S, in analogy to the magnetic moment generated by an electron in a Bohr orbit. A direct analogy with the relationship of orbital angular momentum and magnetic moment (Eq. 8) would suggest that the magnetic moment of the spinning electron should be equal to $\gamma_e\mathbf{S}$, i.e., the magnetic moment due to spin should be directly proportional to the value of the spin and the proportionality constant should be γ_e. However, experimental evidence and a deeper theory show that this is not quite the case and that for a free electron and that Eq. 9 applies.

$$\mu_S = -g_e\gamma_e\mathbf{S} \qquad (9)$$

In Eq. 9 g_e is a dimensionless constant called the g factor or g value of the free electron. and has an experimental value of ca 2. Thus, the simple model which attempts to transfer the properties of an orbiting electron to a spinning electron, is incorrect by a factor of 2. This flaw are is not of concern for the qualitative features of spin.

The following important conclusions can now be made:

(1) since spin is quantized and the spin vector and the magnetic moment vectors are directly related by eq. 9, **the magnetic moment associated with spin, as the angular momentum from which it arises is quantized in magnitude and orientation**;

(2) since the energy of a magnetic moment depends on its orientation in a magnetic field, **the energies of various quantized spin states will depend on the orientation of the spin vector in a magnetic field**;

(3) the vectors μ_S and **S** are both positioned in a cone of orientation which depends on the value of M_S (Figure 10, right);

(4) in analogy to the relationship of the orbital angular momentum and the magnetic moment derived from orbtial motion, the vectors μ_S and **S** are antiparallel (Figure 10, left).

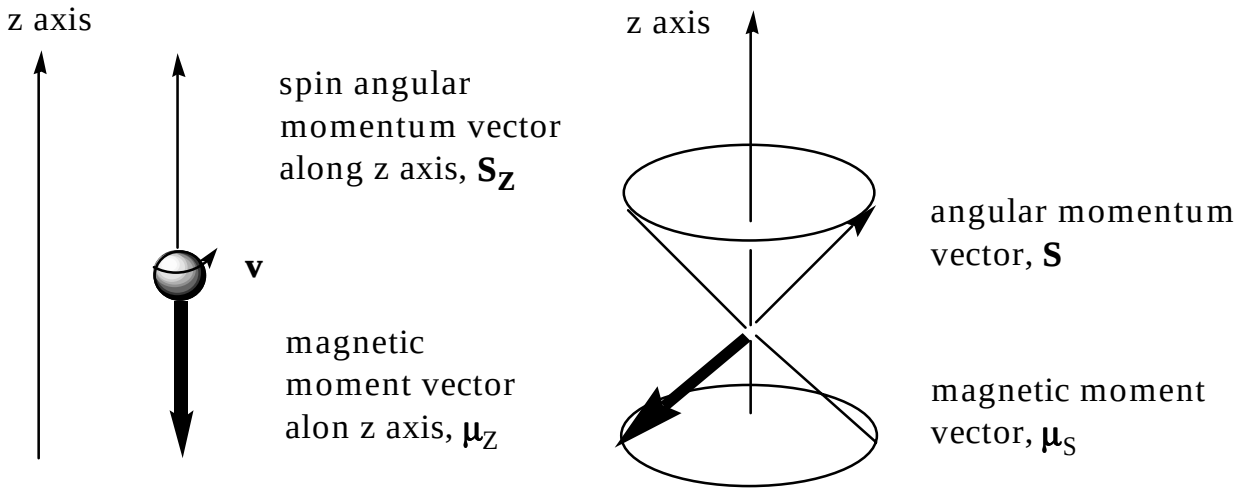

Figure 10. Vector representation of the spin angular momentum, **S**, and the magnetic moment associated with spin, μ_S. The two vectors are colinear, but antiparallel.

5. Classical Magnetic Energy Levels in a Strong Applied Field

In the absence of a coupling magnetic field (zero field situation), the magnetic energy levels due to spin angular momentum are degenerate, i.e., they all have the same (zero) magnetic energy. Let us now consider what happens to the degenerate magnetic energy levels at zero field when a strong field magentic field is applied. We shall examine the results for a classical magnet and then apply these results to determine how the quantum magnet associated with the electron spin changes its energy when it couples with a magnetic field. The vector model not only provides an effective tool to deal with the qualitative and quantitative aspects of the magnetic energy levels, but will also provides us with an excellent tool for dealing with the qualitative and quantitative aspects of transitions between magnetic energy levels.

According to classical physics, when a bar magneti is placed in a magnetic field, H_0, the torque acting on the magnetic moment of the bar magnet is proportional to the product of the magnitude of the magnetic moment, μ, of the bar magentic, the magnitude of the magnetic moment of the magnetic field, $\mathbf{H}_Z$, and the angle θ between the vectors describing the moments. Three important orientations of bar magnetic are shown schematically in Figure 11.

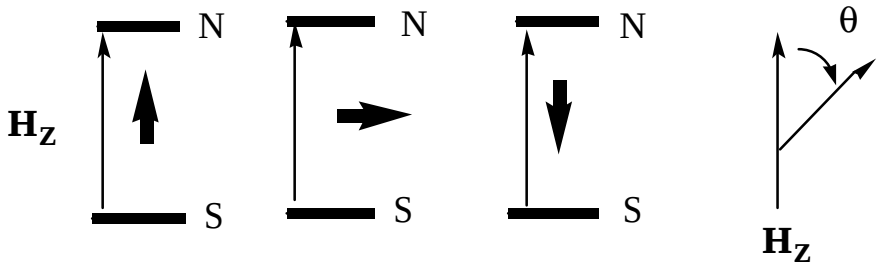

Figure 11. Energies of a classical bar magnet in a magnet field, H_z.

The precise equation describing the energy relationship of the bar magnetic at various orientations is given by equation 10, where μ and $\mathbf{H}_z$ are the magnitudes of the magnetic moments of the bar magnet and the applied field in the Z direction.

$$E\,(\text{magnetic}) = -\mu H_Z \cos\theta \qquad (10)$$

In eq. 10 the negative sign before the quantity on the right of the equation means that the system becomes more stable if the product of $\mu H\cos\theta$ is a positive quantity. The magnitudes (lengths) of the vector quantities $\boldsymbol{\mu}$ and **H** are always positive by definition. So whether the energy of the system is positive (less stable than the situation in zero field) or negative (more stable than the situation in zero field) depends on the sign of $\cos\theta$ (which is positive for q between 0^o and 90^o and negative for θ between 90^o and 180^o. Let us consider the situation for two parallel vectors ($\theta = 0$), two perpendicular vectors ($\theta = 90^o$ or $\pi/2$), and two antiparallel vectors ($\theta = 180^o$ or π). For these cases, $\cos\theta = 1$, 0 and -1, respectively (Figure 11). Thus, we can make the important conclusions that any orientation of the bar magnet with θ between 0 and less than 90^o is stabilizing (the E in Eq. 10 is negtive relative to the zero of magnetic energy) and any orientation of the bar magnet with θ between 90^o and up to 180^o is destabilizing (the E in Eq. 10 is positive relative to the zero of magnetic energy). Importantly, at an orientation of 90^o the magnetic interactions between the applied magnetic field and the bar magnet are zero ($\cos 90^o = 0$), i.e., the same as they are in the absence of a strong field!

From Spin Angular Momentum States to Magnetic Energy Levels

From the classical model for a bar magnet in a magnetic field, we can proceed to deduce the energies of the quantum magnets. To do this, we now proceed to translate the spin states for one, two and three spins into magnetic energy diagramss that will show the relative energetic ordering of the magnetic energy levels. From magnetic energy level diagrams, just as for the electronic energy level diagrams, all possible transitions between different magnetic energy levels can be readily deduced by inspection. The paradigm of selection rules and plausible mixing mechanisms will then provide a means of analyzing magnetic resonance phenomena such as magnetic resonance spectroscopy and intersystem crossing.

We shall consider the energy level diagrams for two extreme situations: (1) zero (or "low") applied magnetic field, i.e., the usual situation under which photochemical reactions are conducted; and (2) a strong ("high") applied field, i.e. the conditions under which magnetic resonance spectrosopy is conducted. The terms high and low will refer to the strength of the applied magnetic field compared to inherent magnetic interactions between the spin states and internal magnetic fields.

Quantum Magnets in the Absence of Coupled Magnetic Fields

In the absence of any magnetic interactions, the vector model of a single electron spin views the angular momentum and magnetic moment as stationary

in space and possessing random orientations in space. There is no pertinent M_S quantum number in this case, because there is no preferred axis of orientation. However, the spin angular momentum of the electron (1/2\) and the quantum number for the total spin, S, are still a good quantum numbers.

As for the case of a single electron spin, at zero field it is convenient to consider a system containing spin correlated electron spins as a mixture of singlet (S) and triplet states (T). Thus, the spin functions given in Table 1 cans be used to describe the system at both zero and high fields. In the absence of magnetic interactions operating on the paired spins, the four states have exactly the same energy, i.e., all four of the magnetic energy levels are degenerate.

Quantum Magnetic Energy Levels in a Strong Applied Field. **Zeeman Magnetic Energies**

We are now in position to determine the energies of magnetic sublevels and the precession rates assoicated with spins in magnetic sublevels as a function of their g-factors and the strength of applied fields. The magnetic energy of interaction of a magnetic moment and an applied field is known as the **Zeeman energy**. Eq. 9 relates the magnetic moment of the quantum magnet with the value of the g factor and the spin. Eq. 11 relates the energy of the quantum magnet to the strength of the applied field, H_0, the magnetic quantum number for the spin orientation, M_S, the g-value of the electron and the universal constant μ_e.

$$E = M_s g \mu_e H_Z \qquad (11)$$

Thus, the magnetic energies (relative to those in zero field) of the singlet, doublet and triplet states are readily computed and are shown in Table 2.

Table 1. Important facets of singlet, doublet and triplet states in an applied magnetic field H_Z.

State	**State Symbol**	**M_S**	**Magnetic Energy**	**Spin Function**	**Vectror Representation**
Singlet	S	0	0	$\alpha\beta - \beta\alpha$	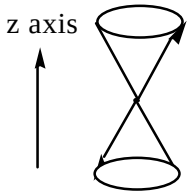
Doublet	D_+	+1/2	$+(1/2)g\mu_e H_Z$	α	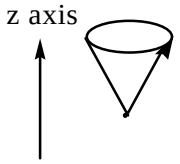
Doublet	D_-	-1/2	$-(1/2)g\mu_e H_Z$	β	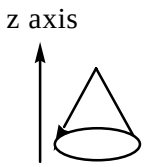
Triplet	T_+	+1	$+(1)g\mu_e H_Z$	$\alpha\beta + \beta\alpha$	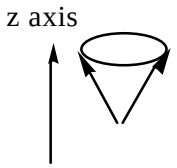
Triplet	T_0	0	0	$\alpha\beta + \beta\alpha$	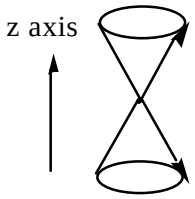
Triplet	T_-	-1	$-(1)g\mu_e H_Z$	$\alpha\beta + \beta\alpha$	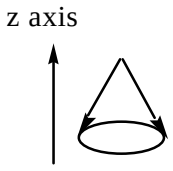

6. Classical Precession of the Angular Momentum Vector

A classical bar magnet (Figure 11) may lie motionless at a certain orientation in a magnetic field. However, if the bar magnet possesses angular momentum, it would not lie motionless, but would execute a precessional motion about the axis defined by the applied magnetic field. A classical analogue of the expected motion of a magnet possessing angular momentum in a magnetic field is available from the classical precessional motion of a rotating or spinning body such as a toy top or gyroscope. The angular momentum vector of a spinning top sweeps out a cone in space as it makes a **precessional** motion about the axis of rotation and the tip of the vector sweeps out a circle (Figure 12 left). The cone of precession of a spinning top possesses a geometric form identical to the cone of possible orientations that are possible for the quantum spin vector, so that the classical model cans serve as a basis for understanding the quantum model. A remarkable, and non-intuitive, feature of a spinning top is that it appears to defy gravity and precess, whereas a non-spinning gyroscope falls down! The cause of the precessional motion and the top's stability toward fallin is attributed to the external force of gravity, which pulls downward, but exerts a torque "sideways" on the angular momentum vector. This torque produces the non-intuitive result of precession. By analogy, in the presence of an applied field, the coupling of the magnetic moment with the field produces a torque that "grabs" the vectors and causes them to precess about the field direction.

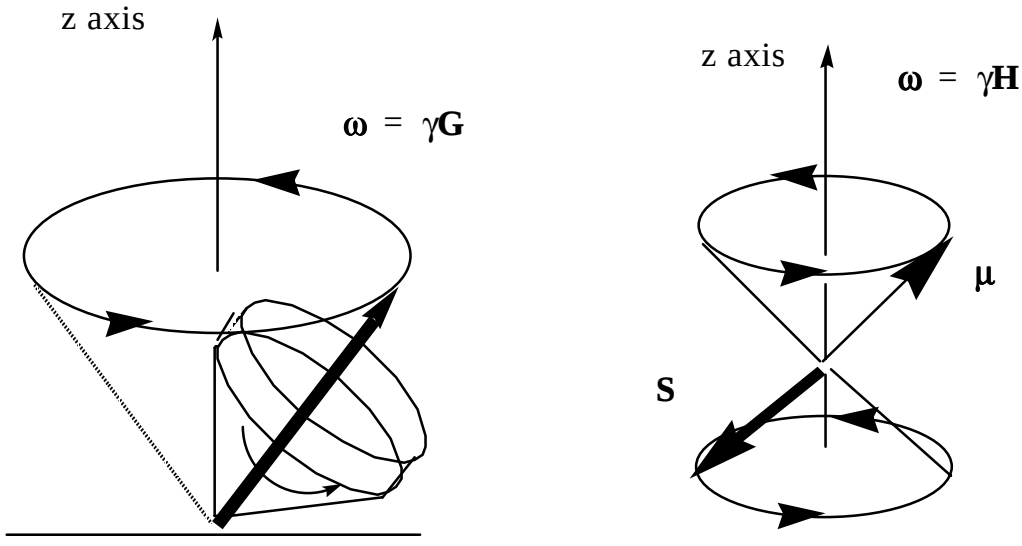

Figure 12. A vector diagram comparing the precessional motion of a spinning top to the precessional motion of spin angular momentum vector **S** and the

precessional motion of the magnetic moment, μ_S in the presence of an applied magnetic field.

The classical vector properties of the angular momentum of a toy top or gyroscope are analogous to many of the important characteristics of the vector properties of the quantum mechanical magnetic moment. The reason for the close analogy is due to the important and **critical connection between the electron's magnetic moment and the angular momentum due to the electron's spin**. For example, the rotating mass of a gyroscope possesses angular momentum which can be represented by a vector whose direction is along the symmetry axis of rotation. A gyroscope in a gravitational field precesses, i.e., the axis of its rotation rotates about the direction of the gravitational field (figure 12 left). What factors determine the **rate of precession** of the gyroscope? The answer is the **force or gravity and the inherent angular momentum of the gyroscope**. If the angular momentum, which is determined by the angular velocity of spin and the mass of the gyroscope, is constant, the rate of precession $\boldsymbol{\omega}$ is determined only by the force of gravity, so that there is a proportionality between the rate of precession and the force of gravity, **G**, as shown in eq. 12, where γ (compare to the magnetogyric ratio in eq. 8 and eq. 9) is the scalar proportionality constant between the precessional frequency and the force of gravity.

$$\boldsymbol{\omega} = \gamma \mathbf{G} \qquad (12)$$

Since the mechanics of the precessional motion of a gyroscope in the presence of gravity are of the same mathematical form as the mechanics of a magnetic moment associated with a spinning charged body in the presence of a magnetic field, we postulate that the vector due to the magnetic moment of the quantum magnet undergoes precessional motion in an applied magnetic field.

Precession of a Quantum Magnetic Moment in an Applied Magnetic Field.

There are several features of the vector representation of a quantum mechanical magnetic moment that are critical for an understanding of how electron spin manifests itself in photophysical and photochemical processes. The first is the **magnitude** of the magnetic moment; second is the **orientation** of the magnetic moment with respect to a defined axis of quantization; the third is the **coupling strength** of the magnetic moment associated with electron spin to other magnetic moments; and the fourth is the **angular frequency** and **direction** of precessional motion made by the magnetic moment about a defined axis of quantization. In order to understand the quantum model, we shall first consider the concrete features of a classical model of a spinning electron and then move to

determine the new features that are imposed on an electron and its spin by the laws of quantum mechanics.

Application of a magnetic field has the effect of producing a torque on the magnetic moment vector in the same way that the force of gravity produces a torque on the angular momentum of a spinnig top (Eq. 12). According to Newton's classic Laws, this torque is equal to the rate of change of angular momentum. For a single electron in a given orbit, the absolute magnitude of the spin angular momentum is fixed, so that a magnetic torque can only be produced by changing the direction of the angular momentum vector, and not its magnitude. The conclusion is that the quantum magnetic moment vector, together with the angular momentum vector (whose motions are identical except for direction in space) must precess about the axis of the applied field because precession allows the direction of the angular momentum to change continuously without changing the magnitude of the angular momentum. If the amount of angular momentum is \, the fundamental unit of angular momentum in the quantum world (i.e., the value of the angular momentum for **S** = 1) then the angular momentum vector and the magnetic moment vector precess about the field direction with a characteristic angular frequency, ω, given by eq. 13, where γ_e is the magnetogyric ration of the electron and **H** is the strength of the magnetic field (one unit of angular momentum is assumed).

$$\omega \text{ (Larmor frequency)} = \gamma_e \mathbf{H} \qquad (13)$$

For a fixed unit of angular momentum of \, the rate of precession, ω, of the spin and magnetic moment vectors about the magnetic field **H depends on the magnitude of both γ_e and H** and is termed the **Larmor** frequency (Figure 12). As mentioned above, this precessional motion is directly analogous to that of the motion of a gyroscope under the influence of gravity. We should remind the reader that the value of ω also depends on the amount of angular momentum, which was assumed to be one unit (\) in the example.

The second important feature differentiating the classical magnet from the quantum magnet is that a classical magnet may achieve any arbritrary position in an applied field (of course, the energy will be different for different positions), but the quantum magnet can only achieve a finite set of orientations with respect to the applied field, i.e., **the orientations of the quantum magnet with respect to the applied field are quantized.** This result is due to the principle of quantization of angular momentum, which can possess only the following values on the z axis, depending on the value of M_S: 0\, \/2, \, 3\/2, 2\, etc., each value of which corresponds to a cone or possible orientations about the z axis. We now show that this feature leads to the conclusion that **the cones of possible**

orientations become cones of possible precess ion for the angular momentum and magnetic moment vectors in the presence of a coupling magnetic fields.

The Quantum Magnet. Precession in the Cone of Orientations.

Individual spin vectors are confined to cones which are oirented to cones which are oriented along the quantization axis. The **cone of possible orientations** (for each value of M_S) of the angular momentum vector also represents a **cone of precession** when the vector is subject to a torque from some magnetic field. When a magnetic field is applied along the z axis, the quantum states with different values of M_S will possess different energies because of the different orientations of their magnetic moments in the field (recall from eq. 9 that the direction of the magnetic moment vector is colinear with that of the angular momentum, so if the angular momentum possesses different orientations, so will the magnetic moment). These different energies, in turn, correspond to different angular frequencies of precession, ω, about the cone of orientations. The energy of a specific orientation of the anglar momentum in a magnetic field is directly proportional to M_S, μ_e and $\mathbf{H}_z$ (eq. 11, previous section).

$$E_Z = \backslash\omega_S = M_S g \mu \mathbf{H}_z \qquad (14a)$$

Thus, the value of the spin vector precessional frequency, ω_S, is given by Eq. 14b.

$$\omega_S = [M_S g \mu \mathbf{H}_z] / \backslash \qquad (14b)$$

From Eq. 14b, the values of ω are directly related to the same factors as the magnetic energy associated with coupling to the field. For two states with the same absolute value of M_S, but different signs of M_S, the precessional rates are identical in magnitude, but opposite in the sense of precession (if the tips of the vectors in Figure 12 were viewed from above, they either trace out a circle via a clockwise motion or via a counterclock wise motion). This opposite sense corresponds to differing orientations of the magnetic moment vector and therefore different energies, E_Z.

From classical physics, the rate of precession about an axis is proportional to the strength of coupling of the angular momentum to that axis. The same ideas hold if the coupling is due to sources other than an applied field, i.e., coupling with other forms of angular momentum. For example, if spin-orbit coupling is strong, then the vectors **S** and **L** precess rapidly about their resultant and are strongly coupled. The precessional motion is difficult for other magnetic torques to break up. However, if the coupling is weak, the precession is slow about the coupling axis and the coupling can be broken up by relatively weak

forces. These ideas will be of great importance when we consider transitions, such as intersystem crossing, between magnetic states.

Since the magnetic moment vector and the spin vector are colinear, these two vectors will faithfully follow each other's precession, so that we do not need to draw each vector, since we can deduce from one vector the characteristics of the other. We must remember, however, that one vector has the units of angular momentum (\) and the other has the units of magnetic moment (J/G). Figure 13 shows the vector model of the different rates of precession for a spin 1/2 and spin 1 state for the possible cones of orientation.

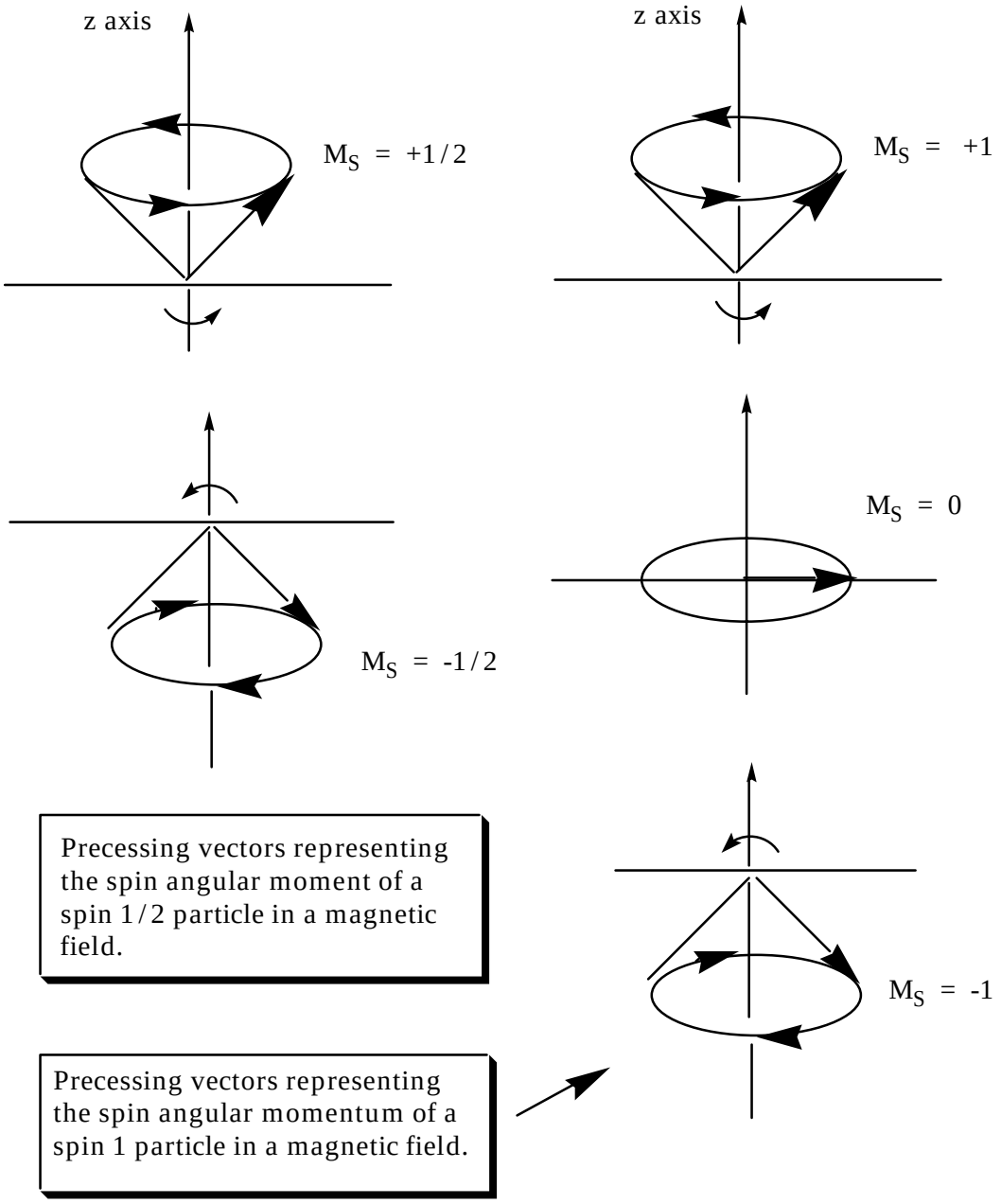

Figure 13. Vector model of vectors precessing in the possible cones of orientation. Only the spin angular momentum vectors are shown. The magnetic moment vectors ($\boldsymbol{\mu}$) (see Figure 11) precess at the same angular frequency as the angular momentum vectors (**S**), but are oriented colinear and 180º with respect to the spin vector. The magnitude of the angular momentum vector for the S = 1 system (right) is twice the magnitude of the angular momentum vector of the S = 1/2 system (left).

Summary

The process of rotation of the quantum magnet's vector about an axis is termed **precession** and the specific precessional frequency of a given state under the influence of a specific field is termed the **Larmor precessional frequency, ω.** We note the following characteristics of the Larmor precession, all of which are implied by eq. 14b:

(1) The value of the precessional frequency ω is proportional to the magnitude of M_S,, g, μ and $\mathbf{H}_z$, where $\mathbf{H}_z$ is the value of a magnetic field interacting with the spin magnetic moment.
(2) For a given orientation and magnetic moment, the value of ω decreases with decreasing field, and in the limit of zero field, the model requires recession to cease and the vector to lie motionless at some indeterminate value on the cone of possible orientations.
(3) For a given field strength, a state with several values of M_S, the vector precesses fastest for the largest absolute values of M_S and is zero for states with $M_S = 0$.
(4) For the same absolute value of M_S different signs of M_S correspond to different directions of precession, which have identical rates, but different energies.
(4) A high precessional rate corresponds to a high energy because a high ω implies a strong coupling field **H** and the magnetic energy corresponds to the strength of the coupling field.
(5) For the same field strength and quantum state, the precessional rate is proportional to the value of the g factor.

Some Quantitative Relationships Between the Strength of a Coupled Magnetic Field and Larmor Frequency.

From eq. 14b and the measured value of γ_e (1.7×10^7 rad s^{-1}) the following quantitative relationship exists between the precessional frequency and the coupling magnetic field for a "free" electron:

$$\omega = 1.7 \times 10^7 \text{ rad } s^{-1} \mathbf{H}, \text{ where } \mathbf{H} \text{ is in the units of Gauss} \qquad (15a)$$

It is also useful to consider the frequency of oscillation, ν (the frequency for which the precessing angular momentum vector sweeps a single circle). The relationship between ω and ν is $\nu = \omega/2\pi$ or $\omega = 2\pi\nu$. The latter relationships lead to eq. 16:

$$\nu = 2.8 \times 10^6 \text{ } s^{-1} \mathbf{H}, \text{ where } \mathbf{H} \text{ is in the units of Gauss} \qquad (15b)$$

Since one complete cycle is equivalent to 2π radians, for a fixed field the value of $\omega$is always greater than the value of ν. The frequency ν is the same frequency associated with the oscillations of a light wave. Through the relationship (Eq. 16) of ΔE. ω and ν, we can readily associate the precessional frequency, ω with the resonance oscillational frequency of radiative transitions,ν and the energy gap between the states undergoing transitions, ΔE.

$$\Delta E = h\nu = \backslash\omega \qquad (16)$$

From eqs. 15 and 16, we can therefore compute that the frequency of precession ω for fields of 1 G, 100 G, 10,000 G and 1,000,000 G is: 1.7×10^7 rad s^{-1}, 1.7×10^9 rad s^{-1}, 1.7×10^{11} rad s^{-1}, and 1.7×10^{13} rad s^{-1} (for oscillation frequency, ν, the values are 2.8×10^6 s^{-1}, 2.8×10^8 s^{-1}, 2.8×10^{10} s^{-1}, and 2.8×10^{12} s^{-1}), respectively. Practically speaking, applied laboratory fields whose strengths can be varied from 0 to about 100,000 G are readily achievable, so that precessional rates ω of the order of 1.7×10^{11} rad s^{-1} ($\nu = 2.8 \times 10^9$ s^{-1}) are achievable by applying laboratory magnetic fields to a free electron spin. Internal magnetic fields resulting from interactions with other electron spins or nuclear spins typically correspond to magnetic fields in the range from a fraction of a G to several hundreds of G. In certain cases, however, strong spin-orbit coupling interactions or strong coupling of two electron spins, can produce magnetic fields of the order of 1,000,000 G or larger, causing precessional frequencies of the order of 10^{12} s^{-1} and greater.

Precession of Electron and Nuclear Spins

The value of the electron's magnetic moment μ_ϵ is proportional to the magnitude of the gyromagnetic ratio, γ_e (eqs. 8 and 9). An analogous expression holds for the magnetic moment of a nucleus, $\boldsymbol{\mu}_n$ (eq. 17, where γ_n is the magnetogyric ratio for a specific nucleus, g_n is the nuclear g factor and **I** is the value os the nuclear spin).

$$\boldsymbol{\mu}_n = g_n\gamma_n\mathbf{I} \qquad (17)$$

Since the value of ω is proportional to μ, it is also proportional to γ. From these relationships, we can deduce that the precessional rate of an electron spin is much faster than that of a nuclear spin of a proton, since γ_e is ca 1000 times larger than γ_p, the gyromagnetic ratio for a proton. The differences can be traced to the difference in the mass of the nucleus and the electron (they both have the same absolute value of charge and angular momentum). To achieve the same angular momentum as an electron, the more massive nucleus need achieve a much smaller angular velocity. Because of this slower velocity, the spinning nucleus

"carries less current" as a spinning charge and therefore generates a smaller magnetic moment. From the definition of γ as $e/2m$ (eq. 7 and 8), it is readily deduced that the magnetic moment of a proton is nearly 1000 times smaller than the magnetic moment of an electron, i.e., the ratio of magnetic moments is proportional to the ratio of the masses for particles of the same spin ($1/2$ \) and electric charge (one unit).

Eq. 18 gives the quantitative relationship of the precessional frequency, ω_p, of a proton's magnetic moment in a field $\mathbf{H}_z$. For a ^{13}C nucleus, the precessional frequency is approximately 4 times less than that of a proton (which possesses the largest value of γ_n of any nucleus.

$$\omega_p = 2.4 \times 10^4 \text{ rad s}^{-1} \mathbf{H}, \text{ where } \mathbf{H} \text{ is in the units of Gauss} \qquad (18)$$

For example, at a field of 10,000 G the precessional frequency of the proton's magnetic moment is 2.4×10^8 rad s^{-1}, which can be compared to the precessional frequency of 1.7×10^{11} rad s^{-1} at the same field strength.

7. Examples of Magnetic Energy Diagrams.

There are serveral very important cases of electron spin magnetic energy diagrams to examine in detail, because they appear repeatedly in many photochemical systems. The fundamental magnetic energy diagrams are those for a single electron spin at zero and high field and two correlated electron spins at zero and high field. The word correlated will be defined more precisely later, but for now we use it in the sense that the electron spins are correlated by electron exchange interactions and are thereby required to maintain a strict phase relationship. Under these circumstances, the terms singlet and triplet are meaningful in discussing magnetic resonance and chemical reactivity. From these fundamental cases the magnetic energy diagram for coupling of a single electron spin with a nuclear spin (we shall consider only couplings with nuclei with spin 1/2) at zero and high field and the coupling of two correlated electron spins with a nuclear spin are readily derived and extended to the more complicated (and more realistic) cases of couplings of electron spins to more than one nucleus or to magnetic moments generated from other sources (spin orbit coupling, spin lattice coupling, spin photon coupling, etc.).

Magentic Energy Diagram for A Single Electron Spin and Two Coupled Electron Spins. Zero Field.

Figure 14 displays the magnetic energy level diagram for the two fundamental cases of : (1) a single electron spin, a doublet or D state and (2) two correlated electron spins, which may be a triplet, T, or singlet, S state. In zero field (ignorning the electron exchange interaction and only considering the magnetic interactions) all of the magnetic energy levels are degenerate because there is no prefered orientation of the angular momentum and therefore no prefered orientation of the magnetic moment due to spin. We can therefore use the zero field situation as a point of calibration of magnetic coupling energy in devising the magnetic energy diagram. The concept is the same as using the energy of a non-bonding p orbital as a zero of energy and then to consider bonding orbitals as lower in energy than a p orbital and anti-bonding orbitals as higher in energy than a p orbital. Ignoring the exchange interaction is not realistic for many important cases. However, the exchange interaction is Coulombic and not magnetic, so we shall "turn it on" after considering the magnetic interactions.

At zero field the D state may be considered as either an α state or a β state, but we cannot distinguish these magnetic states in an experiment without applying a field. Both states have a well defined angular momentum of precisely 1/2 \ but have no defined value of M_S. Similarly, the T state may be considered

as either a αα, ββ or αβ + βα spin function. All three states have a well defined angular momentum of precisely 1 \, but have no defined value of M_S. The S state is characterized as a αβ - βα state at zero field and possesses a well defind value of zero spin angular momentum. Thus, the T state and S states, although degenerate at zero field, are clearly distinguishable through the total angular momentum label.

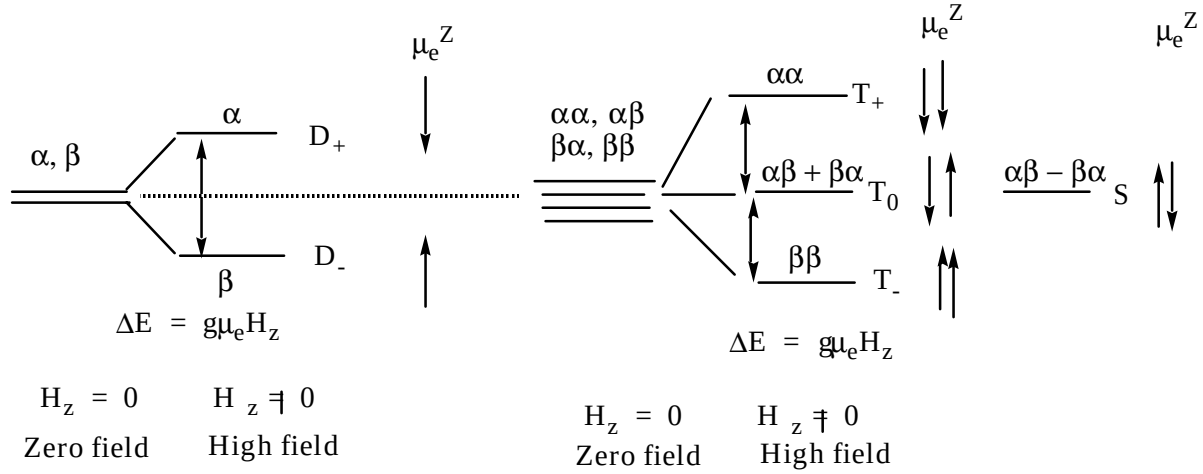

Figure 14. Magnetic energy diagram for a single electron spin and two correlated electron spins.

Thus, at zero field, the magnetic energy diagram for a D, T and S state is quite simple: all the states have the same magnetic energy and that energy corresponds to the zero of magnetic energy. In Figure 14 the degenerate levels are show as being close together and at the energy of zero field. We shall see that even at zero field interactions between spins (electron-electron, electron-nuclear or nuclear-nuclear) can lead to splitting of levels even at zero field.

Magentic Energy Diagram for A Single Electron Spin and Two Coupled Electron Spins. High Field.

Applying an external magnetic field, H_z, removes some of the degeneracies of the D, T and S states through the Zeeman interaction. We now can refer exclusively to the z axis as a reference point, since angular momentum and magnetic moment will be strictly quantized on the z axis. Employing the formula for the quantum magnetic energy of a quantum magnet in a magnetic field of strength H_z (eq. 11), we can readily rank the energies of the levels from knowledge of the value of M_S from eq. 11

$$E_S = g\mu_e H_z M_S \qquad (11)$$

which relates the magnetic energy to the g factor, the inherent magnetic moment of the electron, the field strength and the quantum number for orientation along the z axis. From the formula we have already shown (Table 1) that the β spin state (M_S = -1/2, termed D_-) is lower in energy than the α spin state (M_S = +1/2, termed D_+), remembering that negative values of the magnetic energy are defined as more stable than positive values of the magnetic energy (the magnitudes of g, μ_e and H_z are positive quantities.

The same conclusion concerning the energies of D_- and D_+ is reached by consideration of the physical picture of the spin's magnetic moment in a magnetic field. In Figure 14 the magnetic moments along the z axis(μ_e^z), which determine the observable magnetic enegy diagram, are shown for individual electrons. Since magnetic moments are more stable when they are parallel to a coupling field (Eq. 10), we expect the β spin [$D_-(\ \overline{}\ )H_z(\ \overline{}\ )$] to be lower in energy than the α spin [$D_+(\neg)H_z(\ \overline{}\ )$], since the β spin's magnetic moment is parallel to the direction of H_Z, i.e., it is antiparallel to the direction of its spin angular momentum which is opposed to the magnetic field. The vector representations of the magnetic moments are shown to the right of the energy levels in Figure 14. Thus, from the coupling of magnetic moments shown in Figure 14 we conclude that the D_- state is lower in energy than the D_+ state in a magnetic field, although these two states are degenerate in the absence of a magnetic field.

Similarly, the relative energies of the three levels of the triplet state can be deduced from consideration of the values of M_S or from consideration of the alignment of magnetic moments (Figure 14). We note that the triplet sublevel with M_S = -1 (termed T_-) is lowest in energy, the triplet sublevel with M_S = 0 (termed T_0) possesses 0 magnetic energy on the z axis (the same energy as in the absence of an applied field) and the triplet sublevel with M_S = +1 (termed T_+) is highest in energy. Finally, for two spins the singlet state also possesses M_S = 0 (termed S), possesses 0 magnetic energy on the z axis or on any axis. It is important to note that although the T_0 state possesses a magnetic moment and 1 \ of angular momentum, it possesses zero magnetic moment or angular momentum on the z axis (because M_S = 0). Thus, as far as measurments on the z axis is concerned the S and T states are indistinguishable. This interesting feature will be seen important when we consider intersystem crossing mechanism for S and T interconversions. The same conclusions concerning the relative energies are obtained by consider magnetic moment alignments: $T_-(\neg\neg)H_z(\ \overline{}\ )$ < $T_0(\ \overline{\neg})H_z(\ \overline{}\ )$ < $T_+(\ \overline{\ \ }\ )H_z(\ \overline{}\ )$.

Magnetic Energy Diagrams for Coupling of Electron Spins to Nuclear Spins. Zero Field.

We now consider the magnetic energy diagram for the coupling of a single electron spin (D state) to a magnetic nucleus of spin 1/2. The most important nuclei of organic chemistry either possess spin of zero (^{12}C and ^{16}O) or spin 1/2 (^{1}H and ^{13}C). Either of the latter may be considered as the coupling nucleus in the energy diagrams to be described.

The angular momentum rules for spin coupling are independent of the type of spins (electrons or nuclei) which couple. Thus, when two 1/2 spins couple the possible correlated spin states will be a singlet, S, and a triplet, T, i.e., a single state of spin angular momentum of zero and three states of angular momentum of one, respectively. For both electron electron and electron-nuclear coupling (and even nuclear-nuclear), four spin states are generated, but due to dipolar magnetic interactions, the T state and the S state are not quite degenerate at zero field. In the case of two correlated electrons, the exchange interaction must also be considered.

Consider the states that result from the hyperfine coupling of an electron to a nucleus. Let the labels e and n refer to electron and nuclear spins, respectively. The two correlated states resulting from the coupling be termed T_{en} (electron-nuclear) state and S_{en} (electron-nuclear) state. The magnetic energy splitting of the T_{en} and S_{en} is equal in energy to the hyperfine coupling, a (Figure 15). The hyperfine spitting (a) due to electron-nuclear spin coupling is analogous to the exchange splitting (J) due to electron-electron exchange. However, J is distant dependent whereas hyperfine couplings are usually distant independent and dependent only on molecular structure.

Magnetic Energy Diagrams for Coupling of Electron Spins to Nuclear Spins. Strong Field.

Let α_n be the spin function for the nuclear spin state with angular moment vector pointing in the positive direction of the z axis and let β_n be the spin function for the nuclear spin state with the angular momentum vector pointing in the negative direction of the z axis (this the case for the proton and the ^{13}C nucleus, for which the angular momentum and magnetic moment vectors point in the same direction). Let the subscript e will refer to the analogous electron spin function, α_e and β_e, respectively. In a strong field the S_{en} state ($\alpha_e\beta_n - \beta_e\alpha_n$) and the three T_{en} states ($\alpha_e\alpha_n$, $\alpha_e\beta_n + \beta_e\alpha_n$, and $\beta_e\beta_n$) split into four magnetic levels as shown in Figure 15. The relative energy rankings are readily understood in terms of the magnetic energy of the coupled electron and nuclear

magnetic moments in the strong external field. Since μ_e is roughly 1000 times that of μ_n (recall than $\gamma_e >>> \gamma_n$), and since the strong field is defined as one that is much stronger than the internal (hyperfine interaction) the two levels corresponding to μ_e being parallel to the field (D_-, $M_S = -1/2$, α_e) are much lower in energy than the two levels corresponding to μ_e being antiparallel to the field (D_+, $M_S = +1/2$, β_e). Because the system is in a strong field it is now convenient to classify the states in terms of the individual spins on the z axis. According to the coorelation diagram (Figure 15), the three low field T_{en} states correlate to $\alpha_e\alpha_n$ ($D_+\alpha_n$), $\alpha_e\beta_n$ ($D_+\beta_n$) and $\beta_e\alpha_n$ ($D_-\alpha_n$) states at high field and the low field S_{en} state correlates with the $\beta_e\beta_n$ ($D_-\alpha_n$) state at high field.

The relative energies of the four states at high field are also readily deduced from consideration of the energies of interaction of the electron and nuclear magnetic moments of each state. Within the pair of α_ε levels, one possesses a magnetic moment orientation that is parallel to that of the electron and a magnetic moment orientation that is antiparallel to that of the electron. The lower energy state corresponds to the situation for which the magnetic moments are parallel, i.e., $\beta_e(\ )\alpha_n(\ )$ is lower in energy than $\beta_e(\ )\beta_n(\neg)$. Similarly, for the higher energy pair of levels with α_e, the level $\alpha_e(\neg)\beta_n(\neg)$ is lower in energy than the level $\alpha_e(\neg)\alpha_n(\ )$. Thus, the final energy ranking is $\beta_e(\ )\alpha_n(\ ) < \beta_e(\ )\beta_n(\neg) << \alpha_e(\neg)\beta_n(\neg) < \alpha_e(\neg)\alpha_n(\ )$.

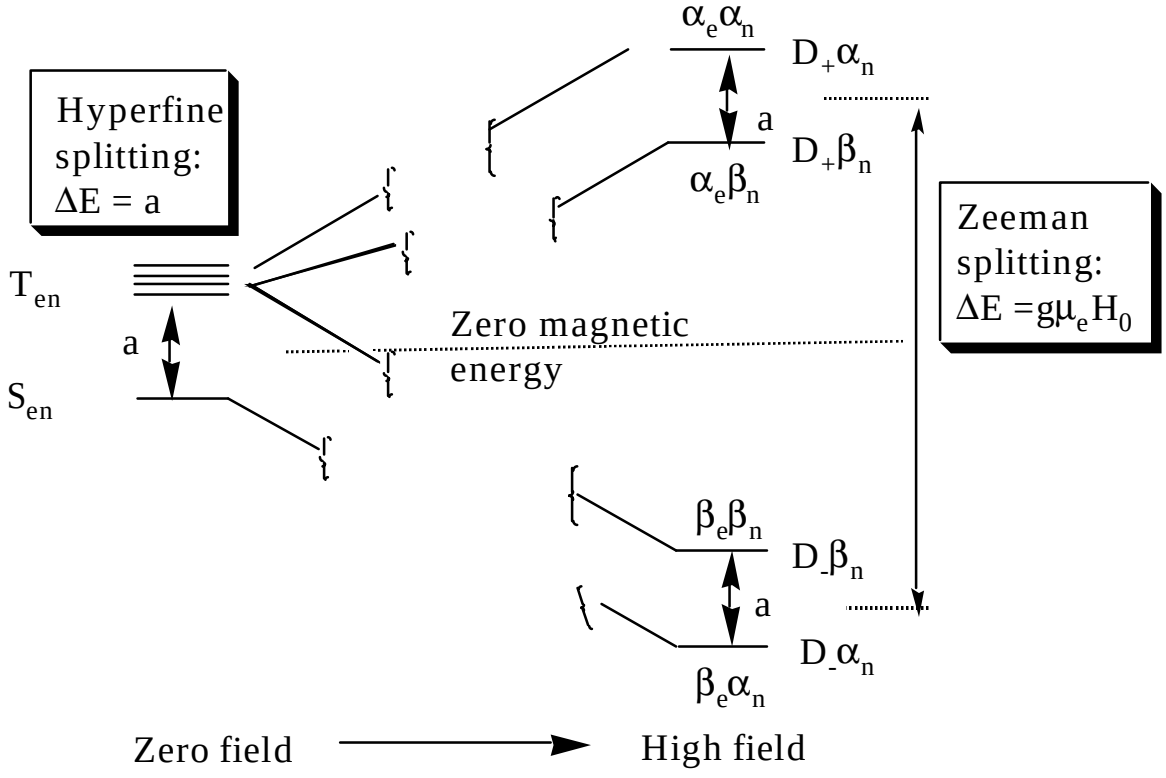

Figure 15. Energy Diagram for the coupling of an electron spin to a nuclear spin 1/2 (e.g., a proton or a ^{13}C nucleus).

Magnetic Energy Diagrams for Two Corrlated Electron Spins and a Third (Nuclear or Electron) Spin. Zero Field.

We now consider two important cases of the coupling of two correlated electron spins (S and T) with a third spin, either that of a third electron or a nucleus of spin 1/2. In zero field the coupling of a S state with a spin 1/2 particle can only lead to one final angular momentum state with a net spin of 1/2 \, i.e, a doublet state, D. The coupling of a T state with a spin 1/2 particle can lead to two possible states: a quartet state, Q, of spin 3/2 \ and and a doublet state, D, 1/2 \. Thus, there are four possible states involved when two correlated electron spins couple with a third spin: S, T, D and Q. As a specific example we consider coupling with a nuclear spin because we wish to emphasize the couplings which cause the important triplet singlet intersystem crossings. Furthermore, the vector model of a nuclear spin coupling is readily extended to other magnetic couplings (spin orbit, spin lattice, etc.) which induce intersystem crossing.

Magnetic Energy Diagrams for Two Corrlated Electron Spins and a Third (Nuclear or Electron) Spin. High Field.

The magnetic energy diagram for two correlated electron spins (Figure 14, right) in a strong field (and absence of electron exchange) consists of two levels at the zero of magentic energy (T and S), one level at lower energy (T_-) and one at higher energy (T_+). Coupling with a nuclear spin of 1/2 will cause a doubling of each level (Figure 16). In the case of T_- and T_+ the levels are split in energy by the hyperfine interaction, a. Since we want to focus on the correlated electron pair, we shall employ the T, S terminology for the electron pair and employ the spin function symbols, $\alpha_n$and β_n to denote the nuclear spin functions. Using the same magnetic energy arguments as above for the T_- pair, the $T_-(\bar{\ })\alpha_n(\bar{\ })$ level will be lower in energy than $T_-(\bar{\ })\beta_n(\neg)$; for the T_+ pair, the $T_+(\neg\neg)\beta_n(\neg)$ level will be lower in energy than $T_+(\neg\neg)\alpha_n(\bar{\ })$ level. An interesting situation applies to the T_0 and S levels when they are coupled to a nuclear spin: **they are not split in energy**. The reason is that the electron magnetic moment of these levels lies perpendicular to the applied magnetic field direction where as the nuclear magnetic moment lies parallel to the applied magnetic field direction. Thus, the electron and nuclear magnetic moments are perpendicular to each other. Recall that when magentic moments are perpendicular to each other (eq. 10), the magnetic interaction between the moments is zero! Another path to the same conclusion is to note that the magnetic energy in an applied field depends

directly on M_S (eq. 11). Since $M_S = 0$ for both S and T_0, the net magnetic energy of couplings of these states in a magnetic field must be equal to zero.

From these considerations the magnetic energy diagram for the coupling of a correlated pair of electrons and a nuclear spin of 1/2 is constructed and shown in Figure 16.

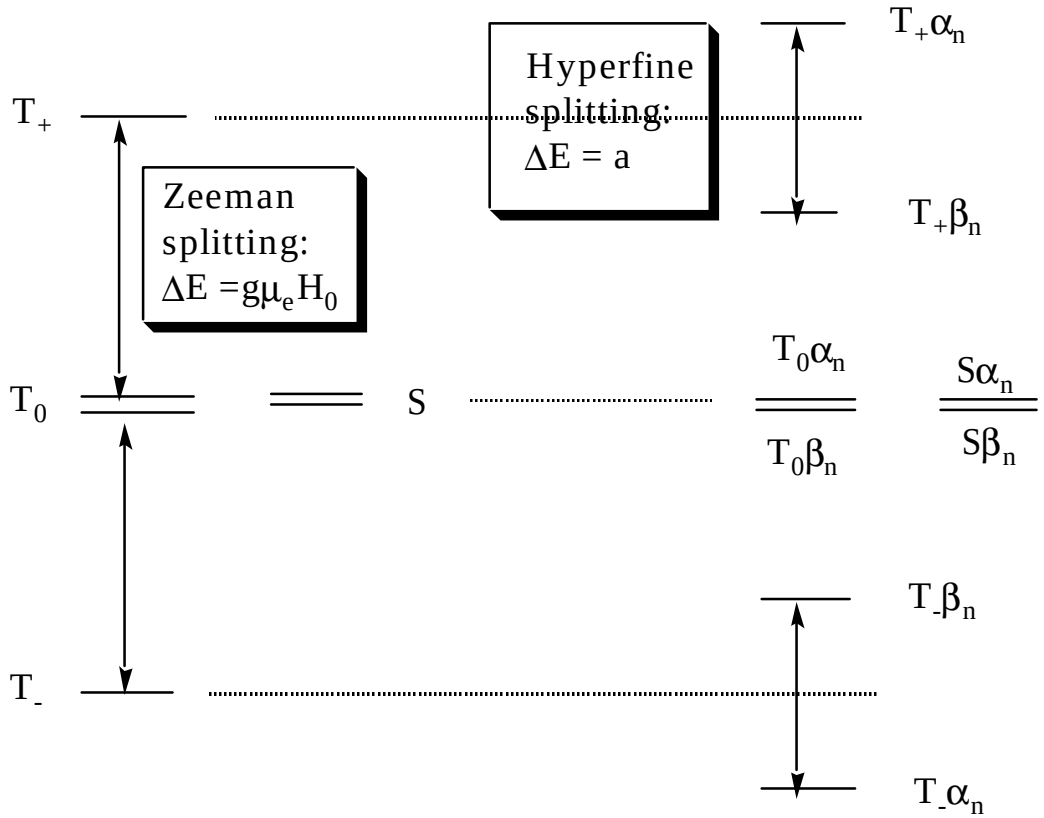

Figure 16. Energy diagram for the interaction of a triplet state and a nuclear spin in a strong magnetic field: left, no hyperfine interaction, right hyperfine interaction turned on.

Magnetic Energy Diagrams Including the Electron Exchange Interaction.

The exchange interaction, J, between two electrons, results in a Coulombic (non-magentic) splitting of the energy of the singlet state from the triplet states. As a result, the energy diagrams shown in Figures 14 and 16 must be modified in the presence of electron exchange. There are four important conditions which are commonly encountered in photochemical systems, two corresponding to zero of low field and two corresponding to high field. The first is the condition for which J = 0 in the presence of a zero (or low) magentic field. Condition I is typical of solvent separated spin correlated geminate pairs and extended biradicals. The second condition is in the presence of zero (or low) magnet field with a finite value of J. Condition II is typical of molecular triplets, spin

correlated pairs in a solvent cage and small biradicals. Condition III occurs at high field for values of J which 0 or are comparable to the Zeeman splitting (i.e., J = 0 or $J \sim g\mu_e H$) and condition IV occurs for values of J which are much larger than the Zeeman splitting (i.e., $J >> g\mu_e H$). these situations will be analyzed in detail in the following sections with a "case history" example.

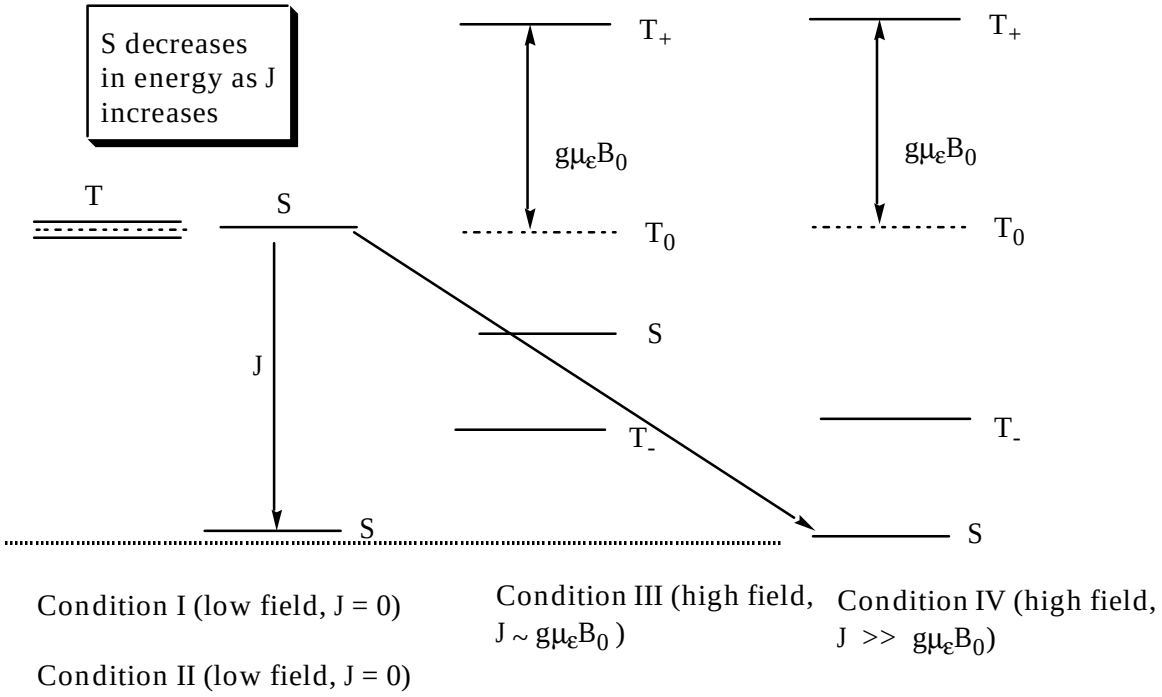

Figure 17. Three important situations of Zeeman splitting and exchange splitting. See text for discusion.

Summary

The magnetic energy diagrams discussed in this section are typical of those encounted in a wide range of photochemical system involving electron spin magnetic resonance (ESR), nuclear magentic resonance (NMR) and intersystem crosssing (ISC). These simple situations capture the critical features required to understand even very complicated situations encountered in practise. We now consider the interactions and couplings which are responsible for ESR, NMR and ISC and presence a concrete example which exemplifies the principles of this chapter.

8. Magnetic Interactions and Magnetic Couplings.

Transitions between the magnetic energy levels discussed in the previous section can be visualized as occuring through the result of magnetic torques exerted on the magnetic moment vectors of an electron spin, or equivalently, as the result of coupling of spin angular momentum to another angular momentum. We shall discuss the magnetic torques as arising from two fundamental magnetic **interactions**: a **dipolar** interaction between magnetic moments and a **contact** interaction between magnetic moments. These arise from some specific source of magnetic moments resulting from the motion of charged particles or spins. The coupling may occur through either a dipolar or contact interaction. In the literature the terms interaction and coupling are used more or less interchangeably. However, we use the term **coupling** to describe the source of the magnetic moment that causes the spin transition.

The vector model allows the dipolar and contact interactions to be visualized in an analogous manner, irrespective of the source of the coupling. In addition, the vector model allows the transitions resulting from the coupling of an electron spin to any magnetic moment to be visualized in an analogous form. These features of the vector model provide a powerful and simplifying tool for discussing magnetic resonance spectroscopy and intersystem crossing through a common conceptual framework.

Couplings of a magnetic field along the z axis.

For example, let us consider the specific example of the intersystem crossing of a T_0 state to a degernate S state or vice-versa (Figure 18, top). On the left and right of the figure the two spins are represented as "tightly" coupled to each other by electron exchange by showing their precessional cones in contactat a common point. For intersystem crossing to occur, the electron exchange coupling must decrease to a value comparable to that of magnetic torques capable of acting on one of the spin vectors, say S_2. This is indicated by showing the spin vectors separated by a line to indicate a "weakening" of the exchange interaction (for example due to separation of the doublet centers in a radical pair or biradical). To cause ISC a coupling is required with a magnetic moment from some source that is capable of interacting with S_2 via a dipolar or contact interaction. As shown the interaction occurs along the z axis and does not cause a reorientation of S_2, i.e., does not "flip" the vector S_2, but rephases S_1 relative to the vector S_1. We may therefore consider the torques as a magnetic field along the z axis which couples spectifically with S_2.

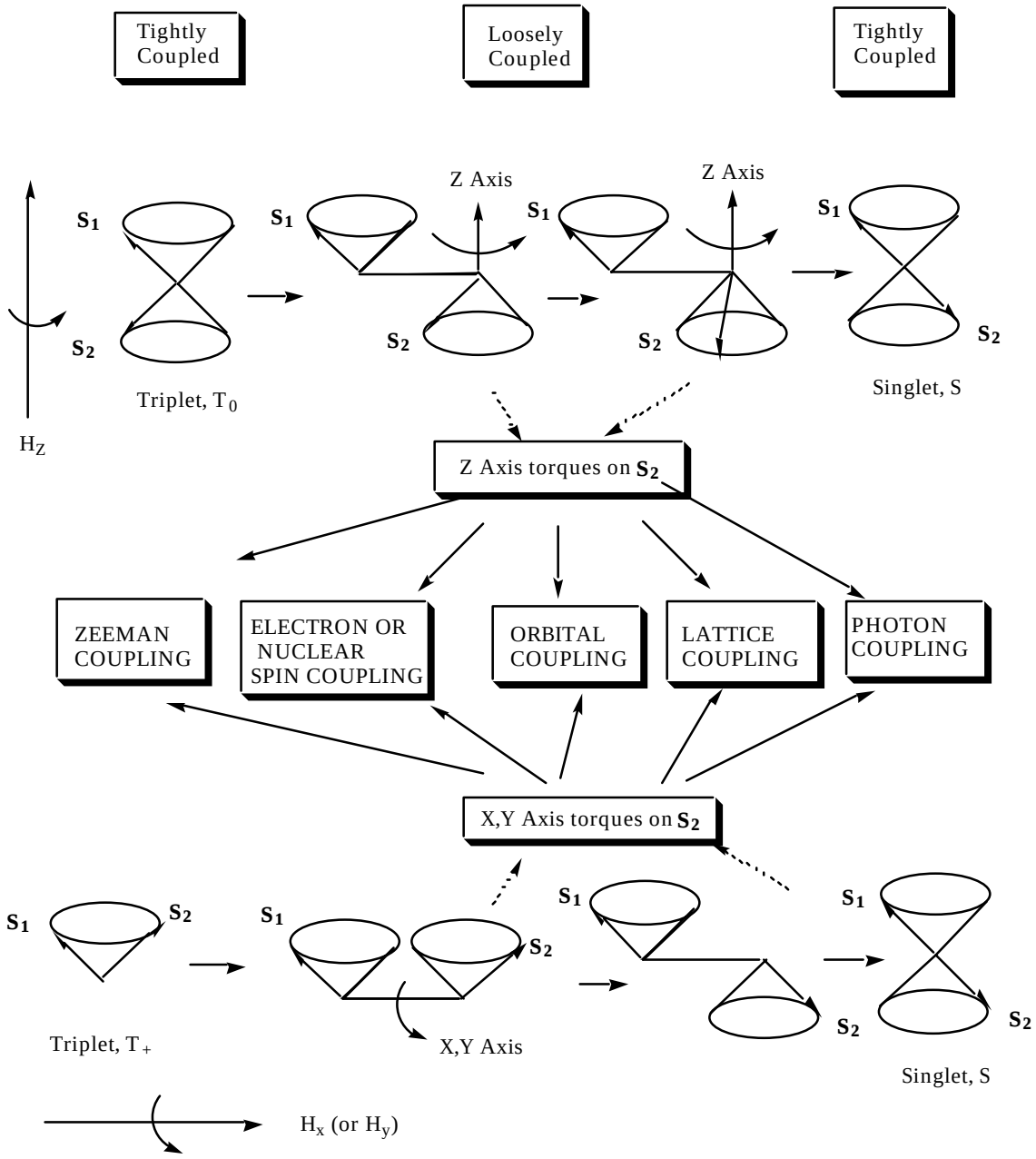

Figure 18. Example of magnetic couplings causing a triplet to singlet (or singlet to triplet transition. The torque on spin S_2 may result from the coupling of the magnetic moment of S_2 with magnetic moments due to any one of a numbers of sources as indicated in the figure.

The situation may be generalized as follows. An electron spin will tend to precess about another electron spin through the exchange interaction or about the magnetic moment produced by some external or internal source. The precessional motion due to exchange must be diminished to a value comparable with or smaller than the magnetic coupling if a transition is to occur. The coupled magnet moment may operate along the z axis or along the x or y axis.

The former coupling produces rephasing of the electron spin and the latter produces spin reorientation.

Couplings of a magnetic field along the x (or y) axis.

The influence of a magnetic field along the x axis is equivalent, by symmetry, to that along the y axis. Thus, the precessional motion of a spin vectror along the x axis is equivalent to precessional motion along the y axis. Therefore, we shall discuss only the x axis, recognizing that the discussion applies also to the y axis. Coupling of a magnetic field along the x or y axis leads to precessional motion about that axis in the same way that coupling to the z axis results in precessional motion about the z axis axis. However, coupling to the z axis does not cause a change in the orientation of the spin, only a change in the precessional frequency. In the case of coupling to the x or y axis, the coupling results in a change in the orientation of the electron spin from α to β (or β to α). As the coupling increases in strength, the precessional frequency increases, leading to a faster frequency of reorientation back and forth between the α and β orientations.

Figure 18 (bottom) shows an examplet of a triplet (T_+) to singlet ISC which results from coupling of the S_2 spin to a magnetic field along the x axis, after it has been decoupled from S_1. The magnetic coupling of S_2 to the x axis causes the spin vector to precess about the x axis. This precessional motion continuously reorients the S_2 spin from the α position to the β position.

In the next section we will develop a vector model for concrete visualization of the coupling responsible for the transitions shown in Figure 18 and spin transitions in general. But first we shall consider briefly (1) the two important magnetic interactions that couple spins to other magnetic moments and (2) the important sources of magnetic moments that can couple to the electron spins and induce transitions.

Dipolar and Contact Magnetic Interactions

A magnetic moment is a magentic dipole, i.e., the magnetic moment gives rise to a magnetic field in its vicinity. Whatever the source of the magnetic moment, the interaction of the field with an electron spin generated may be treated one of two mathematical forms: as a dipole-dipole interaction between the magnetic moment of the spin and the second magnetic moment or as a contact interaction between electron spins. We are interested in the energies associated with each of these interactions. We shall investigate the mathematical forms of the two interactions in order to obtain some intuition concerning the magnitude of the interactions as a function of molecular structure.

Dipole-dipole Interaction

Insight to the nature of the magnetic dipole-dipole interaction is available from consideration of the mathematical formulation of the interaction and its interpretation in terms of the vector model. The beauty of the formulation is that its representation provides an identical basis to consider all forms of dipole-dipole interactions. These may be due to electric dipoles interacting (two electric dipoles, an electric dipole and a nuclear dipole or two nuclear dipoles) or to magnetic dipoles interacting (two electron spins, an electron spin and a nuclear spin, two nuclear spins, a spin and a magnetic field, a spin and an orbital magnetic dipole, etc.).

Classically, the dipole-dipole interaction energy depends on the relative orientation of the magnetic moments (consider two bar magnets). To obtain some concrete insight to the dipolar interaction consider the case for which the two magnetic dipoles, μ_1 and μ_2, are held parallel to one another (this is the case for two interacting magnetic dipoles in a strong magnetic field (Figure 19). We can obtain an intuitive feeling for the nature of the dipole-dipole interaction by considering the terms of the dipole-dipole interaction in eq 19. In general, the strength of the interaction is proportional to several factors: (1) the magnitudes of the individual interacting dipoles; (2) the distance separating the interacting dipoles; (3) the orientation of the dipoles relative to one another; and (4) the "spectral overlap" of resonances that satisfy the conservation of angular momentum and energy. In fact, eq. 19 strictly speaking refers to the interaction of two "point" dipoles (if r is large relative to the dipole length, the dipole may be considered a "point" dipole).

$$\text{Dipole-dipole interaction} \propto [(\mu_1\mu_2)/r^3](3\cos^2\theta - 1)(\text{overlap integral}) \qquad (19)$$

The rate of processes involving dipole-dipole interactions is typically proportional to the **square** of the strength of the dipole-dipole interaction. Thus, the field strength falls off as $1/r^3$ but the rate of a process driven by dipolar interactions falls off as $1/r^6$.

The term involving the $3\cos^2\theta - 1$ (Figure 19) is particularly important because of two of its features: (1) for a fixed value of r and interating magnetic moments, this term causes the interaction energy to be highly dependent on the angle θ that the vector r makes with the z axis and (2) the value of this term averages to zero if all angles are represented, i.e., the average value of $\cos^2\theta$ over all space is 1/3. A plot of $y = 3\cos^2\theta - 1$ is shown at the bottom of Figure 19. It is

seen that the values of y are symmetrical about $\alpha = 90^{o}$. It is interesting to note that for values of $\alpha = 54^{o}$ and 144^{o}, the value of y = 0, i.e., for these particular angles, the dipolar interaction disappears even when the

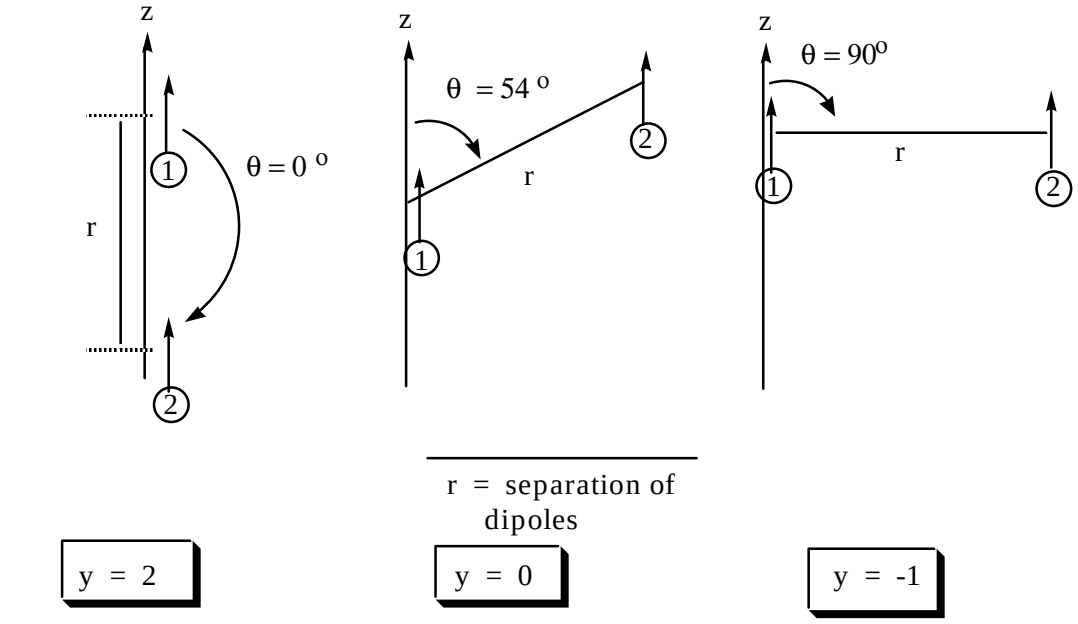

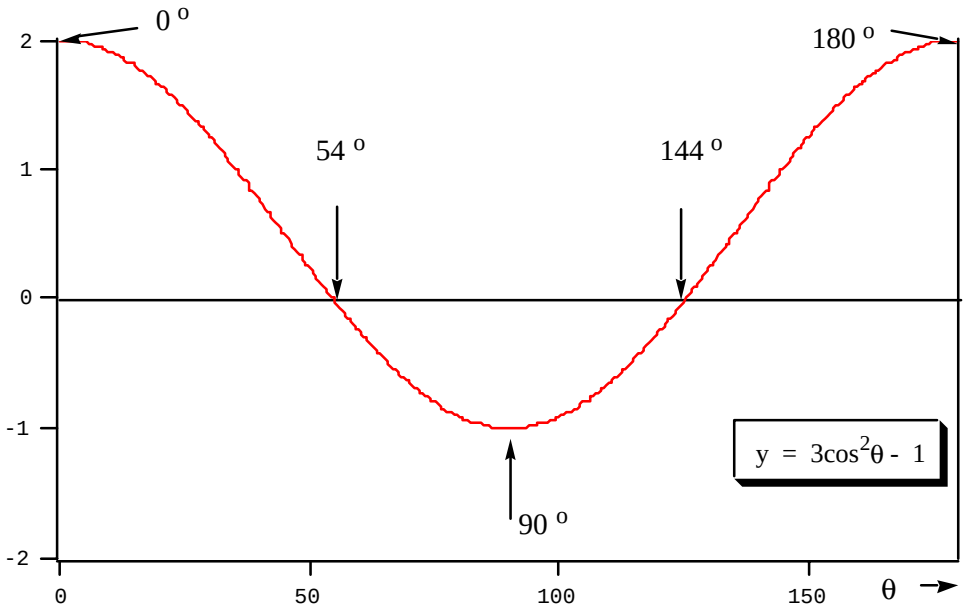

Figure 19. Dipole-dipole interactions of parallel magnetic moments. Top: vector representation of dipoles interacting at a fixed separation, r, and various orientations relative to a z axis. Bottom: plot of the value of $3\cos^2\theta - 1$ as a function of θ.

spins are close in space! This is the familar "magic angle" employed to spin samples in the magnetic field of an NMR spectrometer for removing chemical shifts due to dipolar interactions. It is important to note that certain values of y are positive (magnetic energy raising) and certain values of y are negative (magnetic energy decreasing).

Contact Interaction.

The contact interaction arises when the wave functions for two object overlap in space. The most important cases are (1) the overlap of the electronic wave functions of a spin with the electronic wave function of another spin and (2) the overlap of the electronic wave function of a spin with the electronic wave function of a nucleus. For two electrons in the triplet state the two unpaired electrons are forbidden from "making contact" by the Pauli principle (overlap leads to a triplet singlet splitting, however). However, for an electron and a nucleus, a form of contact is possible and leads to a **hyperfine interaction** between the electron spin and the nuclear spin.

Magnetic interactions can often be well approximated by the dipolar interaction of eq. 19. However, this approximation breaks down when the interacting spins approach and the point dipole approximation is no longer valid. In particular, an electron in an orbital possessing s character has a finite probability of approaching and entering a magnetic nucleus (of, say, a proton). As the electron approaches the nucleus, it brings with it a magnetic moment and discovers that the magnetic field very close to the nucleus is no longer purely dipolar. The interaction of the magnetic moment of the nucleus and the electron spin within the "contact" zone of the nucleus is quite different from the dipolar interaction of the magnetic nucleus and the electron spin when the electron is outside the nucleus. The non-dipolar interaction of an electron spin and the nucleus is termed the **Fermi contact interaction.** For the 1s orbital of a proton, the contact interaction, a, corresponds to an average magnetic field of ca 510 G (ca 1400 x 10^6 Hz) acting on the electron spin. From this simple analysis, we expect that the greater the amount of s character, the larger the value of a, so that there should be a correlation between the value of a and molecular structure. The magnitude of the contact interaction depends on the magnitude of the magnetic moment of the electron, μ_e, and the magnetic moment of the nucleus, μ_p, and the probability of finding the electron at the nucleus, $|\Psi(0)|^2$ (eq. 20).

$$\text{contact interaction} \propto \mu_e \mu_p |\Psi(0)|^2 \qquad (20)$$

Figure 19b shows schematically the dipolar interaction between the electron and the nucleus (left) and the contact interaction between the electron and the nucleus (right).

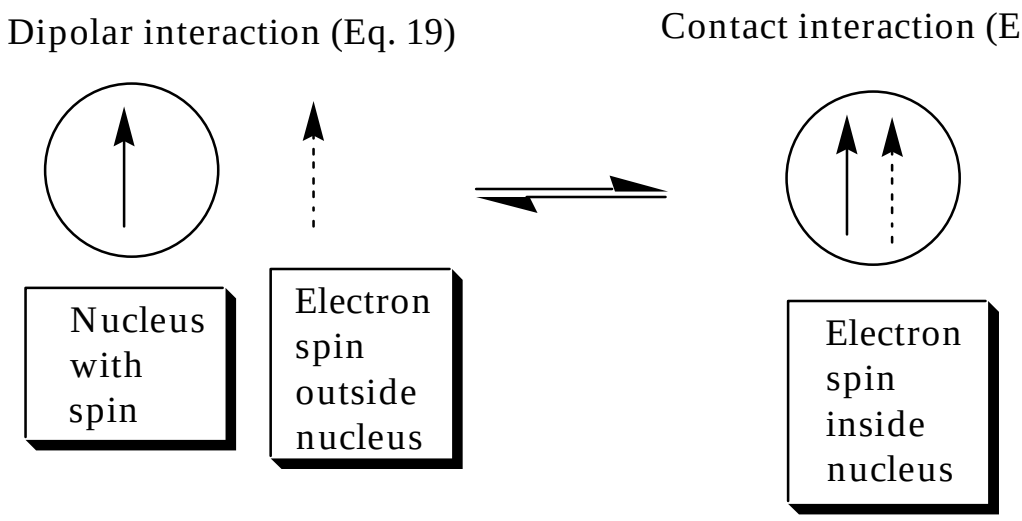

Figure 19b. Schematic representation of the dipolar and contact interactions between electron and nuclear spins responsible for hyperfine coupling.

Because s orbitals are sperically symmetric, the contact interaction does not average to zero as the result of molecular motion, as is the case for the dipolar interaction and that this effect is absent for all other orbitals, because p, d, etc. orbitals possess nodes at the nucleus, so the electron cannot penetrate them. It is also interesting to note that the ideas behind the electron nuclear hyperfine interations are employed to explain the basis of nuclear spin-nuclear spin coupling in NMR.

Couplings of an electron spin with external and internal magnetic fields

The term **external** magnetic coupling refers to applied **laboratory static** or **oscillating** magnetic fields whose strengths and directions can be controlled by the experimenter. The external static fields are those produced by ordinary laboratory magnets. The strengths of the static fields of available laboratory magnets may be varied from 0 gauss (0 Tesla) to over 100,000 gauss (10 Tesla). The external oscillating fields are those produced by electromagnetic radiation. The oscillating fields, in contrast to the static fields, are only effective in interacting with electron spins when the frequency of oscillation is close to, or identical to, the frequency corresponding to the energy gap between two magnetic levels for which a transition is allowed ($\omega = \Delta E$). The strengths, i.e., the intensities (photons / s), of the external oscillating fields may be varied over many orders of magnitude and the frequency of the external oscillating fields may be varied continuously. However, coupling with the magentic moments only occurs when the energy matching condition is met.

The term **internal** magnetic couplings refers to **microscopic static or oscillating** fields whose strengths and directions are due to the electronic and nuclear structures in the vicinity of the electron spin. Whether these couplings are considered static or oscillating depends on the motion and direction magnetic moments in the vicinity of the electron spin. The strengths and frequencies of oscillations of these microscopic fields may vary over many orders of magnitude and are related to the molecular structure and motion of the molecule containing the electron spin and to the molecular structure and motion of the solvent surrounding the electron spin. The most important microscopic magnetic couplings may be classified in terms of the molecular structure in the vicinity of the electron spin as (1) **electron spin-electron orbit** or **spin-orbit** couplings, by which the electron spin experiences magnetic coupling with its own orbital motion (in general the magnetic couplings due to the orbital motion of other electrons is negligible); (2) **electron spin-nuclear spin** or **hyperfine** couplings, by which the electron spin experiences magnetic coupling resulting from nuclear spins; (3) **electron spin-lattice** couplings, by which the electron spin experiences magnetic coupling resulting from the surrounding molecules in the solvent (termed the "lattice" because the origin of the theory of spin-lattice couplings referred to crystal lattices); (4) **electron spin-electron spin** or **electron exchange** couplings, by which an electron spin experiences magnetic coupling resulting from another electron spin.

Coupling mechanisms

In quantum mechanics, a convenient means of classifying the coupling mechanism of an electron spin with other magnetic moments involves the so-called **spin Hamiltonian**. This Hamiltonian contains all of the important magnetic couplings that will influence the energy and therefore the precessional frequency of the electron spin. These couplings of an electron spin vector, $\mathbf{S_1}$, with other magnetic moments are typically of a certain mathematical form given in the followin discussion. These forms have been simplified for the purposes of clarity and are only of qualitative significance. Each may, however, be readily interpreted in terms of the vector model.

(1) A magnetic coupling of the electron spin to the magnetic moment of an applied laboratory field. As we have noted, this **external** coupling is called the **Zeeman** coupling and its contribution to the spin Hamiltonian is $H_Z = g\mu_e \mathbf{H_z} \cdot \mathbf{S_1}$, , where g is the g factor (dimensionless units) for the electron, μ_e is the magnetic moment of the electron in a molecule, H_0 is the strength of the applied laboratory magnetic field and S_z is the value of the angular momentum in the direction of the applied field.. This coupling has the same form if the source is an internal field applied along the z axis, except that the source of the value of the coupling strenght is that of the internal coupling.

(2) The magnetic coupling of the electron spin to the magnetic moment of another electron spin, $\mathbf{S_2}$. This **internal** coupling is called the **spin-spin dipolar fine** coupling and its contribution to the spin Hamiltonian is $H_{DP} = D_e\mathbf{S_1}\cdot\mathbf{S_2}$. The dipolar interaction, as discussed above, averages to zero if the spin system tumbles rapidly because all dipolar interactions averages to 0 for rapidly tumbling systems.

(3) The magnetic coupling of the electron spin to the magnetic moment of a nuclear spin, **I**. This **internal** coupling is called the **spin-nuclear hyperfine** coupling and its contribution to the spin Hamiltonian is $H_{HF} = a\mathbf{S_1}\cdot\mathbf{I}$. There may be a dipolar contribution or contact interaction leading to hyperfine coupling, although in solution the dipolar interaction usually averages to 0 because of rapid tumbling. The major contribution to a for radicals in solution is usually the Fermi contact interaction, which depends on the amount of s character in the orbital containing the unpaired electron. This interaction is distance independent, since the electron and nucleus are in the same radical.

(4) The magnetic coupling of the electron spin to the magnetic moment due to orbital motion of the electron, **L**. This **internal** coupling is called **spin-orbit** coupling and it contribution to the spin Hamiltonian is $H_{SO} = \zeta\mathbf{S_1}\cdot\mathbf{L}$. This coupling depends on overlap of the orbital involving the unpaired spin with other orbitals and is distance dependent for radical pairs and biradicals, but distance independent for molecular triplets and individual radicals.

We note that each term in the Hamiltonian is of the form $H_B = k\mathbf{S_1}\cdot\mathbf{X}$, where k represents a constant which is a measure of the strengths of the magnetic couplings and $\mathbf{S_1}\cdot\mathbf{X}$ represents the vector coupling of the magnetic moments.

In addition to these interactions, the electron spin can also experience a magnetic coupling to the oscillating magnetic fields resulting from molecular motions of the environment. This coupling is called **spin-lattice coupling** and its contribution to the Hamiltonian is mainly in causing transitions between spin states. The magnetic coupling of the electron spin to the fluctuating magnetic moment due to fluctuating magnetic fields due to random motion of molecules in the vicinity of $\mathbf{S_1}$. The frequency of these fluctuations and the intensity of the fluctuation at any given frequency determine the extent of the coupling. Spin-lattice coupling is not strictly expressable in an analogous form to the other internal couplings. However, to a rough approximation this term can be expressed as $H_{SL} = \mathbf{S_1}\cdot\boldsymbol{\rho}_L$, where $\boldsymbol{\rho}_L$ is the "spectral density" of frequencies in the

environment (lattice) that are at the Larmor frequency of $\mathbf{S_1}$ and therefore capable of coupling to the spin.

Finally, the electron spin is influenced by the oscillating magnetic field associated with an electromagnetic field and is termed **spin-photon coupling**. This coupling is responsible for radiative transitions between magnetic states. To a rough approximation this coupling can be expressed as $H_{\backslash\nu} = \mathbf{S_1}\cdot\rho_{\backslash\nu}$

The Electron Exchange Interaction.

The exchange of electrons is a non-classical effect resulting in a splitting of singlet and triplet states as discussed in the previous section as responsible for splitting the singlet state from triplet states. The form of J in a spin Hamiltonian is given by eq. 21. The splitting energy is defined as 2J (a splitting of J above and below the energy corresponding to no exchange). The sign of J may be positive or negative, but in most cases of interest it is negative. In these cases, the singlet state is lower in energy than the triplet.

$$H_{ex} = J\mathbf{S}_1\cdot\mathbf{S}_2. \qquad (21)$$

Although electron exchange is a Coulombic (electrostatic) effect and not a magnetic effect, it influences magnetic couplings in two important ways: (1) the exchange interaction causes the singlet and triplet states to be different in energy; and (2) for the two electrons in a strong exchange situation the spins are tightly electrostatically coupled to each other. When the energy gap, J, is much larger than available magnetic energy, singlet triplet interconversions are said to be "quenched" by J. In addition, since exchange electrostatically correlates the motions of electrons and electron spins, this tight coupling makes it difficult for magnetic couplings to operate on either of the spins and cause intersystem crossing. In this case we view the two spin vectors to be precessing about each other to produce a resultant and it is not longer meaningful to think of the individual spins as components!

The magnitude of J depends on the "contact" region of orbital overlap of the electron spins. This overlap region of two orbitals is usually well approximated as an exponential function such as eq. 22, where J_0 is a parameter which depends on the orbitals and R is the separation of the orbitals in space.

$$J = J_0e^{-R} \qquad (22)$$

Vector Representation of Coupling.

Although there are many different magnetic couplings that can influence the energy levels associated with an electron spin and its transitions, **in each case the specific case of interest can be analyzed in terms of the vector model and the cylindrical symmetry of a coordinate system for which the z axis is the symmetry axis of the cylinder.** In this coordinate system, magnetic interactions along the z axis are effectively **static** and magnetic interactions along the x and y axes are effectively **oscillating.** This means that the magnetic field in the z direction (termed H_z) is static and the magnetic field in the x or y direction (termed H_x or $H_{y)}$ is oscillating.

The essence of understanding the transitions between magnetic states is relating molecular structure and dynamics to the magnitudes of H_z and H_x (H_y), and to the frequency of oscillation of H_x (H_y). We will now attempt to relate the external and internal magnetic interactions operating on the electron spin to molecular structure.

9. Transitions between Magnetic Levels Spin Transitions Between Spin States. Conservation of Spin Angular Momentum

From the magnetic energy diagram derived in the previous sections (Figures 14, 15 and 16), the **possible** magnet transitions are deduced by inspection. They are simply the transitions between any two levels which obey the law of conservation of energy. From this point of view, radiative transitions are possible only for states which differ in energy, since an energy gap is needed to balance the energy absrobed or emitted by a photon. Radiationless transitions are possible only between states which are degenerate or for which there is some source of themal energy to obey the energy conservation law in detail.

However, we now ask which of the possible transitions are plausible, even if energy is conserved. We can deduce the **plausible** transitions between spin states by considering the rules of conservation of angular momentum. The conservation of spin angular momentum defines the plausible transitions as those for which spin angular momentum is preserved during the transition. In general, the total angular momentum and the angular momentum on the z axis must be preserved in any transition between spin states. In addition, of course, energy must be concerved.

Vector Model for Transitions between Magnetic States. Visualization of the Transitions.

The dominant selection rule for plausibility of transitions is that under ordinary circumstances, the spin remains unchanged or will change by one unit of angular momentum, with this change being exactly compensated by an equal and opposite change of angular momentum (not necessarily spin!) as the result of spin coupling. For example, a photon possesses an angular momentum of 1 \, so it can couple to an electron spin and induce any of the plausible transitions for which the spin changes by one unit. This process for conservation of angular momentumis the basis of the rule that for raditive transitions the change in spin must be exactly 1 \. As another example, a proton or a ^{13}C nucleus possesses an angular momentum of 1/2 \, so hyperfine coupling with these nuclei can induce any of the plausible transitions if the change in the nuclear spin angular momentum is exactly the same as the change in the electron spin angular momentum. Similarly, spin-orbit coupling or spin-lattice coupling or couping with an electron spin can induce the plausible transitions.

We now consider the vector description of the magnetic transitions that are important for photochemistry. If the transitions occur radiatively, we are dealing with the field of **magnetic resonance spectroscopy**; if they occur radiationlessly, we are dealing with the field of **magnetic relaxation**. The vector description does not concern itself with the type of magnetic interaction or coupling which causes the transition, so that we can use a general description referring to a transition of a magnetic system involving a single spin ($D \times D$) or two spins ($S \times T$ and $T \times T$).

Coupling of a Single Spin to Another Source of Angular Momentum

Let us first consider the simplest case for the coupling of a single electron spin, $\mathbf{S_1}$ with some other, unspecified source of angular momentum, $\mathbf{H_i}$. The latter is a vector quantity and therefore can be viewed as coupling effectively with $\mathbf{S}_1$ under the proper conditions. What are the proper conditions? The proper conditions are identical for all effective magnetic couplings: (1) the magnetic moment of $\mathbf{S_1}$ must interact with the magnetic moment of $\mathbf{H}_i$ through either the dipolar interaction or the contact interaction and the two vectors must be possess identical Larmor frequencies and phases; (2) the strength of the magnetic coupling between $\mathbf{S_1}$ and $\mathbf{H_i}$ must be greater than the coupling of $\mathbf{S_1}$ to other magentic moments.

Figure 20 shows the process of the coupling of $\mathbf{S_1}$ to $\mathbf{H_i}$ schematically. In the example, the spin function of $\mathbf{S_1}$ (shown as a solid vector) is taken to be α and the orientation of the angular momentum $\mathbf{H_i}$ (shown as an open vector) is taken to be opposite to that of $\mathbf{S_1}$. Since the source of $\mathbf{H_i}$ is not specified, it need not be an electron or nuclear spin and therefore strictly speaking, we should not use the terms α or β (which is reserved for spin functions) to describe $\mathbf{H_i}$ for the general case. However, for clarity we shall use these terms, since the concrete example of coupled spins follows exactly the same principles as any other magnetic couplings. Returning to Figure 20 (left, top), we start by imagining that $\mathbf{S_1}$ and $\mathbf{H_i}$ are positioned in cones or orientation, but are uncoupled. We then couple the two vectors to generate a resultant. If $\mathbf{H_i}$ were a spin 1/2 particle, coupling could produce a final angular momentum state of 0 (singlet, S) or 1 (triplet, T). The triplet coupling is shown in the example. We now imagine that the coupling between $\mathbf{S_1}$ and $\mathbf{H_i}$ is stronger than that of any other source of angular momentum available to $\mathbf{S_1}$. The result of this strong coupling is the the precession of the $\mathbf{S_1}$ and $\mathbf{H_i}$ about their resultant (Figure 20, top right). This precessional motion causes $\mathbf{S_1}$ to "flip" cyclically between the α and β orientations (Figure 20, middle) which we term $\mathbf{S_1}^{\alpha}$ and $\mathbf{S_1}^{\beta}$. This spin flip corresponds to the application of a magnetic field along the x or y axis. Increasing the strength of the coupling along the z axis (Figure 20, bottom) increases the frequency of oscillation (Larmor frequency) but produces no tendancy for reorientation of the spin.

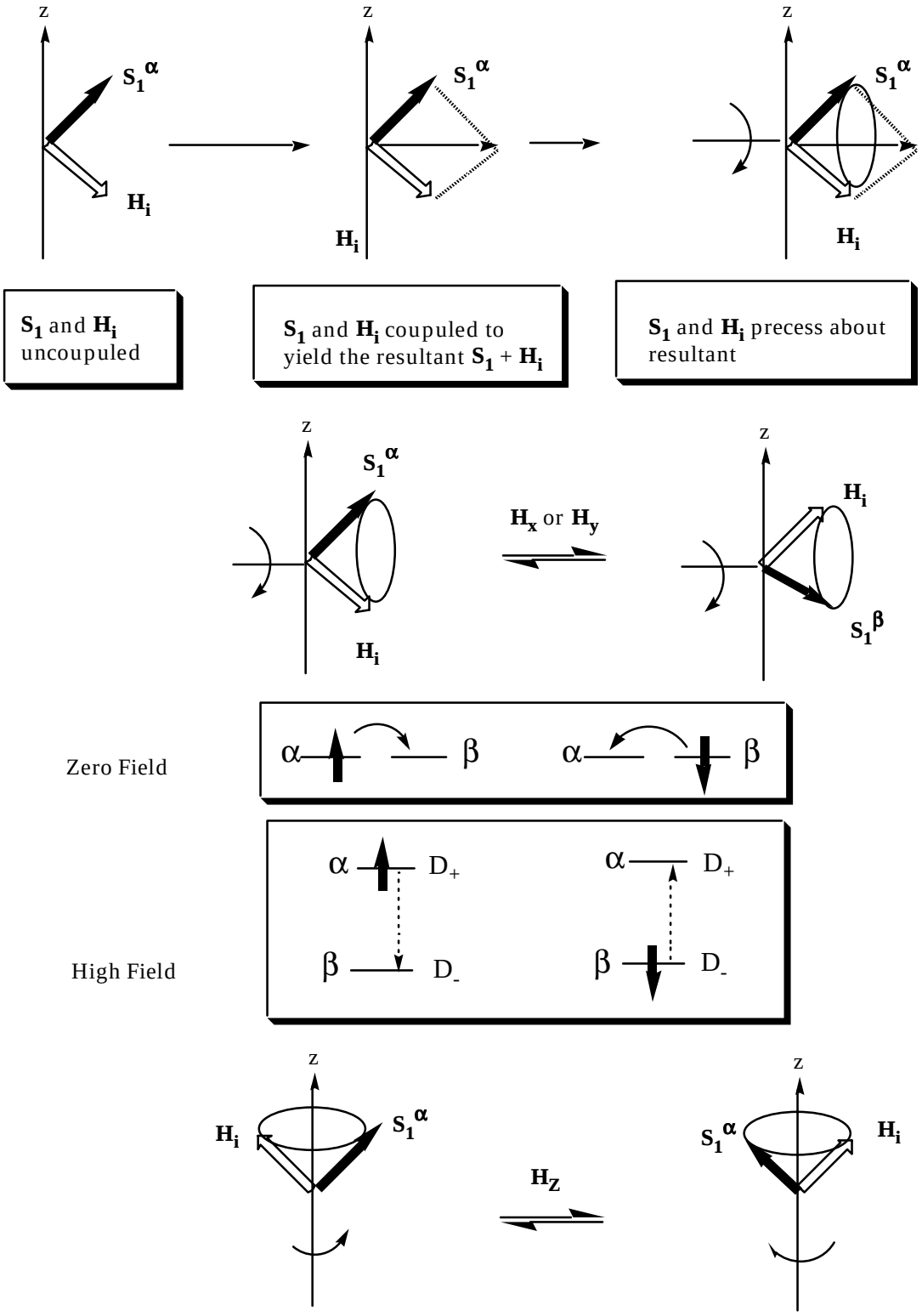

Figure 21. Vectro representation of transitions of a single coupled electron spin, $\mathbf{S_1}$. See text for discussion.

At zero field the conversion of $\mathbf{S_1}^{\alpha}$ to $\mathbf{S_1}^{\beta}$ occurs at approximately the Larmor frequency, ω, which is directly related to the strength of the coupling of $\mathbf{S_1}$ to $\mathbf{H_i}$ (Eq. 15). At high applied field the two states $\mathbf{S_1}^{\alpha}$ and $\mathbf{S_1}^{\beta}$ have different energies because of the Zeeman splitting. As a result, the interconversion of $\mathbf{S_1}^{\alpha}$ to $\mathbf{S_1}^{\beta}$ is "quenched" unless energy is conserved. In a radiative process, energy is conserved by coupling the oscillating magnetic moment of the electromagnetic field which possesses the correct frequency and phase for the transition. In the case of radiative transitions, energy is conserved precisely by the energy of the absorbed or emitted photon, i.e., $\Delta E = h\nu$, where ν is the frequency required to achieve resonance.

In the case of radicationless transitions if the states undergoing transition are not exactly degenerate, then the magnetic energy gap must be made up by coupling with a "third" body. The larger the energy gap the more difficult becomes effective coupling and the transition becomes implaulsible. The energy conserving process for the radiationless transition is accomplished by coupling the transition to the oscillating magnetic field produced by the environment such as the molecules of a solvent. This process is viewed as a magnetic energy transfer between the spin system undergoing transition and some magnetic moments that are oscillating at the correct frequency in the solvent (the oscillating magnetic species are termed the "lattice"). To maiontain energy conservation, the lattice may provide energy or absorb energy and can therefore assist in both absorptive or emissive transitions. With this description fo the lattice we can imagine that the oscillating magnetic moments behave just like the oscillating magnetic field of electromagnetic radiation. Instead of photons, the lattice provides "phonons" to the spin system. The lattice thus behaves analogously to a lamp that emits magnetic phonons or an absorber of magnetic phonons. The overall process is termed **spin-lattice magnetic relaxation** and is simply magnetic energy transfer between spin states. The most important interaction which couples the electron spin to the lattice is usually dipolar. This interaction has exactly the same mathematical form as Förster electronic energy transfer discussed in Chapter XX.

Coupling Involving Two Correlated Spins. $T_+ \varnothing S$ and $T_- \varnothing S$ Transitions.

The visualization of a single spin coupled to a second spin (or any other generalized magnetic moment) is readily extended infigure 21 to the visualization of two correlated spins coupled to a third spin (or any other generalized magnetic moment). In Figure 21 (upper left) two electron spins, $\mathbf{S_1}$ and $\mathbf{S_2}$ are shown as correlated in the T_+ state (the correlation is indicated by showing the resultant vector produced by coupling and precession about the resultant). Now we suppose that a third spin, either an electron spin or a nuclear spin (represented as $\mathbf{H_i}$ in the Figure) is capable of coupling specifically to the spin $\mathbf{S_2}$ (shown in the middle top of Figure 21 in terms of a new resultant and precession about the resultant). As for the single coupled spin in Figure 20, the coupling of $\mathbf{S_2}$ to $\mathbf{H_i}$ causes $\mathbf{S_2}$ to precess about the x or y axis and the α and β orientations. From the vector diagram it is readily seen that this oscillation produced by coupling of $\mathbf{S_2}$ and $\mathbf{H_i}$ causes triplet (T_+) to singlet (S) intersystem crossing.

At zero field the three T sublevels are usually strongly mixed by dipolar interactions between electron spins. Thus, radiationless $T_+ \varnothing$ S ISC is plausible and will depend on the strength of the coupling between $\mathbf{S_2}$ and $\mathbf{H_i}$ and the strength of the exchange interaction. For simplicity, in Figure 21 (bottom) we assume that J = 0. There is no radiative transitions between T and S possible at zero field because there is no energy gap between the states.

At high field the $T_+ \varnothing$ S ISC transition is not plausible by aradiationless pathways. The radiationless pathway is inefficient because it requires some source of magnetic energy conservation by coupling with the lattice. The plausibility of a radiative $T_+ \varnothing$ S transition depends on the relative coupling of the electron spins to one another (value of J) and to the radiative field. If the value of J is very small, the individual spins behave more or less independently so that radiative transitions of each spin ("doublet" transitions) become plausible. The vector diagram for the $T_- \varnothing$ S transition is readily constructed from the symmetry relationships of the T_- vector representation to that of the T_+ vector representation.

Coupling Involving Two Correlated Spins. $T_0 \varnothing$ S Transitions.

As for a single spin, it is also posssible for $\mathbf{H_i}$ to operate on correlated electron spins along the z axis. This situation is shown in Figure 22 for an initial T_0 state. Again under the assumption that J = 0, rephasing along the z axis occurs is if $\mathbf{H_i}$ is coupled selectively to one of the electron spins (say, $\mathbf{S_1}$). This rephasing causes $T_0 \varnothing$ S ISC at low field or at high field if J = 0.

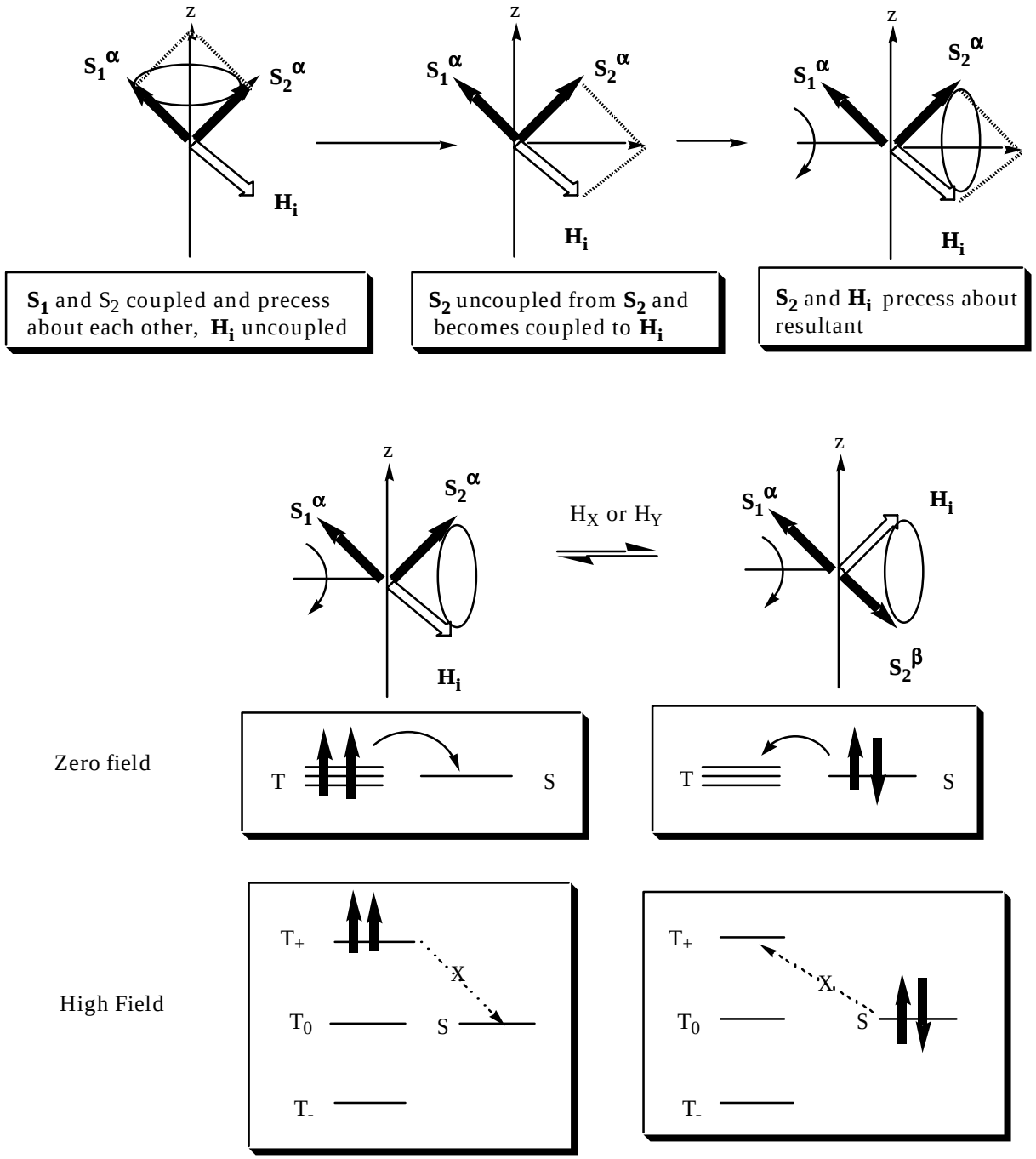

Figure 21. Vector representaion of coupling of two correlated spins with a third spin along the x or y axis. See text for discussion.

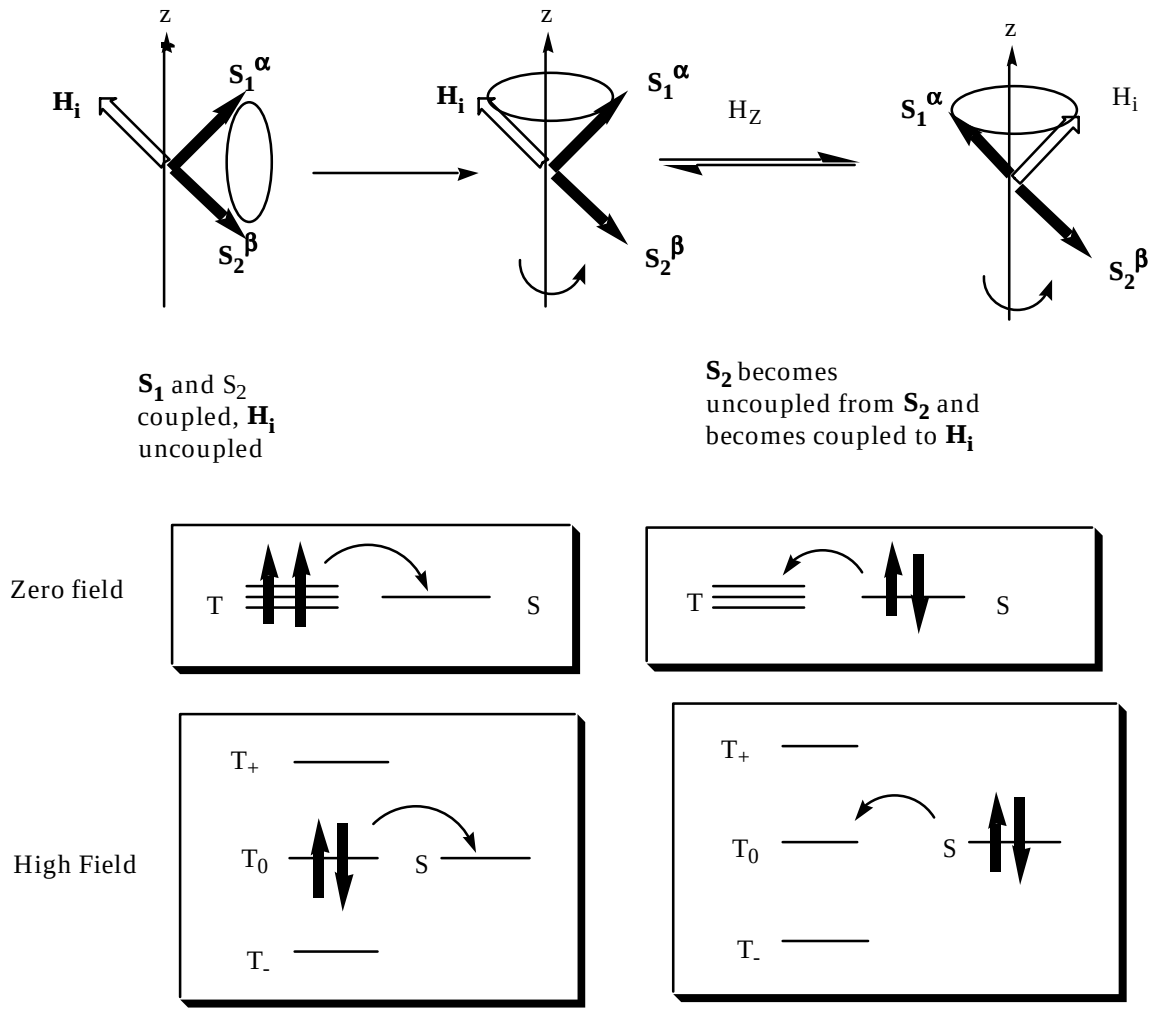

Figure 22. Vector representation of two correlated spins in a T_0 state coupled to a third spin along the z axis. See text for discussion.

10. Magentic Resonance Sectroscopy. The Transition Betweeen Magnetic Dipoles in a Magnetic Field.

Magnetic resonance spectroscopy experiments involve the **radiative transitions** between two magnetic energy levels of a molecule or radical in the presence of an applied laboratory magnetic field. We shall view the theory of magnetic resonance in a relatively primitive manner, but one which should highlight all of the important features of the phenomenon and which should allow a facile transition to an understanding of the features of not only radiative but also radiationless transitions between two magnetic states. The strategy shall be analogous to that employed for the theory of electron spectroscopy, the radiative transitions between electronic states. In order for a radiative transition to be possible between two electronic states, the states must possess an electronic energy difference (ΔE_{el}). In order for a radiative transition to be plausible, the two states must differ in some feature of their orbital structure so that the **oscillating electric field** of the **electro**magnetic field of light can interact with the electrons and drive them into oscillation. For the latter to happen, the frequency of the oscillating electric field, ν, must be such that $\Delta E_{el} = h\nu$. Since the transitions occur only at the frequency ν, we term the phenomenon **electronic resonance** and the technique, electronic (resonance) spectroscopy.

Similarly, in order for a radiative transition to be possible between two magnetic levels or states, the states must possess a magnetic energy difference ΔE_{mag}. In order for a radiative transition between two magnetic states to be plausible, the two states must differ in some feature of their magnetic moments so that the oscillating **magnetic field** of the electro**magnetic** field of light can interact with the magnetic moments and drive them into oscillation. For the latter to happen, the frequency of the oscillating magnetic field, ν, must be such that $\Delta E_{mag} = h\nu$. Since the transitions occur only at the frequency ν, we term the phenomenon magnetic resonance and the technique magnetic resonance spectroscopy. Because of the vector model, we shall move freely between the notion of an light wave oscillating at frequency, ν, and a spin vector precessing at frequency, ω, through the relationships $\Delta E_{mag} = h\nu = \backslash\omega$.

In electronic absorption spectroscopy the light impinges on a sample of randomly reorienting molecules and the light interacts with varying dipole moments to produce electronic transitions, in magnetic resonance spectroscopy, the magnetic moments of electrons and nuclei have definite orientations in space because of the effect of the applied magnetic field. Let us now see how the vector model allow us to visualize radiative transitions between two magnetic states in an applied magnetic field.

The Vector Model for Magnetic Resonance Spectroscopy

We initially consider the simplest cases of magnetic resonance, an electron in the absence of any other electrons or nuclei, i.e., a "free" electron and a proton in the absence of any other nuclei or any electrons, i.e., a "bare" proton. All of the principles are the same for ESR and for NMR. For a proton, as a model for a nuclear spin, the ideas of magnetic resonance are quite analogous. One important difference is that the direction of the spin angular momentum vector of a proton (a positivley charged particle) is in the **same** direction as the magnetic moment vector. This contrasts with the situation for the electron (a negatively charged particle) for which the direction of the angular momentum vector is antiparallel to the magnetic moment vector. Thus, in the case of the proton, although we follow the same rules for energy on the magnetic moment in an applied field, the angular momentum vector pointing in the direction of the field is lower in energy for the proton. The reason for this is that it is the energy of the interaction of the magnetic moment with the applied field that dominates the magnetic energy of the system, and the magnetic energy is generally lower when the magnetic moment vector is parallel to the field. This means that for both a proton and an electron the **lower energy state corresponds to the situation for which the magnetic moment vector is parallel to the applied field**. Following this rule, for the electron the lowest level has the angular momentum vector directed antiparallel to the field (β), but for the proton, the lowest level has the angular momentum vector directed parallel to the field (α). A second important difference is the much larger size of the magnetic moment due to electron spin relative to the magnetic moment for nuclear spin. This factor leads to much smaller Zeeman energy splittings for nuclear spins.

Figure 23 describes the vector model of transitions between magnetic states for a free electron. These transitions are induced by a coupled and oscillating magnetic field, $\mathbf{H_i}$. For radiative transitions, we identify this oscillating magnetic field as that of electromagnetic radiation. Clearly, in order to induce transitions from the α to the β orientations, the oscillating field must be such that it oscillates about the x (or y) axis. We consider some important qualities of photons that are important aspects in visualizing the radiative transitions between magentic levels.

A photon may be viewed as a packet of electromagnetic radiation. The photon possesses a spin angular momentum, $\sigma_{h\nu}$, of 1 \. As a relativistic particle, the spin can have only two projections in space along a selected axis. In the case of a photon, the direction of propagation is the obvious and convenient "z axis". The two possible spin states correspond (Figure 23) to the magnetic vector of electromagnetic radiation moving clockwise around the direction of propagation (spin = 1 \) or counterclockwise around the direction of propagation (spin = -1 \).

These two states of a photon are termed "helicity" states becasuse the tip of the spin vectors trace our a helix as the electromagentic wave propagates in space. The two helicity states in turn correspond to left ($\sigma_{h\nu+} = 1$ \) and right ($\sigma_{h\nu-} = -1$ \) polarized light.

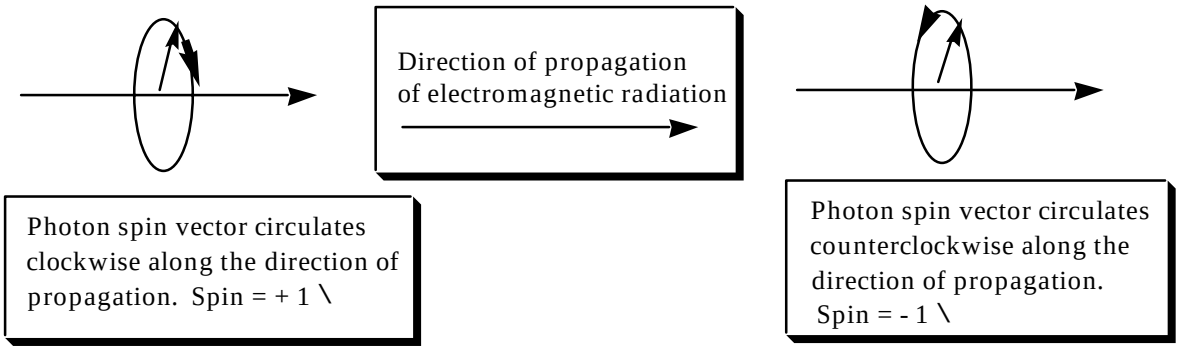

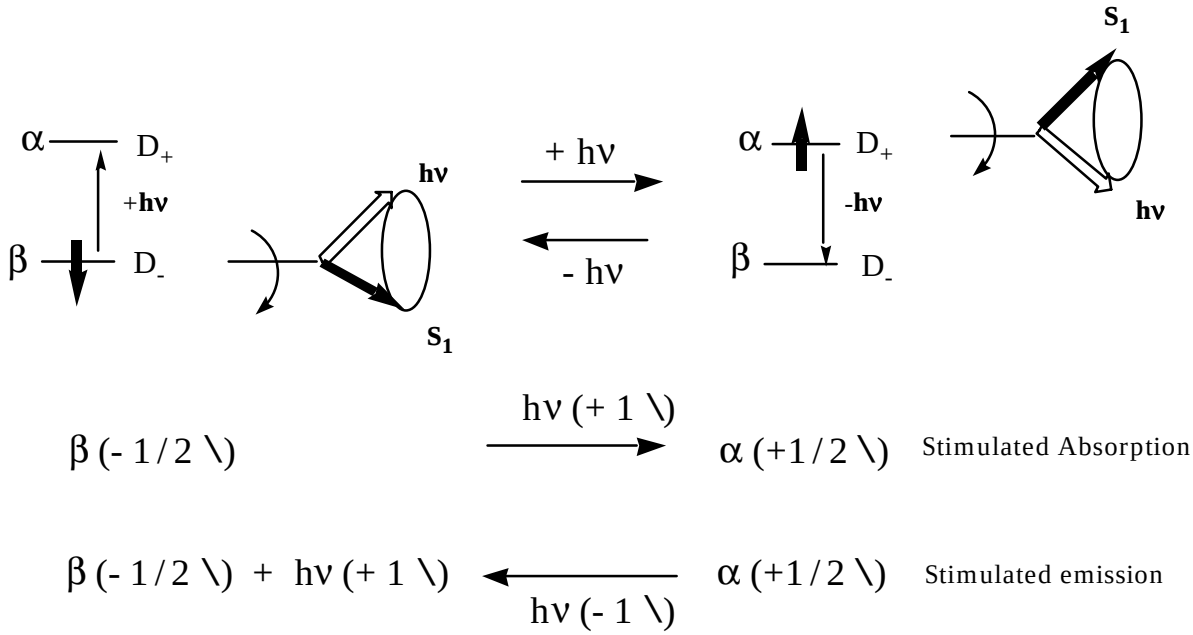

Figure 23. Representation of a photon (top) executing rotation of the magnetic field vecrtor about the direction of propagation of the electromagnetic wave. Representation of the radiative transition (middle) between magnetic energy levels. Equations for the conservation of angular momentum during stimulated radiative transitions (bottom).

Now let us visualize the radiative transition involving the absorption of a photon. Since the photon possess both energy and spin it can couple to en electron spin and supply its spin angular momentum and cause absorption to a

higher energy state, i.e., the $\beta \varnothing \alpha$ transition (Figure 23). Thus, in this case the photon provides the coupling source, the source of conservation of energy and the source of conservation of angular momentum! Althought spontaneous emission between magnetic states is much too slow to compete with other radiationless mechanism of relaxation, a photon can couple with an electron spin and stimulate emission of a photon. This process is shown in Figure 23.

Thus, the vector model represents radiative processes in the same manner as it does the generalized transitions of Figure 20, i.e., the photon's spin is treated in the same manner as a coupling electron spin, or a coupling nuclear spin or any other general coupling magnetic source, $\mathbf{H_i}$.

The absorptive radiative transition from the β state to the α state is analogous to the absorptive radiative transition from one orbital to another. The cones of possible orientation that can contain the spin vector are the analogues of the orbitals that can contain electrons. There are, however, some important differences between electronic transitions and magnetic transitions.

Comparison of Electronic and Magnetic Spectroscopy

Electronic spectroscopy (in the presence or absence of an applied field) involves the jumps of electrons from one orbital to another accompanied by the absorption or emission of a photon. Magnetic resonance spectroscopy (only in an applied magnetic field) involves the reorientation of the magnetic moment of an electron (or a nucleus) accompanied by the absorption or emission of a photon. For consideration of transitions between energy levels the theoretical concepts are completely analogous and we visualize the absorption and emission processes as radiative jumps between energy levels. The conditions for resonance are precisely the same: the photon carries exactly one unit of angular momentum and possesses the energy $\Delta E = h\nu$ so that energy is conserved, angular momentum is conserved and the perturbing interaction of the electromagnetic field possesses the correct resonance frequency and phase.

At a more detailed structural level a number of important differences between electronic and magnetic spectroscopy emerge:

(1) The **interaction** which induces the transition is Coulombic (electrical) in the case of electronic spectroscopy and magnetic in the case of magnetic resonance spectroscopy. This means that the **electrical part** of the electromagnetic wave is the interaction causing electronic orbital jumps, but that it is the **magnetic part** of the electromagnetic wave that causes the reorientation of the magnetic moment. In further detail, the electronic perturbation is visualized as "pushing" or "pulling" electrons along an axis defined by the

molecular structure, whereas the magnetic perturbation is visualized as "twisting" the magnetic moment about an axis defined by the applied field.

(2) The probability of electronic absorption (or emission) depends on the orbitals involved in the transition and the ability of the molecular structure to possess an axis along which the electrons can be induced to oscillate as a result of the orbital transition, since this feature determines the magnitude of the transition dipole which interacts with the electromagnetic wave. The probability of magnetic absorption (or emision) depends on the magnitude of the magnetic moment, which is essentially fixed for an electron or nucleus. As a result the extinction coefficients for electronic absorption is very dependent on molecular structure and vary over orders of magnitude. On the other hand, the extinction coefficients for magnetic absorption are essentially the same for electrons (or a given nucleus) which possess nearly identical magnetic moments. As a result, the probability of magnetic absorption is proportional to the number of magnetic moments (unpaired spins) and is not dependent on molecular structure.

(3) The difference in magnetic energy between the levels involved in the transition are very small compared to electronic transitions. For example, the absorption of electromagnetic radiation in the visible region of the spectrum corresponds to transitions between energy gaps ranging from ca. 40 kcal / mole (red light) to ca. 80 kcal / mole (violet light). On the other hand, the absorption of magnetic energy in an ESR experiment in an applied field of 10,000 G corresponds to an energy gap of about 10^{-3} kcal / mole, the energy of a microwave photon, whereas the absorption of magnetic energy in a NMR experiment involving protons corresponds to transitions between an energy gap of ca. 10^{-5} kcal / mole. For other nuclei the energy gap is even smaller.

(4) The tiny energy gap between magnetic states, even in a strong applied magnetic field leads to an important practical difference between electronic and magnetic spectroscopy. Whereas in electronic spectroscopy the higher energy state is not significantly populated at room temperature, in magnetic spectroscopy the higher energy state is nearly as populated as the lower energy state. Even in a strong magnetic field, there is only a very small difference between the populations of the two states, with the lower state possessing a small excess of population. For example, in an applied field of 10,000 G the populations of the two electronic spin states differ by only 1 part per 100 and the population of the two proton spin states differ by only ca. 1 part per 10,000. This means that in the more favorable case of the electron spin, if one is dealing with an ensemble of 20,001 spins, 10,001 will be in the lower level and 10,000 will be in the upper level!

(5) There are several important consequences of the small energy gap between magnetic levels. The first has to do with the effect on a small energy gap on the rate of spontaneous emission. According to classical theory of spontaneous emission, the rate of such emission is proportional to ν^3. Now, since the rate of spontaneous emission is of the order ot 10^8 s^{-1} for electronic transitions occurring for energies of the order of 20,000 cm^{-1}, the rate of spontaneous radiation is expected to be ca. $(20,000)^3$ or 8×10^{12} times less than emission in the microwave region! In other words the rate of spontaneous emission is of the order of 10^{-4} s^{-1} from one magnetic level to another. This rate is much slower than that for radiationless interconversion of the magnetic states, so that no spontaneous emission is generally observable for transitions between magnetic states. **This means that practically speaking, magnetic spectroscopy has no analog to electronic emission spectroscopy.**

The second important consequence of the small energy gap is indirect and is associated with the nearly equal populations of the two magnetic states and the very slow rate of relaxation of the upper level by radiative or radiationless mechanisms. This consequence is the tendency of the populations of the upper and lower levels to balance exactly after a certain amount of absorption has occurred, i.e., the small excess population of the lower lever is transferred to the upper level by the absorbed photons. When the population of the upper and lower levels are equal, the magnetic system is said to be "saturated" with respect to the absorption of photons. The term means that no **net** absorption of photons will occur because the probability of a photon converting an α spin to a β spin is just as probable as the conversion of a β spin to an α spin. As a result, for each photon that is absorbed to cause a β to α transition, an equally probable stimulated α to β transition occurs so that there is no net absorption of photons. **This means that magnetic absorption spectroscopy is an inherently insensitive technique for measurements at room temperature, because the "effective" transitions leading to the net absorption of photons is proportional to the excess population of spins, which is very small.**

(6) In contrast to electronic spectroscopy, for which the separation of the energy levels do not depend on the strength of the applied field, in magnetic spectroscopy the separation of the energy levels depends directly on the strength of the magnetic field.

Information Avalailable from Magnetic Resonance Spectra

NMR and ESR spectroscopy both provide analogous structural and dynamic information which can be extracted by analysis of the following experimentally observable parameters:

(1) The frequency, ω_i, of the magnetic resonance signal;
(2) The structure of the signal due to an individual spin (or group of equivalent spins);
(3) The shape of the signals;
(4) The intensity of the signals.

We now consider each of these briefly.

The Frequency of an Observed ESR or NMR Signal

Each ESR or NMR signal corresponds to a radiative transition between two magnetic energy levels when the resonance condition is achieved. Thus, for the simplest case of a two level system (Figure 23) each transition can be considered in terms of eq. 23:

$$\Delta E = h\nu = \omega = E_\alpha - E_\beta \qquad (23)$$

The energies E_α and E_β are directly related to the total magnetic field the spins experience and the magnetic moment of the spin. The electron spin being observed in an ESR experiment is always part of a molecule or radical so that it experiences not only the applied field, H_0, but also any other fields arising from magnetic moments that are nearby and interact with the electron spin. Thus, the actual magnetic field at the spin, H_Z, is always a composite of the **exteranl** applied laboratory magnetic field, H_0, and the sum of **internal** fields, $\Sigma\mathbf{H_i}$. The important internal fields are commonly of two types: (1) those due electronic orbital circulations induced by the applied field, H_i and (2) those due to internal field due to the magnetic moments of other spins. In more familiar NMR spectroscopy the first internal field is termed the shielding constant, σ, and leads to the chemical shift, δ, which causes nuclear spins in different chemical environments to undergo resonance at different frequencies (in the presence of a fixed value of an applied laboratory field). In NMR spectroscopy, the second internal field is associated with a spin-spin coupling constant. It is assumed that the reader is familiar with these NMR parameters, so that an analogy can be made with the corresponding ESR parameters.

The basic principles of ESR are as follows. An electron has a magnetic moment $\boldsymbol{\mu}_S = g_e\gamma_e\mathbf{S}$; and in a magnetic field along the z axis (the direction of the magnetic field form south to north pole) the energies of the moment are

restricted to two values, of $g_e\boldsymbol{\mu}_e\mathbf{H}S_z$ where $S_z = 1/2$ and $-1/2$. Thus, the gap between the two energy levels is exactly \, the angular momentum carried by a photon. If the photon possesses the correct energy and frequency, all of the conditions for a transition are in effect. Since $\Delta E = \omega$, when ω is the same as the Larmor frequency, absorption can occur if the photon provides the correct torque to twist it from an α spin to a β spin or *vice versa*, as shown in Figure 23. Experimentally, either the frequency, ν or the magnetic field strength, H_0 is varied until the resonance condition is met (eq. 24). We shall consider the variation of ν because of the close analogy with electronic spectroscopy and because the relationship between the energy gap for the transition and the frequency is direct.

$$\Delta E = h\nu = E_\alpha - E_\beta = g_e\boldsymbol{\mu}\mathbf{H}_0 = \omega \qquad (24)$$

This is the situation for the ESr of a "free electron". In actual experimental systems invovling triplets and radicals, the magnetic currents resulting form orbital circulations induced by the applied field lead to an internal field H_i at an electron spin, just as is the case for a nuclear spin, so that the eq. 24 must be modified to take H_i into account. By convetion, this effect is incorporated in the g-factor as a term that causes a deviation from the g-factor of the free electron (eq. 25), i.e., in the same way that the chemical shift in NMR is defined as the field corresponding to a term σH_0, in ESR, the deviation is considered to be due to a term $g_i H_0$.

$$\Delta E = h\nu = \omega = E_\alpha - E_\beta = g\mu_e H_0 = (g_e + g_i)\mu_e H_0 \qquad (25)$$

Experimentally, since both ν and H_0 can be measured precisely and μ_e is known with precision, g can be extracted with high precision from experimental data.

The Relationship of the g Factor to Molecular Structure: the Spin Orbit Connection

As mentioned above, the g-value in ESR serves a role analogous to the shielding constant, σ, in NMR. Both measure the magnitude of electric currents induced in the electron coulds of a molecule by an applied magnetic field and the extent of the coupling of these currents to a spin magnetic moment. Since the chemical shift provides information about the chemical environment in the vicinity of nuclear spins, we expect the g factor to provide information about the chemical environment of electron spins.

What is the relationship between the g factor for electron spin and molecular structure? The experimental value of the g factor for an electron spin embedded in a molecule is slightly different from that for a free electron (g_e = 2.003). The reason for the difference is that the spin in the molecule experiences magnetic fields due to its environment which effectively add or subtract from the magnetic moment due to the electron spin. For example, an electron, in executing an orbital motion, generates a magnetic moment that can couple with the magnetic moment due to the electron spin, a process termed spin-orbit coupling. We can imagine that the electron "picks up" or "loses" some spin angular momentum as a result of spin-orbit coupling. Thus, the experimental value of g will deviate from the value for the free electron.

The value of g_i (Eq. 25) in a molecular environment is related to the ease with which the applied field, H_0, can "stir up" electric currents that generate magnetic fields which interact with the electron spin. The most important source of such currents is due to the orbital motion of the electron whose spin is being affected. This is reasonable because the "stirring" is related to the ability of the orbital motion to generate angular momentum and therefore a magnetic moment. This is easiest for an electron when it is in an atom, since in an atom the circular motion required for the generation of angular momentum can be readily achieved.

As an example, consider a hydrogen atom (Figure 24) possessing an electron in a 2 p orbital (an electron in a 1s orbital does not possess any angular momentum). We imagine that the 2 p electron can readily move in a circular manner about the nucleus by jumping from a 2 p_x to a 2 p_y orbital. This motion generates angular momentum along the z axis. Application of an external field along the z axis will cause the electron to "jump" from the p_y orbital to the p_x orbital and this motion will produce an induced angular momentum (Figure 13) which, in turn, can couple to the spin through the inherent spin orbit coupling of the system and cause the observed value of g to deviate from the value of g_e.

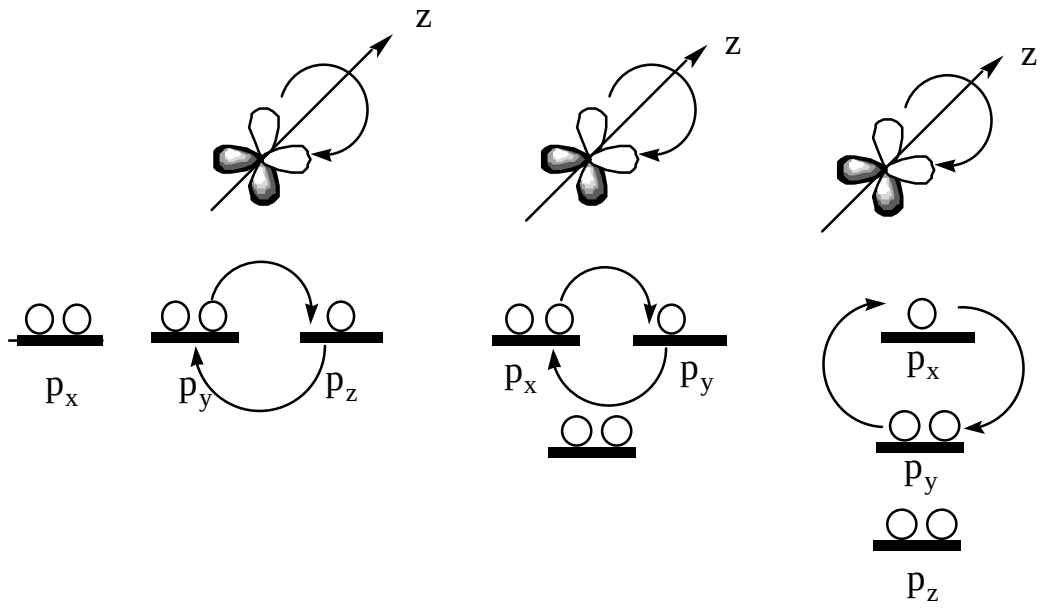

Figure 24. Spin orbit coupling is strongest in organic molecules when jumps between p orbitals can occur on a single atomic center and between a degenerate p orbital. Of the situations shown, the one on the right has poor spin orbit coupling and the ones on the left have good spin orbit coupling.

The strength of the magnetic fields generated by orbital motion is proportional to the magnitude of the spin-orbit coupling constant ζ (see discussion in Chapter XX), which is related to the nuclear charge. In addition, the ability of the electron to make circular orbits is inversely proportional to the energy gap, Δ, between the orbitals involved in the process. Hence the g factor is expected to differ from the value of g_e by an amount proportional to ζ / Δ (eq. 26).

$$g \text{ (measured)} = g_e \text{ (free electron)} - \alpha\zeta / \Delta E \qquad (26)$$

The extent of the deviation of the g factor from g_e can be understood readily in terms of eq. 26. The energy term in the denominator is typical of the results of perturbation theory and reflects the extent to which an applied field can mix in excited states to provide pathways through the molecule for electrons to acquire orbital angular momentum. This induced momentum is then transmitted to the electron spin as an effective magnetic field via the spin orbit coupling, which is proportional to ζ. As the energy separation decreases, the ability of a given field strength to induce currents increases and so the measured g deviates more strongly from g_e. On the other hand, as the spin orbit coupling constant increases, the spin is subjected to a more effective field and the ability to induce fields is also enhanced by the stronger coupling of the spin to the induced fields through the spin orbit interactions.

For organic molecules possessing only H, C, O and N atoms, the value of ζ is generally small. Furthermore, most organic molecules possess a large value of Δ, so that the value of g_i is expected to be small in general for organic molecules possessing an odd electron. For carbon centered radicals, the value of g is close to that for a free electron.

Whether the deviation is to larger values of g or smaller values of g depends on factors such as the sign of the spin orbit coupling constant, but for most organic radicals the measured value of g is in the range 2.010 to 1.990, compared to the value for g_e which is 2.003. Although these differences are small, they can be measured with high accuracy and are excellent experimental parameters for the structure of molecules and radicals possessing an ESR spectrum.

Fine Structure and Hyperfine Structure of Magentic Resonance Spectra.

Although the internal magnetic fields due to orbital circulations modify the frequency at which an electron spin undergoes resonance in a given magnetic field, this factor does not increase the number of magnetic enegy levels, i.e., the g factor modifies the energy gaps between levels and therefore the frequencies of the transitions (eq. 23), but does not change the number of levels. As we have seen in section 7, the interaction of an electron spin with another electron spin or with a nuclear spin does increase the number of energy levels. These new levels lead to new transitions that are said to cause a "splitting" relative to the uncoupled situation. In the case of electron-electron spin couplings, the splittings are termed "fine structure" of the spectrum and in the case of electron-nuclear spin couplind, the splittings are termed "hyperfine structure". Both fine and hyperfine couplings are characterized by parameters, the fine coupling constant and the hyperfine coupling constant, which can be related to molecular structure. These relationships will be discussed in more detail below when examples of ESR spectra are given for a case history example.

The Shape of the ESR Signal.

As in NMR spectroscopy, the shape of the signal due to a single transition provides information on the rate of the radiationless transitions involving the levels undergoing the transition. The shorter the lifetime of the level, the broader the signal. If the total spin remains the same during the radiationless transition, we are dealing with a magnetic **internal conversion**. These conversions are characterized by relaxation of the spin system along the z axis (with a characteristic time, T_1) and relaxation of the spin in the x, y plane (with a characteristic time, T_2). If the total spin changes during the radiationless

transition, we are dealing with a magnetic **intersystem crossing**, which can also be characterized by characteristic times, T_1 and T_2 .

The Intensity of the Magnetic Resonance Signal. Boltzmann Factors and Spin Polarization.

The intensity of a mangnetic resonance signal due to a certain electron spin might be expected to depend on the number of these spins in the sample and the number of photons bathing the spins. This would be true if all of the spins were in one level and none in the other. However, consider the situation for a sample containing "free electrons" for which there are an equal number of spins in the α state and in the β state. According to Einstein's principle of stimulated absorption and emission, a beam of photons (which is not circularly polarized) has an equal probabililty of striking an α spin and stimulting it to emit a photon and form a β spin as it does of striking a β spin and stimulating it to absorb the photon and form the α state. In this extreme case, there would be **no absorption not matter how many spins were in the system!** In order to obtain measurable absorption, there must be an excess of spins in one of the levels.

Thus, in an an actual magnetic resonance experiment, we must consider the fact that we are dealing with a net absorption from only a tiny fraction of the total number of spins in the system. At any temperature, there exists an equilibrium distribution of spins in the upper and lower magnetic states. The specific equilibrium distribution is call the Boltzmann population and its value depends on the temperature and the energy gap according to eq. 27.

$$N_\alpha / N_\beta = \exp(\Delta E / kT) \qquad (27)$$

We now view the experimental form of an ESR spectrum in terms of the Boltzmann distribution. When photons corresponding to the frequency for which $\Delta E = h\nu$ interact with the Boltzmann population of spins, some $\alpha \varnothing \beta$ and some $\beta \varnothing \alpha$ transitions will occur. However, since there are more β spins present when the system is at the Boltzmann distribution, there will be a net absorption at the magnetic field which causes the resonance condition to be achieved, i.e., the value of H_0 for which $\Delta E = g\mu_e H_0 = h\nu$. The same ideas pertain for a proton NMR spectrum, except that the energy gap is much smaller and that the α state is lower in energy than the β state.

In certain cases the rate of relaxation between spin levels is relatively slow and the Boltzmann distribution is not achieved during the time scale of the experiment. In such cases non-Boltzmann or **polarized distribution** of spin levels occur. When spin polarization occurs (we'll discuss mechanisms by which

it may occur in later sections), the intensity of the observed ESR or NMR spectra bear no relationship to the spectrum produced by a Boltzmann distribution. Figure 25 displays schematically a comparison of a Boltzmann distribution and two extreme cases of polarization. Near ambient temperatures, there will be a very slight excess of spins in the lower level for a Boltzmann (Figure 24, left). Since the probability of transitions is related to the difference in populations, the magnetic resonance signe will be relatively weak. If, by some mechanism, a large excess of spins are in the lower level during the time of measurement, the observed signal will be a much stronger absorption than expected based on the Boltzmann distribution. If, by some mechanism, a large excess of spins are in the upper level during the time of measurment, the observed signal will be a **net emission**!

We shall see later on that in many photochemical reactions the primary radical intermediates and the molecules formed from reactions with these radicals are formed with electron spins and nuclear spins that are not at the Boltzmann distribution. This means that there may be more spins in the lower level than there are for the Boltzmann distribution at the temperature of the reactions or **even that there are more spins in the upper level than there are for the Boltzmann distribution at the temperature of the reaction.** The phenomena of generating electron spin polarized radicals is termed CIDEP (chemically induced dynamic electron polarization) and the phenomena of generating nuclear spin polarized molecules is termed CIDNP (chemically induced dynamic nuclear polarization).

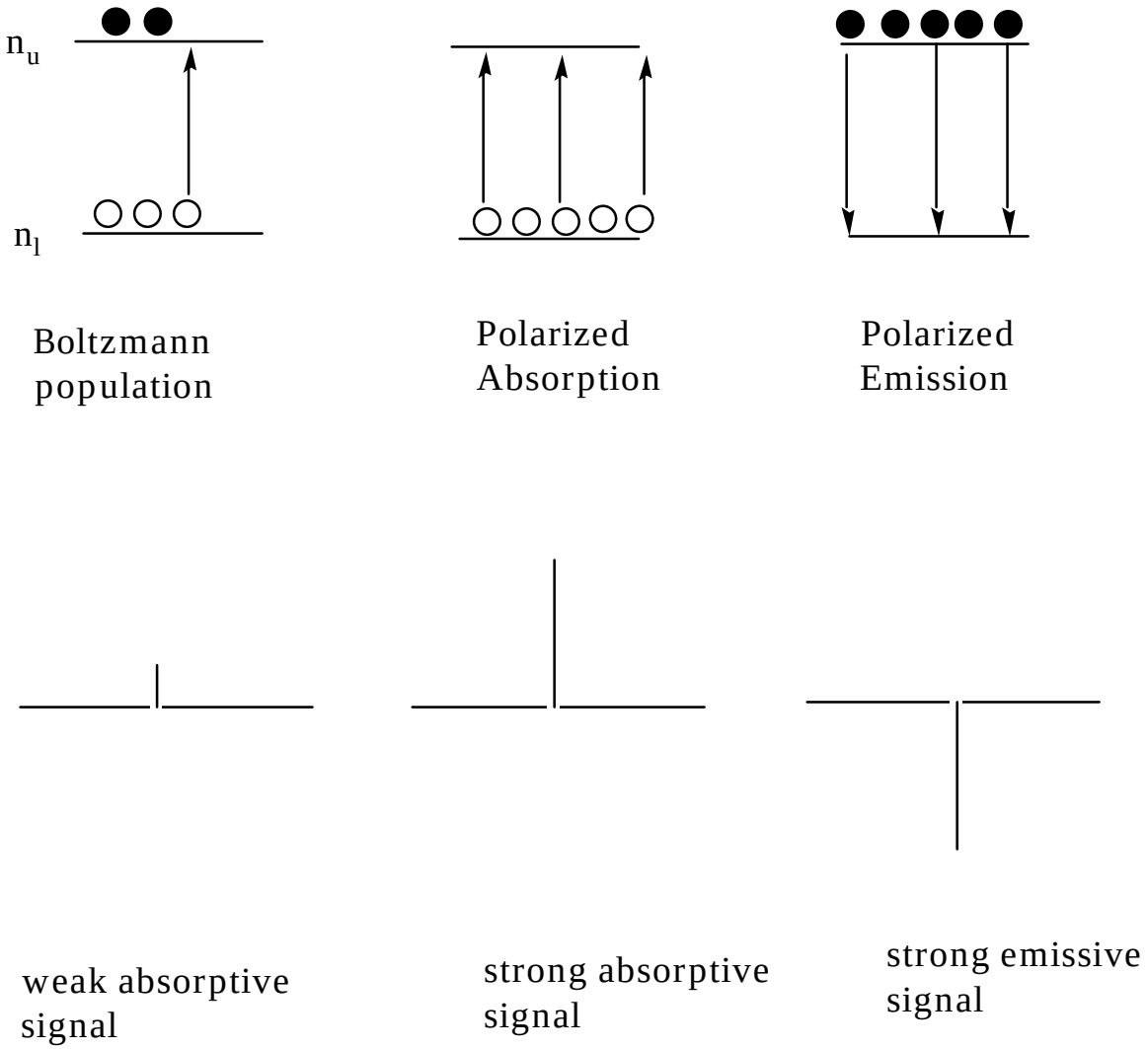

Figure 25. Schematic representation of spin polarization in terms of an energy diagram and in terms of an experimental signal

11. Magnetic Resonance and Spin Chemistry. A Paradigm and a Case History

At the beginning of the Chapter (Figure 1) a paradigm was proposed that a majority of investigated organic photochemical reactions involve photochemical primary processes initiated in the lowest triplet state, T_1, to produce a geminate triplet radical pair (or triplet biradical) which then proceeds to products in secondary reactions. Since many photochemical reactions of organic molecules occur from the triplet electronically excited state and produce triplet geminate radical pairs (or biradicals) as the primary photochemical products, it is important to have a general paradigm to guide the mechanistic interpretation and experimental methods for understanding and investigating such reactions. Figure 26 reviews the key intermediates in such a paradigm. We are now interested in showing how the techniques and concepts of magnetic resonance (radiative transitions between magnetic energy levels) and spin chemistry (radiationless transitions between magnetic energy levels) can elucidate photochemical reaction mechanisms.

In Figure 26 we will consider the following stages of a case history photochemical process:

(1) the intersystem crossing step, $S_1 \varnothing T_1$;

(2) the primary photochemical step, $T_1 \varnothing {}^3RP$;

(3) the intersystem crossing step, ${}^3RP \varnothing {}^1RP$;

(4) the product forming step, ${}^1RP$.

The paradigm we shall develop will be analogous for weakly coupled radical pairs and weakly coupled flexible biradicals, so that for the sake of simplicity, the discussion will mainly refer only to radical pairs. One should keep in mind that in nearly all of the discussion the word "flexible biradical" can be substituted for "radical pair". It is also important to note at this point that if a photochemical reaction is investigated in a NMR spectrometer or in a ESR spectrometer the intermediates in Figure 26 are in a high magnetic field, so that the magnetic energy diagrams must consider the effect of the field on steps 1-4 below.

$$R \xrightarrow{h\nu} {}^1{}^*R \longrightarrow {}^{3*}R \longrightarrow {}^3I \longrightarrow {}^1I \longrightarrow P$$

$$S_0 \longrightarrow S_1 \xrightarrow{1} T_1 \xrightarrow{2} {}^3RP \xrightarrow{3} {}^1RP \xrightarrow{4} P$$

Figure 26. Simplified paradigm of a photochemical process proceeding through a triplet electronically excited state, T_1.

Regions of Chemical Space and Spin Space Explored During a Photochemical Reaction.

We have seen in Chapter XX that electronic surface energy diagram are extremely useful in visualizing the electronic features of photochemical reactions. We shall now combine the "chemical space" of electronic energy surfaces and "spin space" of the vector model to examine a case history of a photochemical reaction. It will be shown that the intersystem crossing step, $S_1 \varnothing T_1$ occurs "vertically" in a region of the energy surface for which the exchange interaction is very large. Thus, this step can be treated in terms of a vertical jump (spectroscopic) of a representative point between energy surfaces described for radiative and radiationless transitions. The remaining steps, $T_1 \varnothing {}^3RP \varnothing {}^1RP \varnothing$ P, involve bond breaking, separation and reencounters of radical pairs and bond formation so that ^3RP and ^1RP constitute a **dynamic radical pair**. These processes involve both horizontal and vertical motion of the representative point on energy surfaces separated by various values of J. We shall see that the variation of J strongly influences the magnetic resonance spectroscopy and the spin chemistry of the dynamic radical pair.

Photochemical α-Cleavage of Ketones as a Case Study

We shall now use a "case study", the α-cleavage reaction of a ketone in its triplet state, to bring together the principles of the vector model to understand magnetic resonance spectroscopy and spin chemistry. Figure 27 shows the four steps 1-4 of the general paradigm of Figure 26 expressed in terms of a ketone, ACOB. We shall examine each of these steps to develop a working paradigm for photochemical reactions proceeding through triplet states of organic molecules.

We proceed with an analysis as follows: (1) For step 1, we shall examine the mechanism of the intersystem crossing step, $S_1 \varnothing T_1$, in zero field and in high field. We shall ask how is angular momentum conserved in this step which involved an obvious change in spin, i.e., what mechanism of coupling is responsible for inducing the spin change? We shall also consider the magnetic resonance spectroscopy of the T_1 state that is formed and how this spectroscopy can provide both information on the mechanism of coupling that is responsible for the intersystem crosssing and the electronic structure of the T_1 state. We shall see that the intersystem crossing step actually "locks" spin information into the triplet and that this spin information may be transferred to the radical pair produced in step 2; (2) For step 2, we shall examine the elementary step of bond breaking in zero field and in high field. We shall also see that step 2 and step 3 are intimately connected through the paradigm of a dynamic radical pair and

that the concept of the dynamic radical pair is required to understand the magnetic resonance and spin chemistry of the system; (3) For step 4, we shall show that the intersystem crossing step of the dynamic radical pair "locks" nuclear spin information into the products, P.

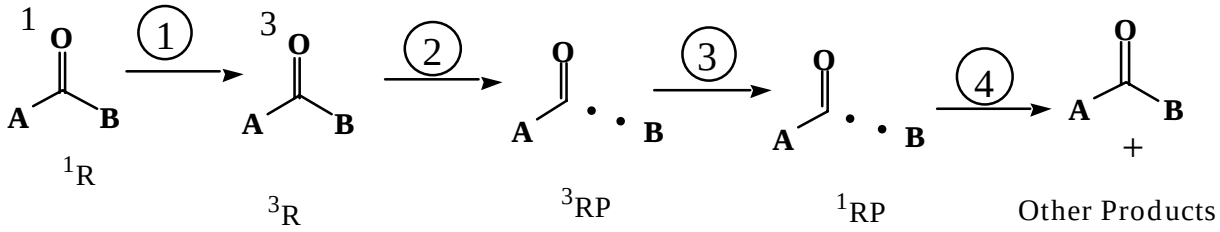

Figure 27. Paradigm for the α-cleavage reaction of ketones.

12. The Molecular Intersystem Crossing Step $S_1 \varnothing T_1$. Zero Field Splitting of the Triplet Levels and Spin Polarization of the Triplet State.

In Section 7 it was pointed out that under certain circumstances the three triplet sublevels may not be degererate at zero field. This will happen when the dipolar interaction between the two electron spins is significant (strong orbital overlap) and does not average to zero (slow molecular motions). Let us now consider how the dipolar interaction modifies the energy diagram for a molecular triplet at zero field and how this modified diagram transforms in high field.

The ESR of Molecular Triplets. The Dipolar Interaction and Zero Field Splitting of the Triplet

We noted numberous times in this chapter that in the absence of magnetic interactions, the magnetic sublevels of a given state of spin angular momentum will be degenerate. We might conclude, therefore, that the three triplet sublevels of a molecular triplet, T_1, of an organic molecule such as a ketone, ACOB, will be degenerate in the absence of an applied field. This conclusion, however, is incorrect because the molecular triplets of organic molecules experience magnetic interactions that cause the triplet sublevels to possess different energies, even in the absence of an applied field. These energy splitting are due to anisotropic dipolar magnetic **interactions** of the unpaired electrons due to the overlap of the orbitals containing the odd electrons and is termed the zero field splitting (ZFS) of triplet states. The source of the dipolar interactions are typically due to one of two types of couplings, either spin orbit coupling or spin spin coupling.

What is the effect of dipolar interactions on the energy level diagram of the triplet? We have seen in section 7 that dipolar interactions between spins average out to zero when the spins undergo rapid isotropic molecular motion about all possible axes. This does not happen for molecular triplets due to the overlap of the orbitals containing the unpaired spins. Because the overlap causes a strong electron exchange, there is a very strong tendency for the two triplet spins to be quantized or fixed relative to each other as a result of the Pauli Principle (requiring the electrons and therefore their spins to be correlated). This correlation can be representated by an axis, which in turn can be related to a molecular axis as shown in Figure 19. We say that the axis tracking the triplet spin follows the molecular axes as the molecule tumbles in solution. This coupling of the molecular axis and the spin axis opposes averaging of the dipolar interaction, which remains finite in the absence of an applied field.

A second important feature of the coupling of the spin to the molecular axes appears when a magnetic field is applied. For technical reasons, ESR spectra are obtained with magnetic fields of the order of 10,000 G or less. The dipolar coupling of many organic triplets is of the order of this field strength, so that the "strong field" limit is not met and the mutual interaction of the two electron spins is of the same order as the interaction of the applied field, H_z. The result is that the ESR spectrum of molecular triplets requires a higher level of theory for interpretation. For example, since the spins interact with each other and the external applied field, the magnetic moment due to the spins does not have a fixed value along the H_z direction. This means that the description of the three triplet sublevels in terms of a "good quantum numnber" M_s = +1, 0 and -1 is not value in general, but depends on the specific orientation of a molecule with respect to H_z. There are, however, three limiting cases for which the quantization in terms of M_s is still valid or a reasonable approximation: (1) in the case of a triplet molecule possessing a cylindrical axis of symmetry in the vicinity of orbital overlap of the two spins when the direction of H_z is along the cylindrical axis; (2) in the case of a triplet for which there is a large separation of the spins or a small orbital overlap; and (3) in the case of a triplet in an applied field that is much larger than the dipolar interaction.

In summary, in considering experimental ESR spectra of molecular triplets, we must alway keep in mind the interaction of the magnetic moment of the molecule as a whole with the field, H_0 and the dipolar interactions of the two spins. The magnetic interaction energy between two electron spins is given the symbol D and is termed the zero field spliting parameter. The reason for this term is that at zero field the dipolar interactions between electron spins still persists, so there are three magnetic energy levels even in the absence of any applied field. We now present a qualitative discussion of how D is extracted from ESR spectra.

Extraction of the Dipolar Interaction from Zero Field Splittings.

At zero field the difference in triplet levels depends on the parameter D, which may be considered as being analogous to a coupling constant such as the exchange interaction, which splits the energy of S and T states, but does not mix them. We can relate D to the vector model by noting that at zero field, the total magnetic moment due to the spin is quantized and therefore may lie in any one of three possible axes of a molecular structure. The three triplet sublevels in the molecular frame are labeled by the axis (or plane) on which they lie, i.e., T_x, T_y and T_z. For the case in which the molecular system has approximate cylindrical symmetry, the energies of the T_x and T_y states are equal. The z axis at zero field is defined as the molecular axis which has zero magnetic energy, i.e., when the

molecule is placed in a magnetic field there would be no magnetic energy along this axis. For ketones, which will be discussed in the following sections, spin orbit coupling dominates the internal magnetic field on the molecular frame and it is experimentally found that for ketones T_z possesses a higher magnetic energy than T_x or T_y as shown in Figure 28. The energy gap between T_z and T_x (or T_y) is effectively equal to the zero field splitting, D.

Thus, at zero field it is possible to measure D by simply observing the transition between the T_x (or T_y) state and the T_z state . Experimentally this is done by measuring some non-magnetic property of the triplet (typically optical absorption or emission) and then applying electromagnetic radiation of varying frequency, ν. When the correct resonance frequency for which $\Delta E = D = h\nu$ occurs, transitions between the triplet sublevels occurs and detected by a change in the non-magnetic property. From the definition of the T_z axis in the molecular frame, it is expected that the application of a magnetic field will not change the energy of the T_z state. Thus, at very high fields, we expect that T_z will transform into T_0, as shown in Figure 28.

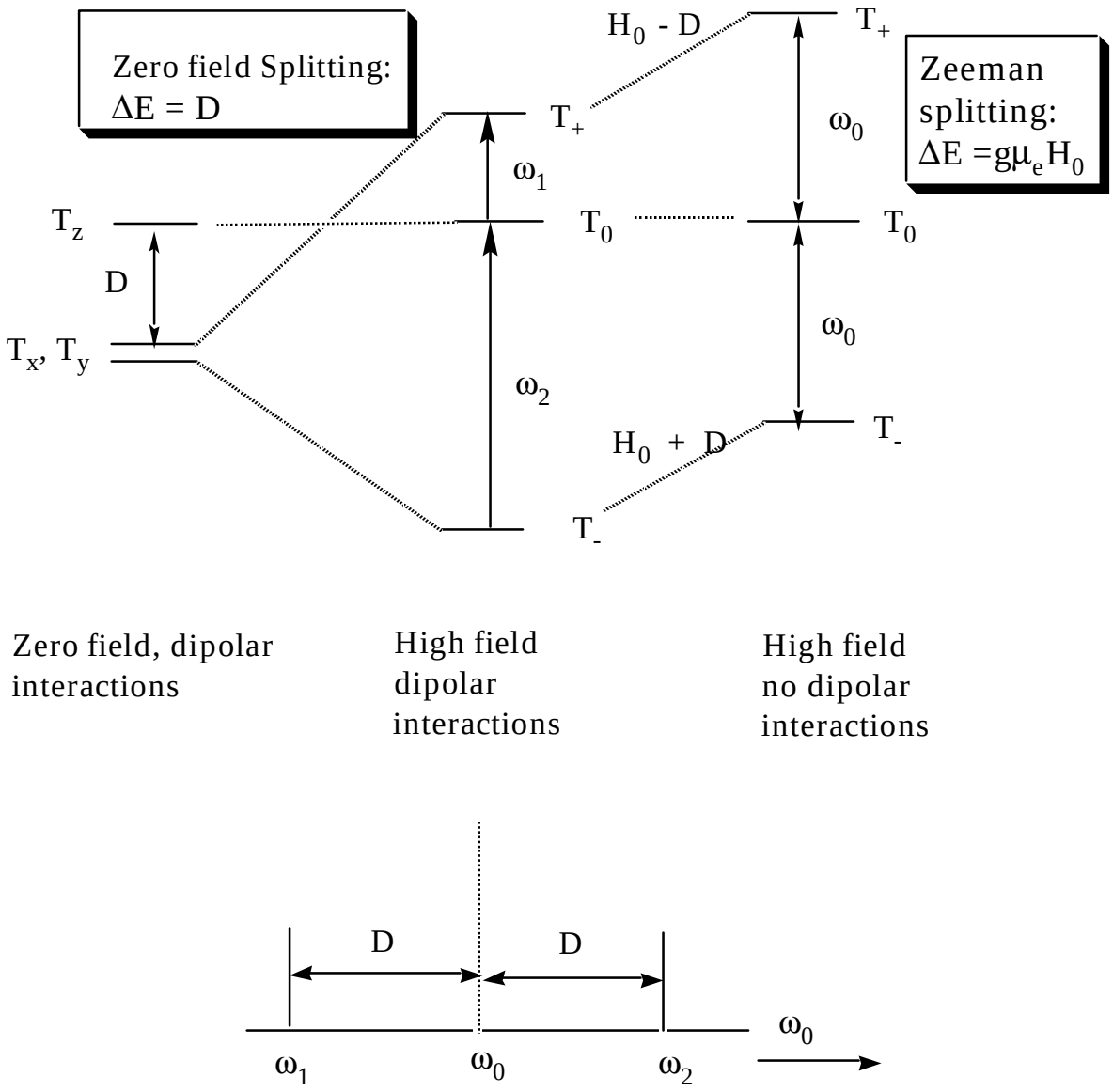

Figure 28. Energy diagram for a molecular triplet at zero and high fields: (a) Zero field in the presence of dipolar interaction; (b) high field in the absence of dipolar interactions; (c) high field in the presence of dipolar interactions.

It is also possible to measure D through magnetic resonance spectroscopy at high field. As mentioned above, in the special case for which the applied field is along the axis of T_z, the interaction energy between the two spins is exactly equal to D. Thus, if we could measure the interaction energy in this special case, we can experimentally determine the value of D from magnetic resonance spectroscopy. (A second quantity, E, is employed to measure the magnetic distinction in the x,y planes. For most organic molecules this quantity is small relative to D and is therefore not considered in this qualitative discussion.)

To obtain an understanding of how D related to an experimental ESR spectrum, let us consider the influence of D on the magnetic energy diagram at zero field and in the presence of an applied field. Figure 28 shows the three triplet sublevels (a) at zero field in the presence of dipolar interaction, D; (b) at high field in the absence of dipolar interactions; and (c) at high field in the presence of a dipolar interactions of strength, D. The parameter D, as for many magnetic parameters, may be positive or negative (which must usually be determined by experiment). The sign of D determines whether the T_- or the T_+ level are raised or lowered in energy in the presence of a high magnetic field. In Figure 28, it is assumed that the sign of D is negative, causing (relative to the case for no dipolar spin-spin interactions) a lowering of the energy of both T_- and T_+, while the T_0 level is unaffected. The corresponding ESR spectrum for this special case consists of two allowed transitions: (T_-/T_0 and T_0/T_+), and the ESR consists of two lines separated by 2D. Thus, from measurement of the ESR of molecules oriented along the H_z axis, the value of D may be obtained from the ESR of the triplet. In the absence of dipolar interactions, the energy gaps for the T_-/T_0 and T_0/T_+ transitions are identical so that the ESR would consist of a single line (of twice the intensity, due to two overlapping transitions).

Experimental Complications in the Measurement of D

The ESR of triplet states is complicated by the enormous magnetic field that the two unpaired electrons exert on each other due to magnetic dipole-dipole interactions. This field varies widely throughout the population of triplet molecules because it is highly orientation dependent, i.e., it is anisotropic (Figure 19). The situation is further complicated because the strength of the anisotropic magnetic field is often comparable to the magnetic field at which ESR measurements are commonly made, so that the external field does not completely govern the direction of the spins. The net result is that the spectrum over all of the population of triplets is broad and the sensitivity of the measurement is low.

In principle, one way to remove these difficulties is to take the ESR of the triplet state of a crystal. In a crystal all of the triplet molecules can be oriented in the same way in the magnetic field so that the angles between the molecular axes and the external magnetic field directions will be the same for all of the molecules. This will eliminate the line broadening due to anisotropy. In this interesting case the ESR spectrum depends on the orientation of the crystal in the magnetic field! For example, the rotation of a naphthalene crystal in a magnetic field causes a variation of a given transition as much as 2000 G. The entire ESR spectrum of a typical organic radical spans only ca. 100 G or less. Therefore, in a

random sample of naphthalene triplets, the spectrum would be distributed over ca. 2000 G and the intensity at any given field strength would be quite weak.

Since a typical sample in an ESR spectrometer consists of molecules in a wide range of orientations relative to the applied field, special considerations must be taken to extract D from experimental spectra. Furthermore, rapid rotation of molecules in solution adds a further complication of line broading due to rotational relaxation. As a results, the D parameters are extracted from samples that are rigidly trapped in a solid, typically in a solid solution or glass at low temperature.

The Distance of Separation of Electron Spins From the Dipolar Interactions.

Because the dipolar interaction depends on orbital overlap, which in turn represents the average distance separating electrons, the zero field splitting parameter, D, (which provides a measure of the dipolar interaction) also provides a means of determining electron distributions and assigning orbital configurations of the triplet state. The effective internal magnetic field, $\mathbf{H_i}$, that one electron expresses on the second electron is given approximately by Eq. 28 (which should be compared to Eq. 19), where R_{12}^3 is the average separation of the electron spins and μ_e is the magnetic moment of an electron spin.

$$\mathbf{H_i} = (\mu_e / R^3)(3\cos^2 - 1) \qquad (28)$$

Since the magnitude of D is directly related to $\mathbf{H_i}$, it is expected that the magnitude of D is proportional to R_{12}^3. However, the value of $\mathbf{H_i}$ depends on the orientation of the spins relative to the applied field because of the $3\cos^2 - 1$ term. For the limiting cases or cylindrical symmetry with the applied field direction parellel to the z direction in the molecular frame, the distance of separation along the magnetic field axis is given by eq. 29. For a separation of spin of 1 Å, the value of D is 1 cm^{-1}, which corresponds to a magnetic field of ca 10,000 G.

$$D\ (cm^{-1}) \sim 10^{-24} R_{12}^3\ (Å) \qquad (29)$$

For the specific example of a ketone triplet (spectrum taken along the z-axis), the ESR will consist of two lines with separation of 2D. For n,π* triplets the value of D is typically 0.3 cm^{-1}, which corresponds to a dipolar magnetic field of ca. 3000 G. Indeed, this is the value of the magnetic field of typical ESR spectrometers.

Intersystem Crossing Step at Zero Field.

At zero field, the spin of a triplet state must be quantized in one of the three molecular axis of a molecular structure. Since spin orbit coupling is typically the dominant mechanism for ISC of ketones, it stands to reason that the $S_1 \varnothing T_1$ ISC will be specific for the molecular axis possessing the highest degree of spin orbit coupling. In other words, there will be spin orbit forces operating on each of the orbitally unpaired electrons of S_1 and these forces will have a certain symmetry with respect to the molecular axes corresponding to the three molecular planes. Thus, the $S_1 \varnothing T_1$ ISC will produce a triplet which is **polarized**, i.e., the ISC process is expected to produce predominantly in one of the three triplet sublevels, T_x, T_y or T_z.

As mentioned above, in the case of ketones, the energetic ordering of the typical zero field levels, determined by dipolar interaction and spin orbit coupling, is typically $T_z > T_x \sim T_y$, i.e., the T_z state, whose axis is along the C=O bond. Since the T_z level is strongly coupled to S_1 by spin orbit coupling, the ISC occurs via a selective $S_1 \varnothing T_z$ process. At temperatures near 4^o K (liquid helium temperature), interconversion of the triplet sublevels is relatively slow, so that the T_z level may be examined with little interference from the unpopulated T_x and T_y states. For example, the phosphorescence of the T_z level will be different from that of the T_x and T_y levels because phosphorescence depends on spin orbit coupling and as we have seen above, the effectiveness of spin orbit coupling depends on the coupling of the spin to the molecular axis!

Intersystem Crossing Step at High Field.

An interesting issue is how the polarized T_z level produced in the molecular frame at zero field might be transformed into one of the T_+, T_0 or T_- level in the presence of a strong applied field. In Figure 29 we note that there is a surface crossing between T_z and T_x as the magnetic field strength is increased. Thus, there are two pathways for the representative point starting from T_z: (1) T_z possesses a "natural" correlation with T_0 at low field and in the absence of mixing or rapid passage through the crossing region, the **diabatic** process $T_z \varnothing T_0$ will occur; (2) if mixing is strong or passage through the mixing region is slow, the **adiabatic** process $T_z \varnothing T_0$ will occur. Whether the adiabatic correlation will occur and how such a correlation can be established experimentally by direct magnetic resonance measurements (by measuring the temperature dependence of the ESR signal) or by monitoring the polarization of the radicals produced by primary photochemical process will be seen. We shall consider below the more photochemically interesting method of determining the adiabatic or diabatic pathway for ISC by observing the spin polarization of the radicals produced in a

primary photochemical step. To do this we must move from the "spectroscopic region of the energy surface" corresponding to vertical electronic transitions of the representative point to the "chemical regions of the energy surface" corresponding to bond breaking. Moving from the spectroscopic region to the chemical regions of the energy surface will be the topic of the following sections.

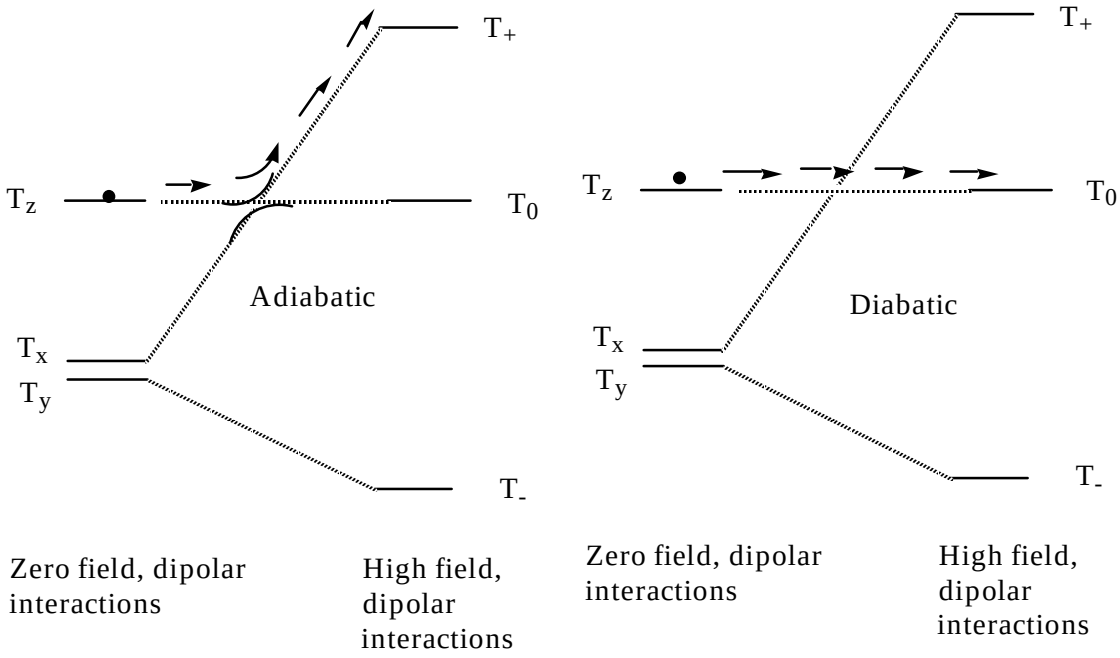

Figure 29. Adiabatic (left) and diabatic (right) trajectories of a representative point starting from the T_z state.

13. Primary Photochemical Reactions. Spinomers

Step 2 in the paradigm of the case history of our ketone photochemistry (Figure 27) is the formation of a geminate radical pair by α-cleavage. In order to understand the subsequent spin chemistry and magnetic resonance spectroscopy associated with this geminate radical pair and the other reactive intermediates, as well as the final product, we must examine in some detail the spin structure and dynamics of the radical pair ACO· ·B. For the spin structure we introduce the concept of ***electronic and nuclear spinomers*** , species which have **identical chemical structures** but differ in some measurable aspect of their spin structure. We shall see that the chemical structure of a radical pair ACO· ·B has a complex spin structure when we consider nuclear spin, electron spin, and the influence of applied magnetic fields. Thus, what looks like a simple structure ACO· ·B can actually be viewed as corresponding to a large number of distinct spinomers. We shall also see that the molecular dynamics (relative diffusional and rotational motions) of ACO· ·B will play an important role in the spin chemistry and magnetic resonance spectroscopy of the system. The distance dependence of the exchange interaction, J (which causes the S and T states to separated in energy) and the influence of J on intersystem crossing and mixing of magnetic energy levels are dominant factors in determing the spin chemistry and magnetic resonance spectroscopy of various spinomers of a dynamic radical pair.

After a consideration and description of the spinomers for some simple examples of the ACO· ·B system, we shall return to an analysis of steps 2, 3 and 4 (Figure 27) of the case history system.

Electronic and Nuclear Spinomers.

The geminate radical pair, ACO· ·B is often described in textbooks with a dot presenting an odd electron on each radical. This model is lacking in any spin characteristics. Thus, at the spinless level, it is expected that a collision between two radicals will lead to the rapid and efficient radical-radical reactions such as formation of a bond to form ACO-B. In this simple model there is no basis for lack of reactivity between two radicals. Taken to its logical conclusion, when radicals are produced in pairs by the cleavage of a bond, they would be expected to react efficiently by bond reformation, since there is no apparent barrier to recombination reactions. This conclusion is contrary to the results of many photoreactions for which triplet radical pairs are produced, but have very inefficient geminate reactivity and form free radicals efficiently. Let us now see what happens to the structure of a primitive, spinless model of the geminate radical pair ACO· ·B when we (1) couple a single nuclear spin (^{13}C on the carbonyl carbon) to one of the odd electrons; (2) introduce correlated electronic

spins to represent the 2 odd electrons; and (3) introduce a strong applied magnetic field.

Enumeration of Spinomers of the ACO· ·B Geminate Radical Pair.

It will be assumed that the ACO· ·B radical pair posseses a well defined chemical structure in terms of bond connectivities. Keeping these connectivities fixed, we seek to enumerate the number of distinct spin structures that are possible when we consider: (1) an istopomeric ACO· ·B pair with a carbonyl carbon atom that is either ^{12}C or ^{13}C; (2) the correlation of the unpaired electrons; and (3) the application of a magnetic applied field.

We start with a "spinless" radical pair, ACO· ·B. The effect of considering isotopes at the carbonyl carbon is to generate two isotopomeric pairs: $A^{12}CO \cdot \cdot B$ and $A^{13}CO \cdot \cdot B$ (Figure 30). These pairs are conventionally termed **isotopomers** (chemical structures possessing the same elemental composition, but different isotopic composition). Without consideration of spin, at the level of the "dot" representation of odd electrons, these two isotopomeric pairs are expected to be comparably reactive except for a weak mass isotope effect.

Next, let us introduce the effect of electronic spin correlation (resulting from electron exchange, J) without respect to the separation of the spins in space (this is important and we shall deal with it when we consider the **dynamic** radical pair below). By introducing electron spin and electron spin correlation, each isotopomer must now be considered as one of two **electronic spinomers:** a triplet, T, or a singlet, S. In the absence of an applied magnetic field, the initial "spinless" structure for a radical pair becomes **four** different electron correlated spinomers, two triplet and two singlet spinomeric structures: ^{12}S, ^{13}S, ^{12}T and ^{13}T (Figure 30). These structures are expected to have different reactivity toward bond forming reactions.

Now let us introduce the effect of a strong magnetic field, $\mathbf{H_0}$, which will cause a Zeeman coupling of the field to the electron and nuclear spins. The Zeeman effect orients the magnetic moments of all the electronic and nuclear spins of the pairs along the field direction. For the $A^{12}CO\cdot\ \cdot B$ pair, the two electronic spinomers, ^{12}T and ^{12}S, will split into the **four Zeeman electronic spinomers** (Figure 30)**:** ^{12}S, $^{12}T_-$, $^{12}T_0$, and $^{12}T_+$. For the $A^{13}CO$ B pair, the two structures ^{13}S and ^{13}T will break up into **eight nuclear-electronic Zeeman spinomers** (Figure 30): $^{13}S^{\alpha,\beta}$, $^{13}T_-^{\alpha,\beta}$, $^{13}T_0^{\alpha,\beta}$, and $^{13}T_+^{\alpha,\beta}$, where the superscript indicates the nuclear spin orientation in the field. Thus, our analysis of the hypothetical radical pair leads to the conclusion that the simple idea of a radical pair, ACO· ·B, involving simply two orbitally unpaired electrons becomes quite

interesting and complex when electron correlation, a magnetic field, and even one nuclear spin is introduced. This hypothetic pair, a three spin system, contains most of the important features of spin systems.

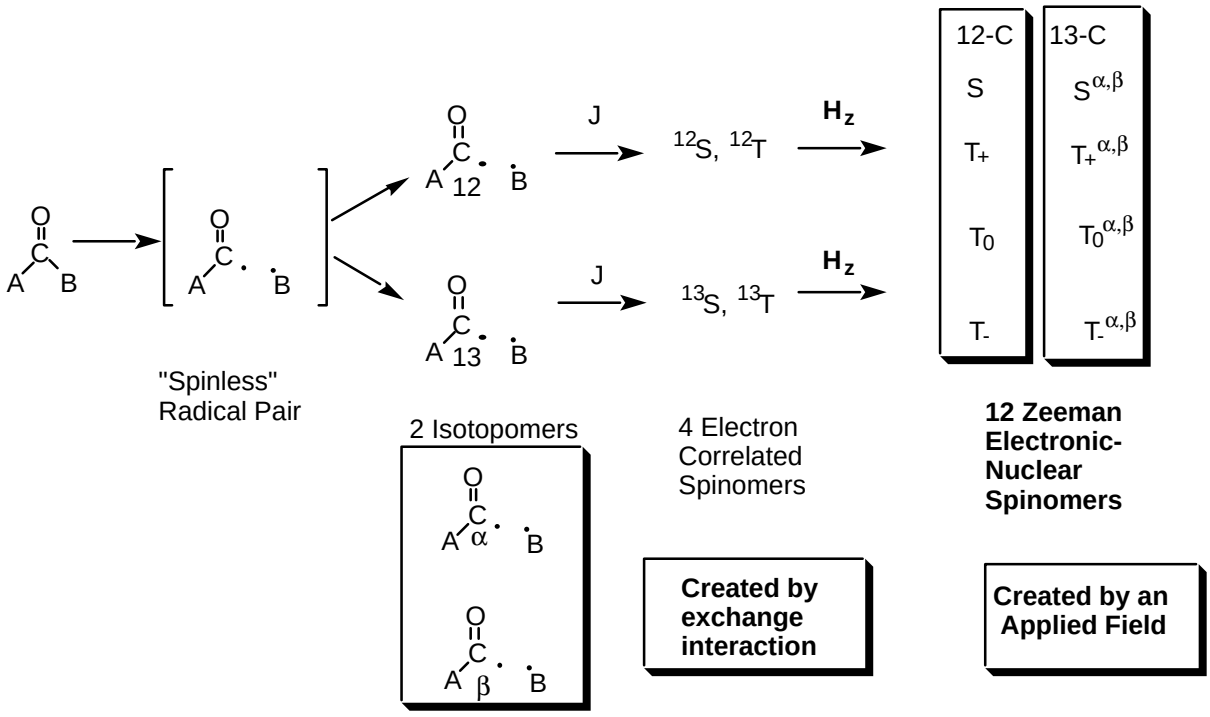

Figure 30. Evolution of spinomers as the result of introducing electron exchange, a magnetic isotope and an applied field.

It is important to recognize that **each of the 12 spin states shown in Figure 30 correspond to completely independent and distinct spin species.** A radical pair can be in one of these states or the other, but cannot be simultaneously in more than one of these states at any instant. For example, each state potentially possesses a distinct rate of intersytem crossing, a distinct ESR spectrum and distinct chemical reactivity. There will be a certain rate of interconversion of spinomers for each of the two isotopomers. For example, the four electronic Zeeman spinomers of the $A^{12}CO$ B pair will possess a certain rate of interconversion, <u>but only the S state will be capable of undergoing radical pair combination reactions</u>. All of the 8 nuclear-electronic Zeeman spinomers of the $A^{13}CO\cdot$ $\cdot$B are capable of interconversion, <u>but only the $S^{\alpha,\beta}$ pair is reactive toward radical pair combination reactions</u>. The S states will not display any ESR signal (they do not possess net electron spin to couple with an applied field!). The ^{13}C containing radicals will show ESR spectra with hyperfine splitting and the ^{12}C containing radicals will not show hyperfine splitting. We shall see that even in solution the selection rules for interconversion of spinomers are strict and that angular momentum and magnetic energy must always be conserved.

As a further example of the differences between isotopomers and spinomers, a radical pair containing ^{14}C at the carbon is an isotopomer of the $A^{12}CO$ B radical pair, but not a spinomer because both ^{12}C and ^{14}C have a nuclear spin of 0. Thus, magnetically, ^{12}C and ^{14}C behave qualitatively the same, so that in terms of spin the $A^{14}CO\cdot\ \cdot B$ pair is identical to the $A^{12}CO\cdot\ \cdot B$ pair, but qualitatively different from the $A^{13}CO\cdot\ \cdot B$ pair!

We now consider an extension of the radical pair model to a more realistic <u>dynamic</u> radical pair by introducing the critical feature of <u>molecular dynamics</u> which recognizes the feature that, in solution, the two partners of a pair undergoing random diffusional motion influences the electron correlation due to electron exchange and the magnetic interactions which are distance dependent.

14. The Dynamic Radical Pair in Zero Field.

The triplet geminate radical pair produced in the primary photochemical step 2 of figure 27 is not a static structure but, because of its diffusional and rotational dynamics, constitutes a **dynamic** system and therefore is termed a **dymanic radical pair**. We need to analyze the dynamics of the pair at three levels: (1) the level of molecular dynamics whereby the partners of the pairs may be collision partners in a solvent cage or be separated by one or more solvent molecules and may interconvert between these situations; (2) the level of spin dynamics whereby intersystem crossing and rephasing of spin occur; (3) the level of chemical dynamics whereby the partners of the pair undergo chemical reactions through bond formation, scavenging or radical pair rearrangements or fragmentations. In order to keep this riot of molecular dynamic activity organized in our minds in physical space, spin space and time, we result to a combination of energy surfaces, the vector model and conventional molecular structures. Effectively in exploring with our imagations we need the same tools as when we explore an unfamiliar territory: a map, a clock and a compass. The map is the energy surface (molecular structures are the geographical identifiers on the map), the clock is the time scale on which the interactive dynamics occur and the compass is the magnetic field that tell us about spin orientation.

Electronic Energy Surfaces and Molecular Dynamics.

We need to keep track of the several interacting dynamic events that are occuring simultaneously in the primary photochemical step of Figure 27, i.e., the ^{3}ACO-B $\varnothing$ ^{3}ACO$\cdot$ $\cdot$B process. We start by considering an energy surface description of the process (Figure 31). The triplet surface is shown as decreasing in energy and the singlet surface as increasing in energy as the carbon carbon bond stretches and then breaks. The energy gap between the triplet and singlet states is considered to be due to the exchange interaction, J. When the bond is broken and the partners of the pair separate by a solvent molecule or two, the exchange interaction is expected to decrease to negligably small values, so that the singlet and triplet surfaces are effectively degenerate and no longer change in energy with further separation. A representative point is shown moving down the surface (At zero field, the S_1 $\varnothing$ T_1 intersytem crossing is assumed to have occured to a specific triplet sublevel, T_z. We will return to this point when we consider the ESR of the radical pair).

Definition of Terms for Radical Pairs

In order to understand the behavior of the representative point we must consider its molecular, spin and chemical dynamics as it moves alont the triplet surface. Let us consider each of these dynamics separately and start with the

molecular dynamics which are represented schematically at the bottom of Figure 31. We shall employ the following terms to describe the molecular dynamics and structures of the pair.

1. **Geminate radical pairs.** A radical pair whose fragments are "born together" and share the parentage of a common precurson molecule, e.g., step 2 of figure 27.

2. **Free radicals or random radicals.** Radicals which have separated to a distance for which non-geminate reaction with radicals has a higher probability than geminate reaction.

3. **Random (or free radical) pairs.** A radical pair formed by an encounter of two free or random radicals. As one tracks the representative point as it makes an excursion down a dissociative triplet surface starting from the parent triplet excited state (^{3}*R) all the way to a separation of radicals that is so large that the pair becomes statistically distributed in space with radicals from other dissociations (right of Fsigure 31). Such a radical "pair" no longer is geminate in the sense that it becomes more probable that reencounters will occur with radicals from other dissociations than with the original geminate partner. At this point each partner of the original geminate pair is considered a "free radical" or a "random radical".

4. **Solvent cage**. The first shell of solvent molecules which surround a molecule or a radical pair (geminate or random). A pair in a solvent cage undergoes repeated collisions before one of the partners can find a "hole" in the cage wall and become separated by a solvent molecule.

4. **Contact radical pair.** A radical pair (geminate or random) whose partners are in a solvent cage without a solvent molecule between them, i.e., the pair is in contact through repeated collisions. A contact pair is able to react to form molecules through combination reactions directly if it is in the singlet state and the partners of the pair can achieve the appropriate geometry and energy required for reaction. A contact pair in the triplet state is inert to combination reactions because of Wigner's spin conservation rule for elementary chemical reactions.

5. **Solvent separated radical pair.** A radical pair (geminate or random) whose partners are separated by one or more solvent molecules.

Visualization of the Primary Photochemical Step: ^{3}ACO-B $\varnothing$ ^{3}ACO· ·B in Zero Field. The Dynamic Radical Pair.

Imagine the behavior of the representative point during the primary photochemical bond cleavage, ^{3}ACO-B ∅ ^{3}ACO· ·B, in zero field. The point begins to move along the triplet surface as the bond stretched and eventually breaks (Figure 31). Immediately after the bond has broken, the radical pair is produced as colliding neighbors that are born together in a solvent cage (termed the **primary, geminate collisional pair**, step (1) bottom of Figure 31). As the result of random thermally induced motions (the molecular dynamics), the partners of the pair eventually diffuse apart out of the solvent cage (producing a **geminate, solvent separated pair**, step (2) Figure 31, bottom). The solvent separated pairs make random excursions in space and time. Some of the excursions (step 3a in Figure 31, bottom) cause the geminate pair to return to the contact state in a solvent cage (such excursions are termed **reencounters** and such pairs are termed **secondary, geminate collisional pairs**). Some of the excursions lead to separation of the partners of the pair to distances so large (step 3b in Figure 31) that further diffusional trajectories (step 4 in Figure 31 are more likely to have each partner randomly encounter radicals other than the geminate partner (pair that encounger to form contact pair from such excursions are termed **random, collisional pairs**).

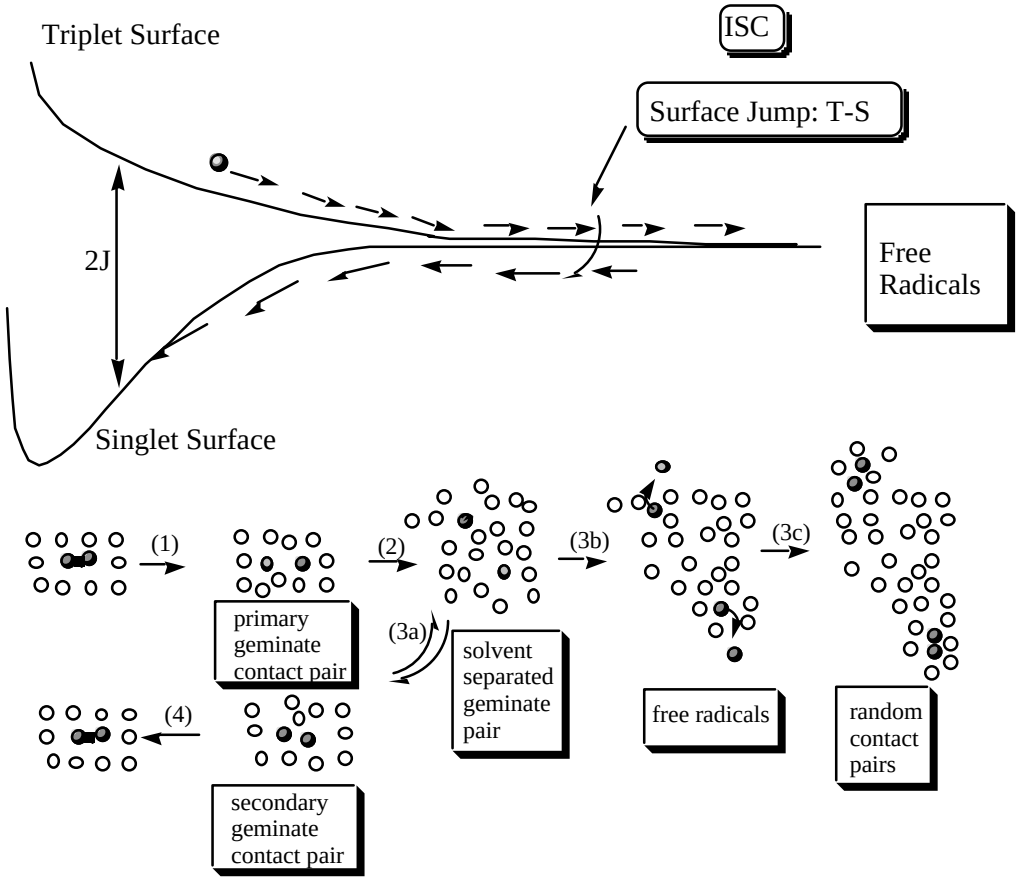

Figure 31. Surface energy diagram displaying the spin and molecular dynamic features of a dynamic radical pair.

The importance of the dynamic model of a radical pair to spin chemistry derives readily from consideration of the behavior of the triplet electronic energy surface on which the radical pair is created and the singlet electronic energy surface which the pair must reach in order to become reactive as a pair. As is shown in the top half of Figure 31, the energy separating the triplet and singlet surface is a strong function of the distance of separation of the pair in physical space. This is due to the fact that the exchange interaction, J, which is the most important contibutor to the energy gap between the S and T surfaces, falls off exponentially as the electrons in the bond being cleaved are separated in physical space. **When J is large compared to available magnetic couplings, it controls the correlated precessional motion of the two odd electron spins of the pair in spin space.**

It is only during the trajectories when the pair is not in contact that intersystem crossing is important, because only under these circumstance can the electron spin experience torques that are effective enough to cause a rephasing ($S\text{-}T_0$) or spin flip ($S\text{-}T_{\pm}$), i.e., it is essentially only during the excursions out of the collisional state that ISC can be induced by the weak magnetic interactions avaliable to induce reorientation or rephasing of the electron spins of the pair, because only for large excursions does the value of J decrease to values close to zero. It is our goal to be able to move fluently from a conventional structural description of the pair through a representative point on an electronic energy surface to one which simultaneously considers the dynamics of the vectors in spin space and the molecular dynamics in physical space of the solvent.

Regions of Magnetic Interactions for a Triplet Electronic Excited State and a Triplet Radical Pair in Zero Field

Consider the breaking of a carbon-carbon bond in an α-cleavage reaction of a triplet ketone. Figure 32 depicts a representative point moving down the triplet surface as the bond breaks. What are the regions for which the point can "jump" from the triplet surface to the singlet surface? Let us consider four regions along the energy surface at which the ISC might occur: (1) a region for which the bond is strongly stretched, but not quite broken; (2) a region for which the bond is completely broken and a contact, collisional pair in a solvent cage is produced; (3) a region for which the pair has separated by at least one solvent molecules; and (4) a region for which the pair is separated to such large distances that the geminate character is lost, i.e., the probability of reaction of random pairs is much greater than the probability of reaction of geminate pairs.

Visualization the Spin Dynamics. Intersystem Crossing in Geminate Radical Pairs in Zero Field.

In the previous sections we have considered the simultaneous visualization of the motion of the representative point along energy surfaces and the molecular dynamics of the diffusional motion of the radical pair after the bond breaks. We now seek to visualize, in zero field, the spin dynamics simultaneous with conventional chemical structures of the pair, which are shown at the bottom of Figure 32. A vector model representation of the triplet is shown on the upper surface and a possible T_+-S ISC is shown (Recall that $S_1 \varnothing T_z \varnothing T_+$ pathway is expected for the cleavage of the ketone triplet). The vector representation showns initial strong coupling of the two individual spin vectors in T_+. This representation means that the two spins are phase and orientation correlated and precess precisely in step. The chemical structure corresponding to this vector representation has the orbitals of the two radicals of the pair overlapping strongly and because of the overlap, strong electron exchange (large J) occurs. We now consider the plausibility of ISC in the various regions of the energy surface explored by the representative point. We must recall that we are dealing with a dynamic representative point for the system that can only move on the triplet or singlet energy surface.

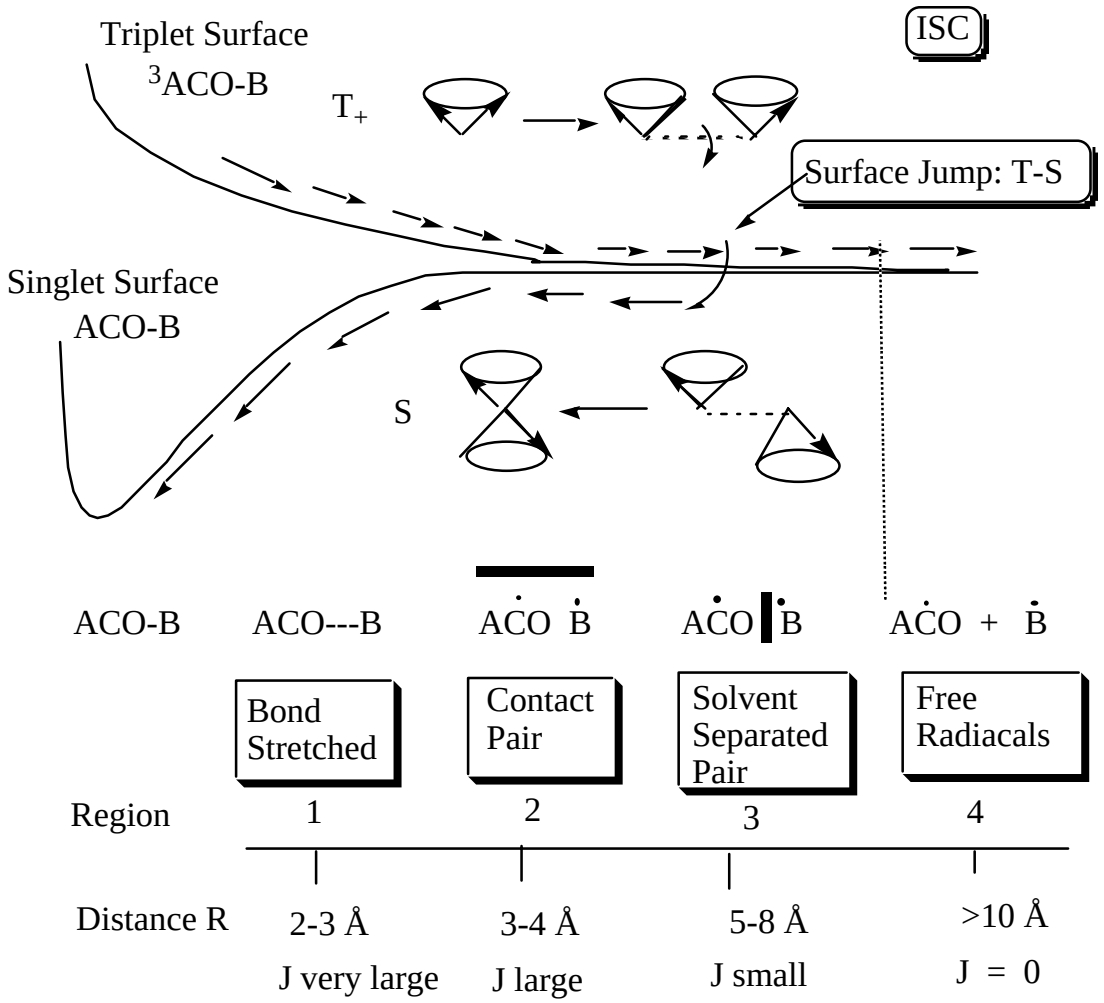

Figure 32. Distance dependence of spin correlated radical pairs. See text for discussion.

The Bond Breaking Step. $T_+ \varnothing {}^3RP$

In the primary cleavage step, $T_+ \varnothing {}^3RP$ to form ACO· ·B (**region 1**, Figure 31, ca < 3Å separation of the partners of the pair), the carbon carbon bond is stretched and then eventually broken. Is ISC palusible during the bond breaking step? The answer is, generally it is not plausible because the act of bond breaking (the time it takes the representative point to "fly through" region 1) takes of the order of a vibrational time period (10^{-13} s) whereas the rate of spin precession in organic molecules is of the order of 10^{-10} s. Thus, the spin vectors are "frozen" in spin space during the time period in which the bond is broken, i.e., the orientation and phase of the spin vectors are identical as the representative point passes through region 1. This conclusion is equivalent to **Wigner's spin selection rule which says that in any elementary step of bond making or bond breaking, the spin state of the reactant and product must be**

identical. This situation may be viewed as a "horizontal" Franck-Condon selection rule for the spin vector: horizontal displacements on a dissociative energy surface occur faster than changes in the angular displacement of the spin vectors, thus, spin orientation is preserved when a bond breaks on a disociative surface. Just as the Franck-Condon Principle is based on inability of nuclei motion to follow electronic reorganization when an electronic transition occurs, the Wigner Principle is based on the inability of spin motion to follow electronic reorganization when a bond is made or broken. As in the conventional Franck-Condon Principle, for which nuclear configuration is preserved upon rapid vertical jumps of the representative point, Wigner version, spin configuration (orientation or phase) is concerved upon rapid horizontal jumps of the representative point.

In addition to the kinetic problem associated with ISC in region 1, these is a second problem associated with coupling magnetic moments of the spins to induce ISC. The value of J is expected to be much larger than any available magnetic interaction for the pair, so that the coupling required for ISC is implausible. Thus, from both the kinetic standpoint and the coupling standpoint, *ISC is considered as implausible in region 1* and this conclusion is incorporated into our working paradigm of the dynamic radical pair.

Trajectories of the Dynamic Radical Pair.

Figure 32 schematically displays three regions of importance (regions 2, 3 and 4 of Figure 32) to the dynamic radical pair. In **region 2** (ca < 4Å separation), the value of J is still expected to be much larger than any available magnetic interaction for the pair, so that ISC will be inhibited. Thus, contact radical pairs experience large values of J compared to magnetic interactions because the single and triplet are split in energy and do not mix; the pair behaves as a spin 1 system, and ISC is difficult. We say that in the contact state the electron spins are strongly correlated. Although we conclude that ISC is implausible when the pair is in the contact state, the kinetic problem of rapid and irreversible passage through region 1 is not present. As a result, if the contact state is particulary long lived or if an exceptionally strong magnetic mixing is avaliable to the pair, ISC may result. However, as a rule in a non-viscous solvent for typical organic radicals, *the paradigm assumes that ISC is implausible in the contact pair. (region 2)*

The solvent separated radical pair experiences a rapidly diminishing exchange interaction, which is expected to falloff exponentially (Eq. 22) in value with separation of the spins. In **region 3** (ca 5-8 Å separation) the value of J is expected to be comparable to the available magnetic interactions for the pair, so that ISC is plausible. We say that for the solvent separated pair the electron spins are weakly correlated. By weakly correlated we mean that the two electron

spins, although correlated, begin to behave as if there were independent doublets. If the pair jumps from the T surface to the S surface, the molecular dynamics may either carry the singlet solvent separated pair toward a reencounter (3a in Figure 32) or toward the formation of random radicals (3b ∅ 4) in Figure 32. Thus, depending on the trajectory followed, either a geminate cage reaction or free radical formation will occur.

In **region 4** the electron correlation is 0 (J = 0) because of the large separation between the unpaired electrons. In Figure 32 the spins are shown as correlated up to a certain point (dotted vertical line) and beyond this distance the pair is separated so far that the exchange interaction can be considered to be zero. Thus, beyond this point the magnetic interactions are so weak that the pair is considered as uncorrelated. Hypothetically, if there were no different magnetic interactions experienced by either spin, then the phase and orientational features of the initial triplet would be preserved even at infinite distances of separation! However, it is more likely that weak magnetic interactions which are not dependent on the separation of the radicals, such as electron spin-lattice coupling, electron spin orbital coupling and electron spin-nuclear hyperfine coupling, will cause the spins to lose the phase and orientational correlation imposed by the exchange interaction. In this region the pair is not well represented as a singlet or triplet, but as a pair of doublets, i.e., neither the phase nor the orientation of the spin on one center influences the phase or orientation of the the spin at the other center.

Order of Magnitude Estimates of ISC.

We can obtain some insight to the magnitude required for magnetic effects to uncouple the exchange interaction and allow ISC by considering the relationship between the precessional rate, ω (in units of rad / s), and the exchange energy, J (in units of gauss, G). The rate of precessional motion of the electron spins that are coupled by the exchange coupling is given by eq. 30, which is analogous in form to Eqs. 12 and 13.

$$\omega_{ex} = 2J/\backslash \qquad (30)$$

From various modeling of organic radical pairs the value of J falls off roughly exponentially as a function of separation of the radical pairs. An approximate expression for this function is $J \sim 10^{10}10^{-R}$, where the units of separation are Å and the units of J are in G. This, means that the following relationships hold for the four regions of Figure 31: Region 1, $J \sim 10^{12}$ G; region 2, $J \sim 10^{8\text{-}9}$ G; region 3, $J \sim 10^{2}$ G; region 4, J ~ 0 G. We can compare these values of J to the magnitude of hyperfine couplings of typical organic radicals (100 G) and it is clear that only in region 3 is ISC plausible, unless some exceptionally strong coupling or very long

lifetime is available in region 2. We can also compare these estimates to the value of a the magnetic field of 1,000 G (of the order of typical ESR spectrometers). We note that the applied field will control the spin motion of solvent separated (weakly correlate) geminate pairs and free radicals, but not contact pairs. Let us now consider the influence of application of a high field on spin chemistry and then consider the magnetic resonance spectroscopy of the pair in the three resgions of the energy surface.

15. The Dynamic Radical Pair at High Field

We now consider the dynamic radical pair in a high magnetic field. These are the typical conditions under which magnetic resonance measurements are made and under which ISC of the pair may be strongly influenced by the coupling of electron and nuclear spins to the applied field. First let us consider the effect on the applied field on the triplet and singlet energy surface (Figure 33). At zero field there is a single triplet energy surface because the three triplet sublevels (T_-, T_+ and T_0) are degenerate. At high field the three surfaces are split in energy, with T_0 maintaining the same magnetic energy it had at zero field, with T_- decreasing in energy as the result of Zeeman coupling and with T_+ increasing in energy as the result of Zeeman coupling.

Figure 33, as Figure 32, can be analyzed in terms of four regions: (1) region 1 for which the singlet triplet splitting is much larger than the Zeeman energy; (2) region 2 for which the singlet triplet splitting is of the order of the Zeeman interaction; (3) region 3 for which the singlet triplet splitting is zero, but the dynamic pair is geminate and is likely to experience reencounters; and (4) region 4 for which the singlet splitting is zero but the dynamic pair is separated to such large distance that the probability of a reencounter is vanishlying small and the pair can be viewed as a random pair or free radicals. We note in particular from the standpoint of ISC, that ISC of the geminate dynamic pair is not likely in region 1 (large S-T gap quenches ISC), that in region 2 a $T_-\varnothing S$ surface "crossing" occurs and provides a pathway for ISC and that in region 3 a $T_0\varnothing S$ surface "touching" occurs and provides a pathway for ISC.

ESR spectrum of weakly correlated dynamic spin pairs. Spin Correlated Radical Pairs in Regions 2 and 3.

As discussed above, a dynamic geminate radical pair experiences a fluctuation between large values of J (contact pair, region 2, Figures 32 and 33) and weak value of J (solvent separated pair, region 3, Figure 32 and 33). Irreversible separation of the pair into random radicals competes with the oscillation of the pair back and forth between the contact and solvent separated states, i.e., reencounters. Let us now consider the ESR spectra expected for the pair in each of the regions. In region 2 if the magnitude of J is sufficiently large, the ESR spectrum is expected to be similar to that of the molecular triplet discussed in section 12. However, in fluid solution, because of the effects of dipolar interactions between the coupled spins and molecular rotation, the ESR spectrum is not a series of relatively sharp lines corresponding to transitions between well defined magnetic energy levels, but a is a broad, difficultly measurable spectrum corresponding to a wide range of transition for each possible molecular orientation in the magnetic field.

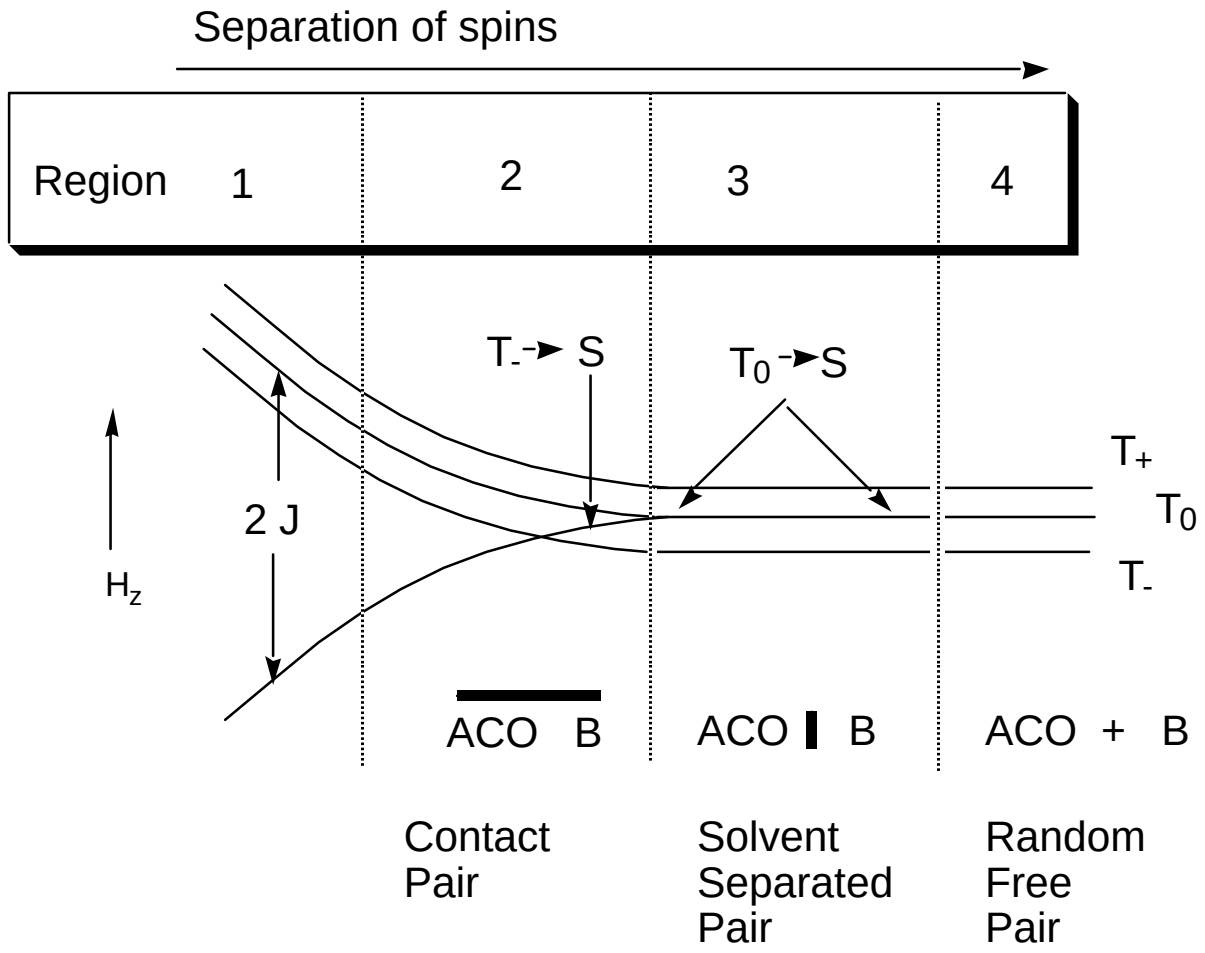

Figure 33. Effect of Zeeman splitting on the energy surface for the α-cleavage of a triplet ketone.

However, in region 3 the magnitude of J is small relative to the Zeeman coupling so that the spins are weakly correlated to each other, but strongly coupled to the applied field. It is therefore possible to consider a pair in this region as **spin correlated radical pair** (SCRP) whose ESR is determined by the doublet character of the individual radicals. Furthermore, during the excursions between the contact and separated states the radical partners of the pair undergo many rotations so that the dipolar magnetic interactions are small (Eq. 28) and may be averaged to zero. As a result, the ESR of a dynamic radical pair is expected consider of relative sharp signals and to be observable if an ESR measurement can be made during the lifetime of the dynamic radical pair. Experiments are possible through time resolved ESR instruments which are capable of time resolutions of ca 100 ns. However, dynamic geminate radical pairs in homogeneous solutions generallly possess lifetimes much shorted than 100ns, the lifetime of the geminate pair must be extended by some sort of constraint which delays separation into random radicals. This can be done either

molecularly by attaching the spins through a flexible covalent linkage or supramolecularly by adsorbing the spins non-covalently in a constrained space such as a micelle.

As a model for the ESR of SCRP, we consider the magnetic energy diagram shown in Figure 34 for our prototype geminate pair, ACO· ·B. In the absence of any exchange interaction T_0 and S have precisely the same energy and the Zeeman splitting of T_- and T_+ from T_0 are identical. Thus, the ESR consists of a single line due to two overlapping transitions at ω_0 ($T_- \varnothing T_0$ and $T_0 \varnothing T_+$, Figure 34, left). In the presence of an exchange interaction that is weak relative to the Zeeman interactions, and in the presence of some coupling of the S and T_0 states (through hyperfine coupling, spin orbit coupling, etc.) the S and T_0 states split and create the new energy level diagram shown in Figure 34 (middle).

The number of transitions observed experimentally will depend on the extent of state mixing and electron exchange, which will determining the probability of transitions between the various levels. For example, if the mixing is strong, transitions between the nominal S and T levels can be observed. On the right of Figure 34 is shown one of the simplest cases: the net effect is raising the energy of the T_0 state so that the $T_- \varnothing T_0$ transition occurs at higher frequency than the $T_0 \varnothing T_+$ transition. When such is the case, the frequency difference between the transitions can be related to the magnitude of the electron exchange, J. Inspection of the energy diagram shows that the splitting between two adjacent transitions is equal to J, the singlet triplet splitting. The situation is exactly analogous to that for NMR splitting for which the separation between adjacent transition is equal to the nuclear spin-spin splitting.

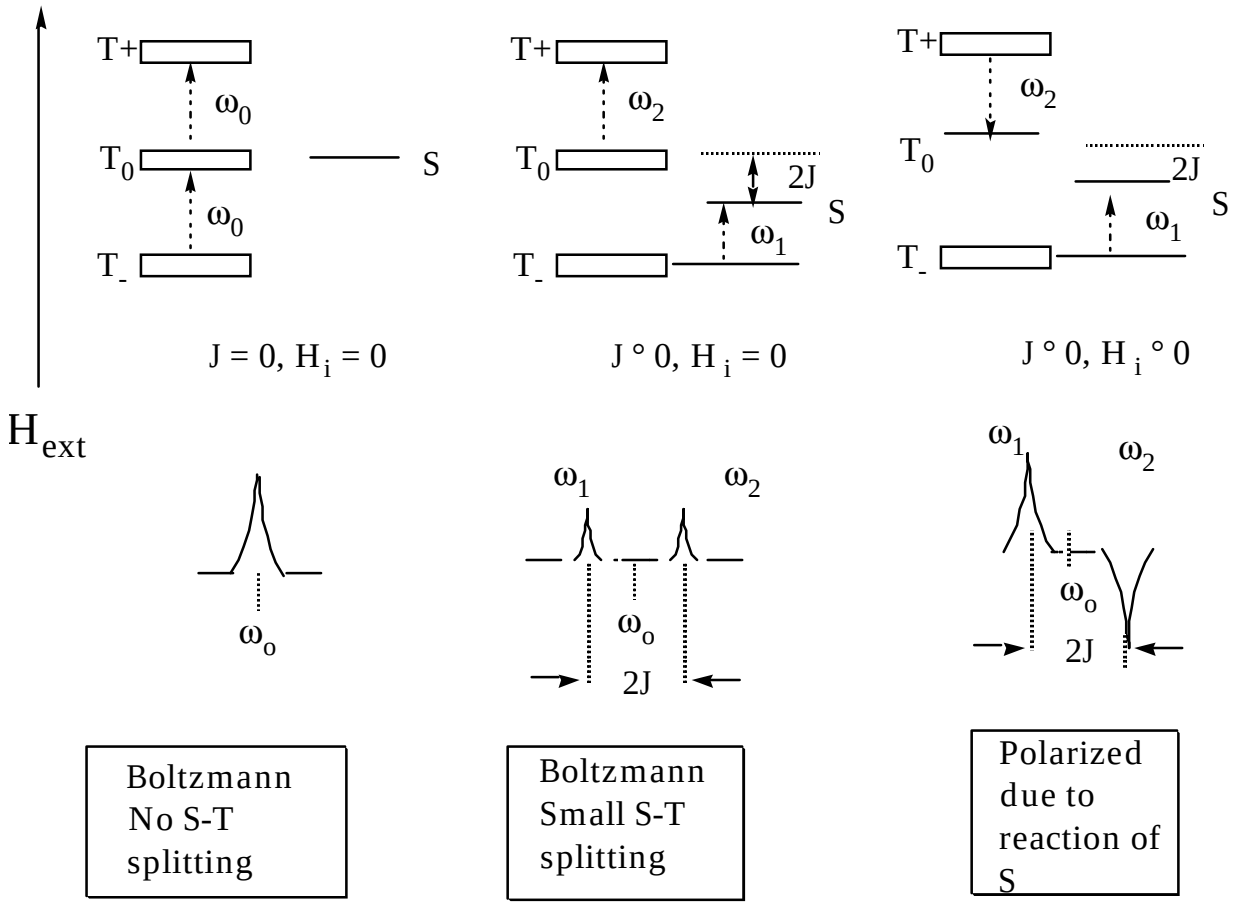

Figure 34. Schematic representation of the effect of exchange interaction and S-T mixing on the ESR spectrum of a weakly spin correlated radical pair.

The ESR of a spin correlated dynamic radical pair in homogeneous solution has not been observed by conventional ESR spectroscopy, but has been observed through time resolved polarized ESR spectroscopy. The basic idea behind the polarization is that because of the mixing of the S and T_0 levels, the T_0 level is selectively depleted through ISC and as a result the T_- and T_+ states are "overpopulated". Since the probability of radiative transitions is related to population differences (Eq. 27, Figure 25) the probability of transitions to T_0 from the T_- and T_+ states occur well above the probability of transitions due to the Boltzmann population. The experimental result is that instead of two absorptive signals corresponding to the weaker Boltzmann population (Figure 34, middle), there will be one absorptive signal at low frequency (ω_1) and an enhanced emission signal at high frequency (ω_2). This is a striking prediction and is observed experimentally for many biradicals and supramolecular radical pairs in micelles. For these systems the conditions for a long lived geminate pair are optimal.

ESR of Radicals Produced from Spin Selective Intersytem Crossing.

We have seen that the intersystem crossing step, $S_1 \varnothing T$ leads to the specific population of one of the three triplet levels and that for a ketone this is typically the highest magnetic sublevel (T_z). The selectivity results from spin orbit coupling, which favors the coupling of the spin to the z axis of the molecular frame. Immediately after ISC, the T_z level is overpopulated and the lower energy T_x and T_y levels are underpopulated relative to the equilibrium populations dictated by the Boltzmann distribution (Figure 29). The spin system will begin to rapidly equilibrate the three triplet sublevels through spin lattice relaxation. However, if the triplet unders a reaction to produce a radical pair ($^{*3}R\varnothing\ ^{3}RP$), the overpopulation of the T_z may be carried over to the radicals of the geminate pair and then to the free radicals after pair separation. The time scale of spin lattice relaxation among the triplet sublevels is of the order of 10^9 s^{-1}. Thus, the rate of α-cleavage must be of this order to compete with spin lattice relaxation and carry the polarization over to the radicals, ACO· ·B (for simplicity we ignore hyperfine coupling). If this occurs the resulting free radicals are overpopulated in the D_+ levels. .

Figure 35 schematically shows the process $S_1 \varnothing T_z \varnothing T_+ \varnothing$ ACO· (D_+) + B· (D_+). The time of spin relaxation of free radicals is of the order of microseconds, which is well within the time scale of conventional time resolved ESR spectroscopy, so that polarized radicals can be readily detected experimentallyTypically, the ACO· radical has a smaller g factor ($g_1 \sim 2.001$) than B· ($g_2 \sim 2.003$) radicals that are carbon centered. The observed spectrum of the radicals consists of two signals, one for each radicals and is identical in frequency to that for the radicals at the Boltzmann; however, the **entire** spectrum is in **emission** rather than absorbtion. Experimentally, the observatino of such an emission is evidence that the $S_1 \varnothing T_z \varnothing T_+$ steps have occured and that $S_1 \varnothing T$ ISC is spin sublevel selective. Thus, this example shows how the time resolved ESR of free radicals, produced by the reaction of triplets, can provide indirect information on the S_1 to T ISC crossing step preceeding the formation of a triplete radical pair! It is an excellent example of "spin memory" and the fact that even in solution at room temperature spin

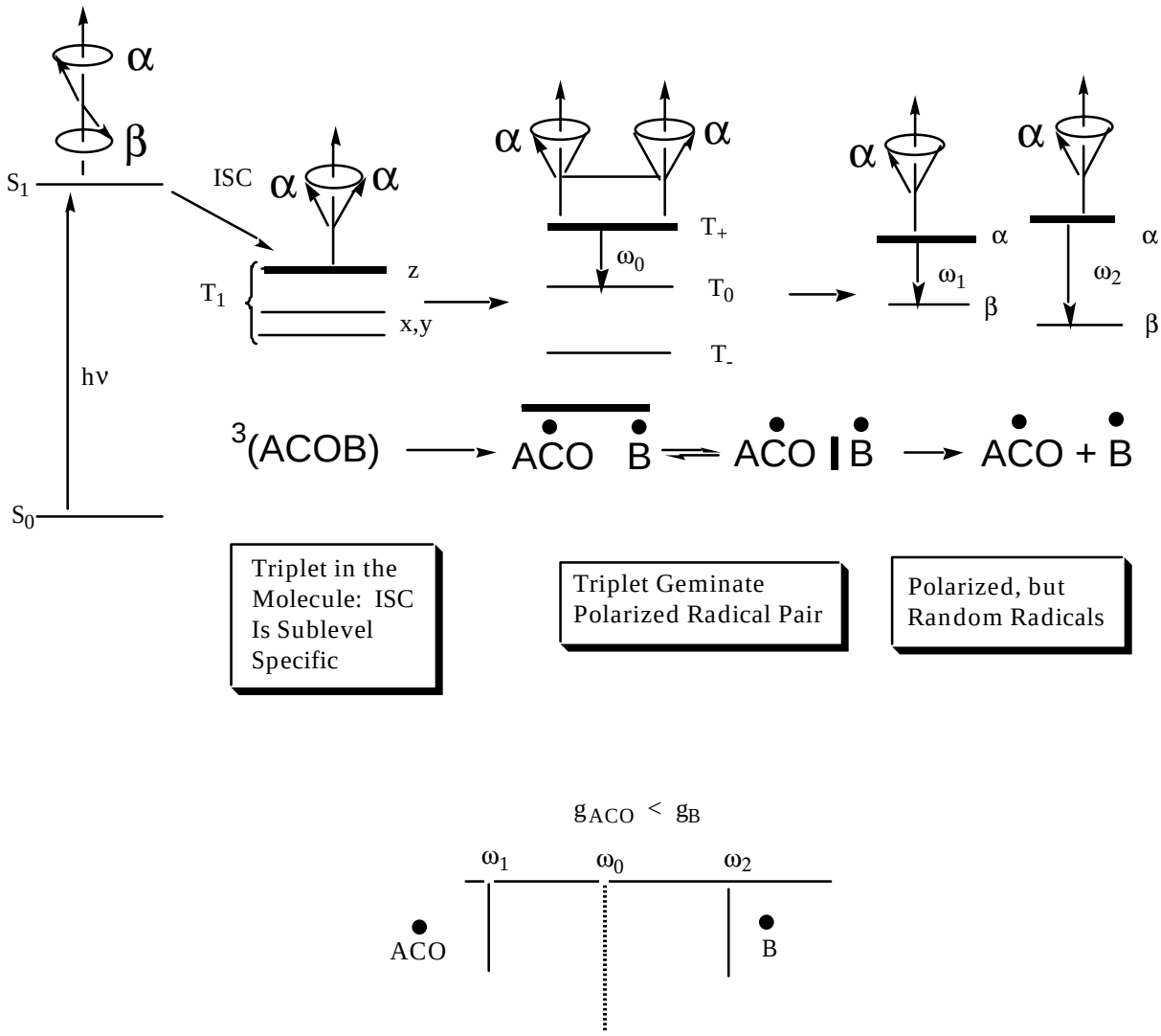

Figure 35. Schematic of the pathway of electron spins from sublevel ISC to cleavage to form spin polarized random radicals.

relaxation may be sufficiently slow as to be measured by both direct (polarized radicals) and indirect means (inferred mechanism of polarization).

ESR of Radicals Containing a Hyperfine Coupling

Radical pairs in regions 2 and 3 possess correlated electron spins. We have seen how the correlation or coupling of two electron spins can influence observed ESR spectra and how ESR spectra of correlated electron spins can lead to information on the electronic structure of triplet states and the mechanism of ISC. Now we consider the coupling of a single electron spin with a magnetic nucleus influences the ESR spectrum of a radical and the ISC of a radical pair. In actual cases it is usually the rule that an electron spin will be coupled to more

than one nuclear spin. However, the basic featurtes of the ESR of an electron spin coupled to a single nulcleus of spin 1/2 will reveal most of the basic features of the ESR of carbon radicals, the most important family of radicals invovled in organic photochemical reactions.

ESR of Radical Pairs in Regions 3 and 4.

The energy diagram for an electron coupled to a nuclear spin of 1/2 is shown in Figure 15. Figure 36 compares the energy level diagram for the spinomeric radicals $A^{12}CO\cdot$ and $A^{13}CO\cdot$. We recall from Eq. 14 that the frequencies, ω, at which the ESR signals of radicals without hyperfine couplings are observed is related to the energy differences between the energy levels. These energy differences are readily computed for our simple example of a single hyperfine coupling from Eq. 31. We note that the magnetic energy of the hyperfine levels depend on two quantum numbers: M_S the quantum number for the electron spin and M_I the quantum number for the coupled nucleus. In addition the energy depends on the hyperfine coupling constant, a and the Zeeman terms, g_1, μ_e, and H_Z.

$$E_{SI} = \backslash\omega = M_S g_1 \mu_e H_Z + M_I M_S a \qquad (31)$$

The energies of the magnetic levels, computed from Eq. 31, are listed in Figure 36. The frequencies for the ESR transitions are obtained by dividing the right hand of Eq. 31 by \ (Eq. 32).

$$\omega = [M_S g_1 \mu_e H_Z + M_I M_S a]/\backslash \qquad (32)$$

The frequencies of the ESR signals for the $A^{12}CO\cdot$ and $B\cdot$ radicals (a assumed to be zero) occur at frequencies $g_1\mu_e H_Z/\backslash$ and $g_2\mu_e H_Z/\backslash$, where g_1 and g_2 are the g factors of the $A^{12}CO\cdot$ and $B\cdot$ radicals, respectively.

From Eq. 32 we note that in the absence of hyperfine coupling (a = 0), the frequency at which the signal is observed depends only on the g factor and the magnetic field strength. In the presence of a single hyperfine coupling, the energy levels correspond to those of Figure 36. Recall that the allowed ESR transitions are between the levels for which the electron spin changes orientation ($\beta_\varepsilon \varnothing \alpha_e$) but the nuclear spin orientation is conserved. The observed spectrum of the radical $A^{13}CO\cdot$ thus consists of two lines, whose frequencies, ω_1^{α} and ω_1^{β}, are given by Eq. 33 and 34, for $M_s = +1/2$ and $M_s = -1/2$, respectively. We label the frequencies ω_α and ω_β for the quantum numbers $M_s = +1/2$ and $M_s = -1/2$, respectively.

$$\omega_1^{\alpha} = g_1\mu_e H_Z / 2\backslash + a/4 \qquad (33)$$

$$\omega_1^{\beta} = g_1\mu_e H_Z / 2\backslash - a/4 \qquad (34)$$

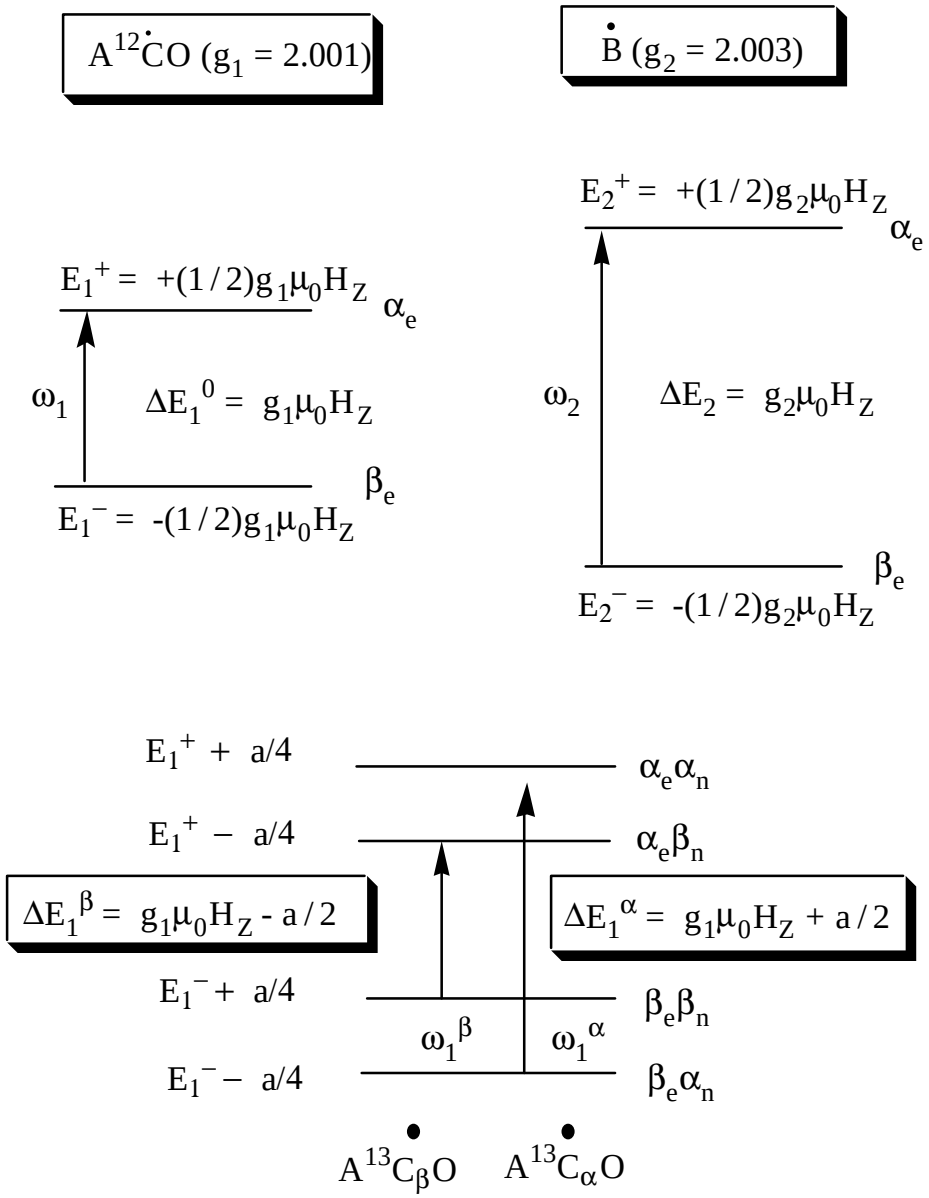

Figure 36. Energy level diagrams for the radicals $A^{12}CO$, $A^{13}CO$ and B. See text for discussion.

The ESR of the $A^{12}CO$ and $A^{13}CO$ radicals

Figure 37 displays the ESR spectra of a solution containing an equal number of $A^{12}CO\cdot$ and B· radicals (top) and a solution containing an equal number of $A^{13}CO\cdot$ and B· radicals (bottom). In the absence of hyperfine coupling the spectrum of the (separated) $A^{12}CO\cdot$ and B· radical pair consists of two signals: one at $\omega_1 = g_1\mu_e H_Z/\backslash(A^{12}CO\cdot)$ and one at $\omega_2 = g_2\mu_e H_Z/\backslash(B\cdot)$. For a typical g_1 of 2.001 for the $A^{12}CO\cdot$ a radical and a typical g_2 of 2.003 for the B· radical, the ESR signal of the $A^{12}CO\cdot$ radical will occur at lower frequency, since ω is directly proportional to g at a fixed field.

In the presence of the single ^{13}C hyperfine coupling, the spectrum of the (separated $A^{13}CO\cdot$ and B· radicals consists of three signals: one at $\omega_2 = g_2\mu_e H_Z/\backslash(B\cdot)$ and two split symmetrically by a/2 Gauss about the frequency $\omega_1 = g_1\mu_e H_Z/\backslash$. The signal at lower frequency is labeled ω_1^{α} and corresponds to the ESR of the spinomer $A^{13}CO(\alpha_n)$, i.e., the carbonyl radical possessing a nuclear spin with α orientation with respect to the magnetic field. The signal at higher field is labeled ω_1^{β} and corresponds to the ESR of the spinomer $A^{13}CO(\beta_n)$, i.e., the carbonyl radical possessing a nuclear spin with β orientation with respect to the magnetic field. Since ω_1 is the frequency for the $A^{12}CO\cdot$ transition, then the frequencies of the ω_α and ω_β transitions are given by Eqs. 35 and 36, respectively. Thus, the ESR spectrum of the free $A^{13}CO\cdot$ and B· radicals consists of three signals consists of three lines: (1) a low frequency line whose frequency is $\omega_1^{\beta} = \omega_0 - (a/2)/\backslash$; (2) a medium frequency line whose frequency is ω_2; and a high field line whose frequency is $\omega_1^{\alpha} = \omega_0 + (a/2)/\backslash$. A typical hyperfine coupling for a $A^{13}CO\cdot$ radical is 120 Gauss.

$$\omega_1^{\alpha} = \omega_1 + (a/2)/\backslash \qquad (35)$$

$$\omega_1^{\beta} = \omega_1 - (a/2)/\backslash \qquad (36)$$

In Figure 37, a vector model representation of the magnetic basis of the hyperfine coupling is shown. A nucleus with an α orientation possesses a magnetic moment vectors that points in the direction of the applies field. Thus the electron experiences not only the applied field, H_z, but also the hyperfine field a/2, which augments the applied field. The electron precesses **faster** in the higher field $H_z + a/2$ than it does in H_z alone. On the other hand, a nucleus with an β orientation possesses a magnetic moment vectors that points opposed to the direction of the applied field. Thus the electron experiences not only the applied field, H_z, but also the hyperfine field a/2, which dimunishes the applied

field. The electron precesses **slower** in the higher field $H_z - a/2$ than it does in H_z alone.

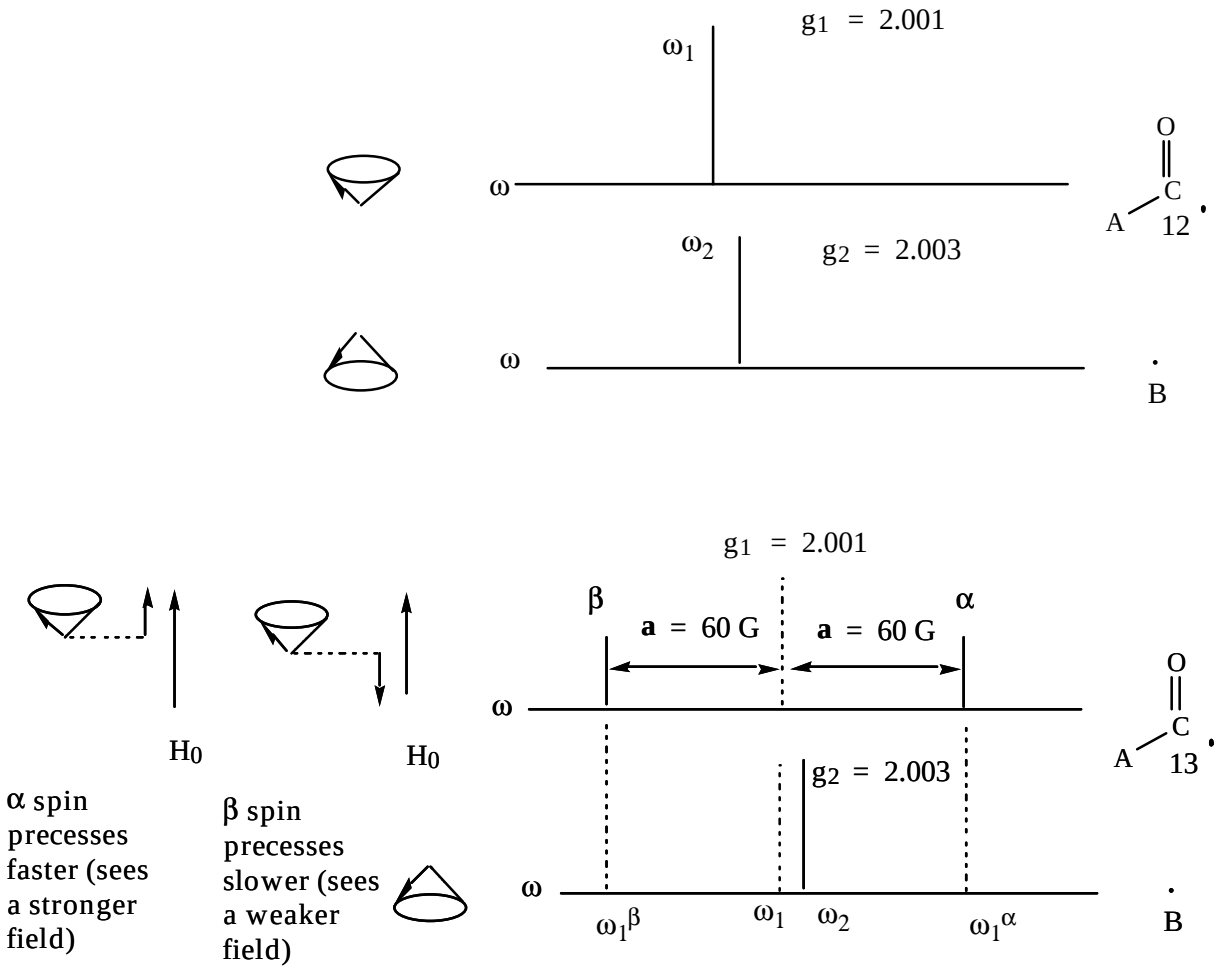

Figure 37. Schematic of the ESR of two spinomeric free radical pairs. Top: the $A^{12}CO$ B pair. Bottom: the $A^{13}CO$ B pair.

16. Reactions of the Radical Pairs. The I∅ P Step of the Paradigm

Let us consider the product forming step in the general photochemical paradigm, i.e., the I∅ P process shown in Figure 1. From the discussion of this chapter, we see that this step, for which the primary photochemical product is a geminate triplet dynamic radical pair, $^3I_{GRP}$, is not a simple elementary step involving passage of a representative point over a single energy barrier. Instead the I∅ P "step" is a complex set of steps involving molecular diffusion dynamics, spin dynamics and chemical dynamics and extensive motion of the representative point back and forth along the energy surface. It is convenient to classify the pathways from I to P as two types:
(1) formation of products produced from reactions of geminate pairs, and
(2) products produced from random pairs. Geminate pairs are born together and can be traced back to a primary photochemical event of the same parent molecule, whereas random pairs result from encounters or "free radical" partners that were generated in independent primary photochemical events. Geminate products produced by reactions of geminate radical pairs are often termed "cage" products or "recombination" products, but these terms are ambiguous, since random pairs also require encounters and formation of a caged pair to form products, and often the same products are produced by geminate or random pairs.

There are two methods, one chemical and one spectroscopic that can be employed to distinguish between the products of geminate and random radical pairs. The chemical method involves sorting the geminate and random pair reactions through **chemical scavenging** experiments which selectively scavenge the free radicals leading to random pairs leaving behind only products due to geminate pair reactions. The spectroscopic method involves the sorting of the geminate and random pair reactions through the NMR determination of the nuclear spin orientation in the products. The latter method, termed chemically induced dynamic nuclear polarization (CIDNP) provides a nice example of how the interplay of molecular, spin and chemical dynamics results in an unusual spectroscopic observation which provides detailed information on the structure and dynamics of the radical pair leading to isolated products, i.e., the I∅ P step of Figure 1.

We employ our case study pair, I = ACO· ·B, to exemplify how chemical and spectroscopic methods can be employed to sort out the reactions of geminate and random pairs.

Chemical Sorting Geminate and Random Radical Pair Reactions. Scavenging of Free Radicals.

Singlet radical pairs, random or geminate, undergo two typical reactions when they are in the contact state (Region 1) in a solvent cage:
(1) combination and (2) disproportionation. The former involves bond formation between the radicals to generate a molecule, and the latter involves hydrogen transfer between the radicals to form two molecules. We need only consider one of the two in our case study and we select the simpler process, combination. However, we emphazise that the discussion is appropriate for either combination or disproportionation products of radical pairs.

Let us assume that the triplet, geminate pair, ACO· ·B, produced by the primary process of α-cleavage of ^{3}ACOB, may undergo two pathways to form radical pair combination products: (1) geminate pair recombination to form the combination product ACOB (Eq. 37.) and (2) random pair combination to form ACOCOA, ACOB and BB (Eq. 38).

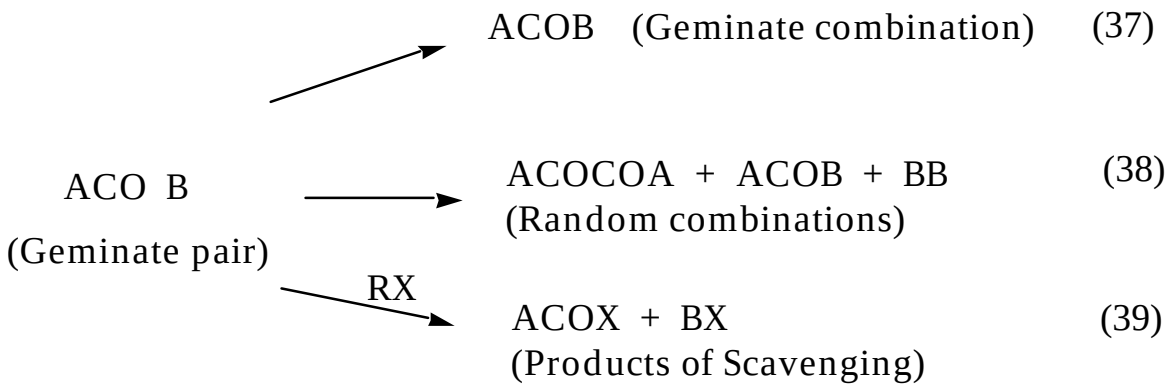

The two products ACOCOA and BB (Eq. 38) cannot be geminate products based on simple atomic composition considerations, i.e., each requires the dissociation of two precursor ACOB molecules. However, the ACOB product could arise from either a geminate combination (Eq. 37) or a random combination (Eq. 38). These two possibilities can be distinguished through chemical scavenging of free radicals. Suppose a molecule RX (here X may be a halide such as Cl or Br) reacts very rapidly with each of the free radicals ACO· and B·. If the rate of reaction of the free radicals with RX is fast enough, then at a high enough concentration of RX, all of the radicals that do not undergo geminate combination to form ACOB (Eq. 37) can be scavenged by RX to form the products shown in Eq. 39. **When this is the case, the ACOB formed through the combination of free radicals will be absent from the reaction mixture and the ACOB formed must result entirely from geminate combination.** We note that Eqs. 37 and 38 are spin dependent reactions because the product molecules are singlets, i.e., they are forbidden when the pair is in the triplet state. However, the scavenging reaction, Eq. 39 is spin independent since the reactants

and products are doublets (although the orientation of the doublet spin in the reactants and products must be identical.

The efficiency of geminate combination reactions (Eq. 37) is termed the "cage effect" and may be defined in terms of the fraction of geminate pairs that are generated to those undergoing recombination. However, the fraction of geminate pairs formed is difficult to determine experimentally. Instead, the quantum yield for the cage effect is often determined. The quantum yield for the cage effect is defined as the number of geminate combinations relative to the number of photons absorbed. It is also possible to define the cage effect in terms of the probability of combination without determining the fraction of geminate pairs formed. This technique involves the use of an optically active ketone and the measurement of racemization that occurs as a function of the extent of photolysis.

Spectroscopic Sorting Geminate and Random Radical Pair Reactions. Chemically Induced Dynamic Nuclear Polarization (CIDNP).

NMR spectra taken during a photochemical reaction sometimes result in unusual features: some signals possess a phase which is in emission rather than an absorption and some signals possess an enhanced absorption intensity which is much stronger than expected for the number of moles of material in the sample. Furthermore, when the source of photochemical excitation is removed, the emission and enhanced absorption signals disappear rapidly but can be regenerated when the exciting source is reestablished. Extensive investigations have shown that these unusual NMR features occur only for signals due to the products of reactions of free radicals and radical pairs, e.g., such as those of Eqs. 37-39. The "dynamic radical pair" theory we have employed in this chapter was, in fact, developed to explain the phenomena of NMR spectra showing emission and enhanced absorption, which is termed "*chemically induced dynamic nuclear polarization*" or more usually referred to as CIDNP.

We now briefly review the Wigner spin selection rules for elementary chemical steps that form a natural conceptual framework for understanding the fundamental principles of CIDNP.

Wigner Selection Rules for Reactions of Radical Pairs.

An elementary chemical step is conceptually defined as the passage of a representative point over a single bond making or bond breaking barrier on an energy surface. Wigner's Spin Selection Rule states that spin angular momentum must be conserved (unchanged) in any elementary chemical step. Thus, *electron*

and nuclear spin must be conserved during any elementary chemical step, such as the making or breaking of a chemical bond in a combination reaction such as Eq. 37. The same principle holds for radiative or radiationless transitions since the conservation of angular momentum is as fundamental as the law of conservation of energy.

The application of Wigner's rule to the geminate reactions of dynamic radical pairs leads to the following principles of CINDP:

(1) Combination reactions depend on the **electronic spin** state of the dynamic radical pair, reaction from the singlet being allowed and reaction from the triplet being forbidden;

(2) Combination reactions depend on the **nuclear spin** of the dynamic radical pair, the rate of intersystem crossing of a dynamic radical pair depending on the orientations of the nuclear spins that are hyperfine coupled to the electron spins in the radical pair.

Thus, although the electron spin controls bond formation and therefore combination reactions directly, the nuclear spin indirectly determines the rate of bond formation through hyperfine coupling which influences the rate of intersystem crossing. According to the principles stated above, a triplet radical pair (geminate or random) cannot undergo combination reactions (the product, Eq. 37, is a singlet!) and therefore **a triplet geminate radical pair is chemically inert**. In order to form a product the triplet geminate pair must undergo ISC to a singlet geminate radical pair. As we have seen in the previous section, different nuclear spin orientations cause electron spins to precess at different rates. We shall now see how the influence of nuclear spin orientation on electron spin precession in turn can cause intersystem crossing to occur faster for some nuclear orientations than for others, so that combination or "cage" reactions starting from a triplet pair will occur faster for the spin orientations that cross more rapidly to the singlet state. Thus, the two CIDNP principles lead to the conclusion that **the reactivity of a radical pair depends on the spin orientation of the nuclei present in the pair.** We now employ the vector model to understand the nuclear spin dependence of chemical reactivity.

Vector Model of CIDNP.

Figure 38 presents a schematic vector model that will assist in understanding how the orientation of nuclear spin could influence the rate of intersystem crossing of a geminate triplet pair and how the different rates of ISC for different nuclear orientations lead to the ^{13}C CIDNP spectrum observed when A^{13}COB is photolyzed in an NMR spectrometer. We must point out that

we are observing ^{13}C NMR, which results from the spinomeric pair $A^{13}C_{\alpha}O$ B and $A^{13}C_{\beta}O$ B and that the spinomeric pair $A^{12}CO$ B does not enter into the analysis (because ^{12}C does not have a nuclear spin and therefore does not have an NMR!). Next we point out that the experiment is being performed in the high field of an NMR spectrometer so that the energy surface of Figure 33 applies in our analysis of CIDNP. Finally we note that the same ideas will apply to ^{1}H or other magnetic nuclei occurring in organic molecules (^{31}P, ^{19}F, etc.).

Let us now follow the vector description of the two unpaired electron spins from the molecular triplet state through the formation of products from geminate pairs and free radicals. In the triplet state, ^{3}ACOB, the two electron spins are tightly coupled by the exchange interaction (Region 1 of Figure 33). The triplet geminate radical pair produced by α-cleavage is originally born as a primary contact pair (Region 2 of Figure 33), and must become a solvent separated pair (Region 3 of Figure 33) in order to undergo $T_0 \varnothing$ S intersystem crossing. In Figure 38 we show these situations in terms of tightly coupled electronic spins in the molecular triplet and in the contact pair and loosely coupled spins in the solvent separated state. The trajectories from the contact state to the solvent separated state and the subsequent reencounter is termed a **random walk diffusion of a dynamic radical pair.** If during these random walks a triplet geminate pair undergoes ISC to form a singlet geminate pair, upon reencounter (return to Region 2) in the contact state a recombination reaction can occur, i.e., the originally cleaved bond can reform. In Figure 38 we visualize this process as it would occur in a strong magnetic field, i.e., one for which only the T_0 and S states of the pair are capable of undergoing ISC, because only these two states are capable of becoming degenerate in a strong magnetic field.

In Figure 38 the spinomer, $A^{13}C_{\beta}O$ B is shown undergoing a faster $T_0 \varnothing$ S ISC than the $A^{13}C_{\alpha}O$ B pair. If this is correct, the geminate product of combination (ACOB) will be enriched in β nuclear spins and the scavenging product (ACOX) will be enriched in α spins! We now need to justify the hypothesis that the β orientation of ^{13}C nucleus lead to a faster ISC than the α orientation of ^{13}C nuclei. Let us now see how inspection elementary quantum mechanical relations and the ESR spectra of Figure 37 leads to the conclusion that the $A^{13}C_{\beta}O$ B pair undergoes ISC faster than the $A^{13}C_{\alpha}O$ B pair.

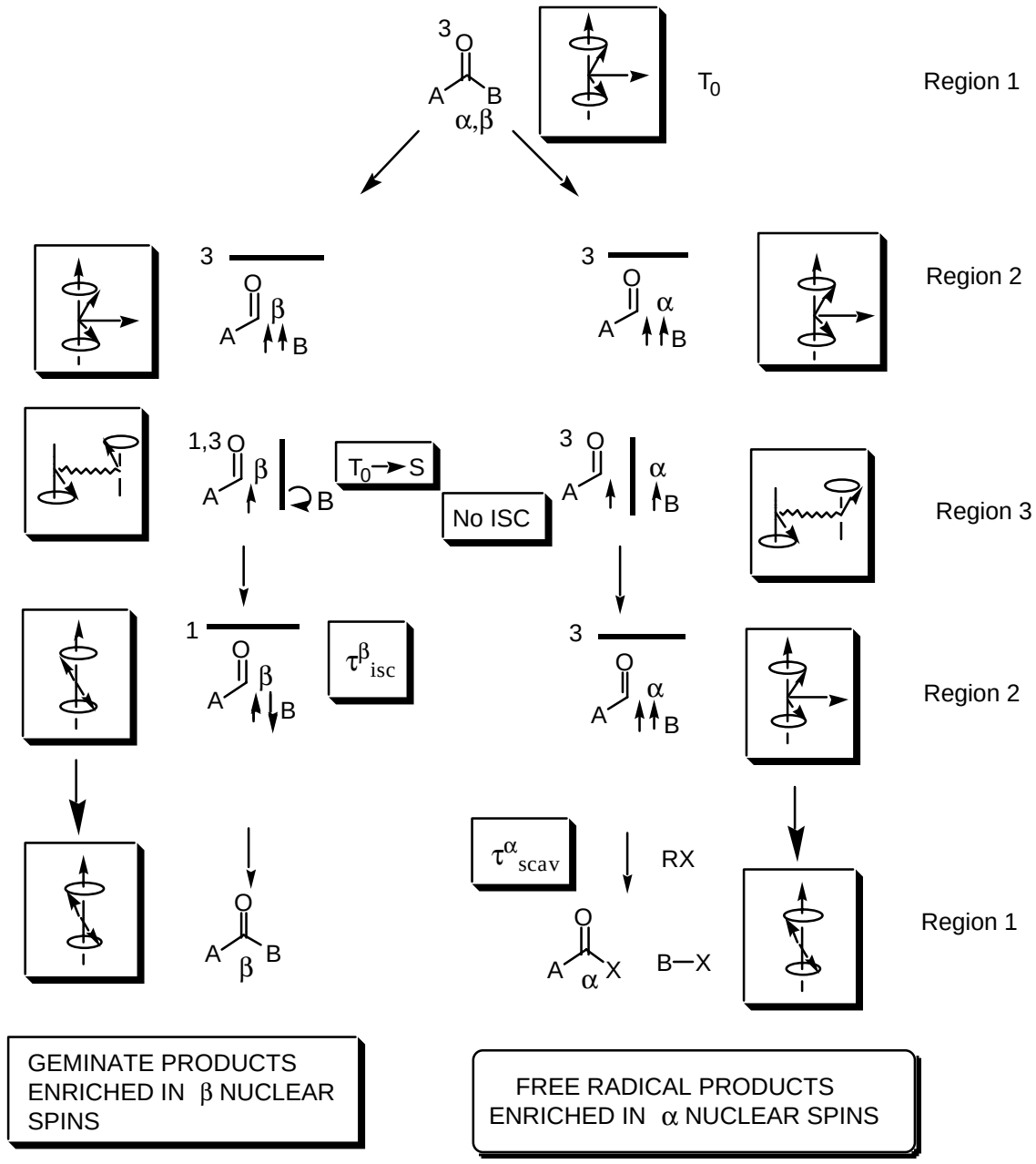

Figure 38. Vector model of the nuclear spin sorting that occurs in the dynamic radical pair. See text for discussion.

The connection between ESR spectroscopy and CIDNP

As discussed above, since both ESR spectra and NMR spectra are experimentally observed at high fields, the pertinent energy diagram for the dynamic radical pair under condition of magnetic resonance observation is given by Figure 33. At high field we are dealing only with T_0-S ISC (since T_+ and T_- are split off resonances from S) and strong coupling of the electron and nuclear spins

to the z-axis. Thus, at high field, the issue of ISC is which spinomeric radical pair, $A^{13}C_{\alpha}O$ B or $A^{13}C_{\beta}O$ B, undergoes more rapid **spin rephasing** about the z-axis? In other words, which spinomeric pair has the greatest difference in precessional frequencies, $\Delta\omega$? For example, if $\Delta\omega = 0$, then both partners of the pair will possess identical precessional rates, and the electron spins would never get out of phase and ISC would not occur! **It is the difference in magnetic fields due to g factors and hyperfine coupling that cause the spins to precess at different rates so that $\Delta\omega$ is not equal to 0.** Recalling that the precessional rates of an electron spin depends on the orientation of the nuclear spin (Figure 37), we can now determine which spinomeric pair is rephased more rapidly by simply considering the frequencies at which the lines occur in the ESR spectra of the spinomeric pairs. We will then consider the more generalized form of the rephasing process.

In Figure 39 the ESR spectrum of the $A^{13}C_{\alpha,\beta}O\cdot$ radical is shown as two lines occurring at frequencies ω_1^{α} and ω_1^{β}. The line at ω_1^{α} corresponds to the "pure" electron spin transition $D_-^{\alpha} \varnothing D_+^{\alpha}$ and the line at ω_1^{β} corresponds to the "pure" electron spin transition $D_-^{\beta} \varnothing D_+^{\beta}$. For each of these transitions the nuclear orientation is unchanged. The ESR apectrum of the B· radical is shown as a single line at ω_2.

To determine which spinomeric geminate pair undergoes more rapid ISC we need to compute which possesses the larger value of $\Delta\omega$, where $\Delta\omega$ is the difference in the precessional rates of each spinomer. $\Delta\omega$ is simply the absolute difference in the precessional rate (ω_1^{α} and ω_1^{β}) for each spinomeric $A^{13}CO$ radical and the precesional rate of the B radical (ω_2). From Eqs. 35 and 36, we may compute the **difference in precessional rates for the spinomeric pairs** from Eq. 40 and 41.

$$\Delta\omega_{\alpha} = \omega_1^{\alpha} - \omega_2 = (g_1\mu_e H_Z + a/2)/\backslash - (g_2\mu_e H_Z)/\backslash =$$

$$\Delta\omega_{\alpha} = [(g_1 - g_2)\mu_e H_Z + a/2]/\backslash = [\Delta g\mu_e H_Z + a/2]/\backslash \qquad (40)$$

$$\Delta\omega_{\beta} = \omega_1^{\beta} - \omega_2 = (g_1\mu_e H_Z - a/2)/\backslash - (g_2\mu_e H_Z)/\backslash$$

$$\Delta\omega_{\beta} = [(g_1 - g_2)\mu_e H_Z - a/2]/\backslash = [\Delta g\mu_e H_Z - a/2]/\backslash \qquad (41)$$

From Eqs. 40 and 41 we see that the absolute magnitudes of $\Delta\omega_{\alpha}$ and $\Delta\omega_{\beta}$, which determine the differences in ISC rates at high field, depend on the following factors: (1) the magnitude of the difference in g factors of the radicals

forming the pair; (2) the sign of the difference in g factors; (3) the magnitude of the hyperfine coupling constant, a; and (4) the sign of a. Thus, whether $\Delta\omega_\alpha$ is larger or smaller than $\Delta\omega_\beta$ depends on both magnitudes and signs, so that the ISC rates of the spinomeric pairs will depend on the same factors. Let's see how this all works out for our case study pair.

The sign of a for the $A^{13}CO$ radical is positive. Since the g factor for the $A^{13}CO$ radical (g = 2.001) is smaller than the g factor for the B radical (g = 2.003), Δg (= $g_1 - g_{2)}$ is negative. Inspection of Eqs. 40 and 41 show that from the ESR parameters of the spinomeric $A^{13}CO$ B radical pairs, the absolute value of $\Delta\omega_\beta$ is **larger** than the absolute value of $\Delta\omega_\alpha$, because in Eq. 41 two quantities are being added together and both are **negative**, whereas in Eq. 40 the same quantities are being added but one is **negative** and the second is **positive**. The same conclusion is reached graphically from inspection of the ESR spectra shown in Figure 39. The magnitudes of $\Delta\omega_\alpha$ may be read from the ESR spectra directly as the difference between the lines $\omega_1{}^\alpha$ and ω_2 and $\Delta\omega_\beta$ may be read from the ESR spectra directly as the difference between the lines $\omega_1{}^\beta$ and ω_2. It can be seen by inspection of Figure 39 that the difference between $\omega_1{}^\beta$ and ω_2 is **greater** than the difference between $\omega_1{}^\alpha$ and ω_2. This is, of course, what is expected since Eqs. 40 and 41 simply are mathematical representations of the ESR spectrum of the spinomer pairs.

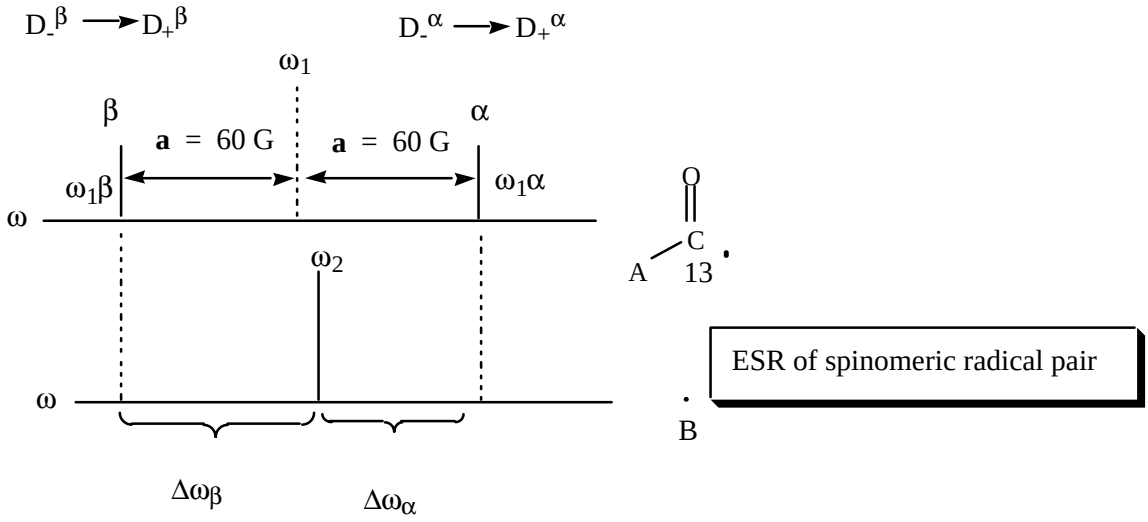

Figure 39. Comparison of the ESR spectrum of the radical pair and the NMR spectrum of the ACO radical.

Finally, let us consider how the vector model leads to the same qualitative conclusion concerning the faster ISC of the pair possessing the β spin. The magnetic field "felt" by the electron spin of B is independent of nuclear spin and

depends only on the magnitude of the applied field and the value of g_1. However, the magnetic field "felt" by the electron spin of the $A^{13}CO$ radical depends not only on the magnitudes of the applied field and the value of g_1 but also on the value of the orientation of the nuclear spin. When the nuclear spin is in the α orientation, the magnetic moment due to the nuclear spin is along the z-axis, the electron of $A^{13}C_{\alpha}O$ feels a **stronger** field than the applied field (see vector diagram of figure 37). When the nuclear spin is in the β orientation, the electron of $A^{13}C_{\beta}O$ feels a **weaker** field than the applied field (see vector diagram of figure 37). Because the ACO radical has a smaller g factor than the B radical, the ACO radical inherently precesses more slowly than the B radical. If a magnetic field is added to the ACO radical it will precess more rapidly and at a rate that is more similar to the B radical. Therefore the **difference** in precessional rates will become smaller and ISC will become **slower.** On the other hand, if a magnetic field is subtracted from the ACO radical it will precess more slowly and at a rate that is less. Therefore, the **difference** in precessional rates will become larger and ISC will become **faster** than the B radical. These ideas are captured by the vector model in Figure 37 where the projection of the nuclear spin on the z-axis is shown for the α and β orientations. For the α orientation the electron spin on $A^{13}C_{\alpha}O$ feels a field 60 Gauss stronger than H_Z, and for the β orientation the $A^{13}C_{\beta}O$ radical feels a field 60 Gauss weaker than H_Z.

In Figure 36, the transitions between E^- levels (or transitions between E^+ levels) correspond to NMR transitions (e.g., $\beta_e\alpha_N \varnothing \beta_e\beta_N$) because for these transitions, **the nuclear spins, not the electron spins undergo reorientation**. Although the NMR spectra of radicals are technically difficult to observe because of line broadening resulting from the electron spin coupling to the nuclear spin, the radical $A^{13}CO$ does in principle possess an NMR spectrum, which is shown schematically in Figure 39. The separation of the levels in Figure 36 do not take the nuclear Zeeman coupling into account. When this is done, the energy gaps for nuclear transitions become different in energy and the difference in transition frequencies is equal to the hyperfine coupling constant. Just as the ESR spectrum of the electron spin of the $A^{13}CO$ radical is split into two lines separated by the coupling constant of 60 gauss, **the NMR spectrum of the nuclear spin of the $A^{13}CO$ radical is also split by the same amount**. The NMR spectrum of the $A^{13}CO$ radical may be considered in the same way that any AX NMR spectrum is considered, except that the nucleus is coupled to an electron possessing an enormous "chemical shift" many orders of magnitude larger than any nuclear chemical shift. For example, the "center" of the NMR spectrum of the $A^{13}CO$ radical in a magnetic field of 10,000 gauss is at a frequency of ca. 10×10^6 s^{-1} (Megahertz), whereas the "center" of the ESR spectrum of the $A^{13}CO$ radical in a magnetic field of 10,000 gauss is ca. $28{,}000 \times 10^6$ s^{-1} (Megahertz). The typical

variation of chemical shifts for ^{13}C NMR spectra is ca. 100 x 10^{-6} (10,000 gauss) = 1 gauss. The hyperfine splitting of 120 gauss of the radical is thus two orders of magnitude greater than the entire normal range of NMR chemical shifts for molecules.

CIDNP Resulting from Nuclear Spin Orientation Dependent ISC

We have now justified the more rapid ISC for the triplet $A^{13}C_{\beta}O\cdot\ \cdot B$ geminate dynamic radical pair relative to the $A^{13}C_{\alpha}O\cdot\ \cdot B$ geminate radical pair. For an extreme case, if the rate of triplet to singlet ISC for the β spin containing pairs were fast enough, we could imagine that after a time (τ^{β}_{ISC}) all of these pairs might undergo combination reactions upon reencounters after ISC. If the rate of ISC of the pairs containing the α spins is slow relative to the time τ^{β}_{ISC}, the partners in the pair will separate to form free radicals that can be completely scavenged within a time τ^{α}_{SCAV}. In this extreme scenario, the $A^{13}C_{\beta}O\cdot\ \cdot B$ pairs undergo exclusive recombination to form $A^{13}C_{\beta}OB$ after a time of ca. τ^{β}_{ISC} and the free radicals $A^{13}C_{\alpha}O$ would be scavenged to form $A^{13}C_{\alpha}O$ after a time of ca. τ^{α}_{SCAV}. This extreme case is shown schematically at the top of Figure 40.

If the ^{13}C NMR spectrum of the system were observed after time τ^{α}_{SCAV}, there would be no radicals left and the "P∅ I" process would be complete. Figure 40 shows schematically the population of the nuclear spin levels at this point. From Figure 40 we note that the β level of the combination product, ACOB would be overpopulated. Because of the overpopulation of the β level, stimulated downward transitions would be more favored than stimulated upward transitions and the spectrum of the geminate coupling product would appear as an emissive line (Figure 40) rather than the usual, much weaker absorption spectrum of a solution containing an equivalent molar amount of ACOB (Boltzmann spectrum shown bottom left of Figure 40). The **position** of the line is the same for both Boltzmann and polarized spectra because it is the energy level **populations**, not the energy gaps between levels (which determine line position) that are influenced by the processes producing CINDP.

If the ^{13}C NMR spectrum is taken after scavenging occurs, the spectrum would result from stimulation of nuclear spin levels that are tremendously overpopulated in the α level (Figure 40). Thus, stimulated upward transitions would occur but the intensitive of the transitions and the observed signal would be far greater than is observed under normal (Boltzmann) conditions. Thus, the ^{13}C NMR spectrum of the scavenged products would appear in enhanced absorption. If there were no nuclear spin relaxation which occurred in the radicals before geminate reaction and scavenging reaction, the enhancement

intensities of emission and absorption would be roughly equal because they would be much stronger than the signal

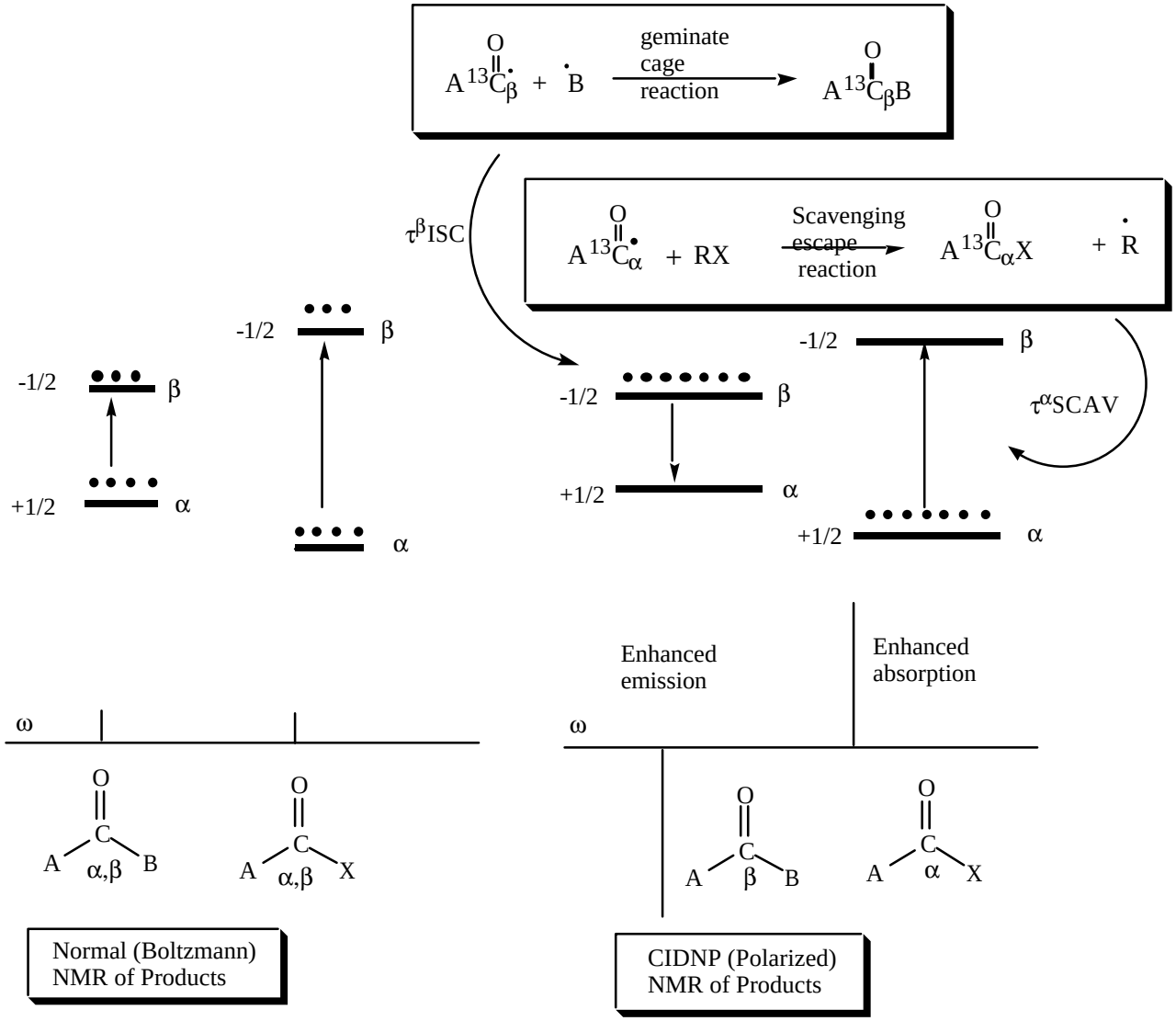

Figure 40. Conventional (left) and CIDNP spectra of the combination and scavenged products from the photolysis of ACOB in an NMR spectrometer. See text for discussion.

due to the Boltzmann intensity. Typical ^{13}C nuclear spin relaxation times are of the order of seconds, which sets an upper limit to the effective time after a photolysis that a CIDNP spectrum can be observed.

In summary, if hyperfine coupling determines the ISC of the $A^{13}CO\cdot\ \cdot B$ radical pair and the formation of the geminate coupling product, $A^{13}COB$, the resulting NMR spectra possess some remarkable features: (1) the signal for the

recombination product $A^{13}COB$ would be an "emissive" signal rather than the normal absorptive signal, and the scavenged $A^{13}COX$ product would be an absorptive signal that is much stronger in intensity than expected from the number of moles of product produced; (2) if the exciting light is extinguished, the entire NMR spectrum would disappear in a matter of seconds or less as the ^{13}C nuclei undergo relaxation; (3) upon reirradiation, the NMR spectrum of an emission for the $A^{13}COB$ product and a strong absorption for the $A^{13}COX$ product would reappear; (4) these processes might be repeated over and over again with little loss of signal if the amount of ketone required to produce the signal is quite small relative to the ketone employed.

Kaptein's Rules. Applications of CIDNP to Photochemical Reactions

Eqs. 40 and 41 and the vector model form the basis of **Kaptein's rules** which allow a prediction of the origin of a product showing a certain CIDNP polarization, i.e., either geminate cage or escape, **if the primary geminate pair is a triplet (the most common case)**. The rules may also be applied to the less common situation for which a singlet radical pair is the primary product. In this case the rules for the sign of the CIDNP are reversed because the formation of a geminate cage product becomes disfavored by more rapid ISC of the geminate pair.

The vector model of Figure 22 shows schematically the T_0 S ISC. The vector description shows that ISC requires a rotation of one electron spin vector relative to the other about the z-axis. ISC occurs when the electron spin vectors of the triplet, originally 0^o out of phase, twist to become 180^o or π radians out of phase. Let τ_α be the time it takes to make this twisting motion for the $A^{13}C_\alpha O$ radical and let τ_β be the time it takes to make this twisting motion for the $A^{13}C_\beta O$ radical. The two times τ_α and τ_β are equal to the inverse of the difference in precessional rates $\Delta\omega_\alpha$ and $\Delta\omega_\beta$ given by Eqs. 40 and 41, respectively.

In principle, Kaptein's rules (an abbreviated form given in Table 2) can be applied to determine any one of the three parameters for reaction starting from a geminate triplet radical pair, if the other two parameters are known: (1) the magnitude and sign of the difference in g factors; (2) the magnitude and sign of the hyperfine coupling constant; and (3) the geminate (cage combination) or free radical (cage escape) nature of products. Since spectroscopic parameters 1 and 2 are generally available from ESR spectra, the third, chemical, parameter is commonly determined by CIDNP experiments.

In some cases, parameters 1, 2 and 3 are known. In such situations, the multiplicity of the exciting state may be deduced from CIDNP data, since triplet precursors of radical pairs will lead to one set of predictions for the observed CIDNP spectrum and singlet precursors of radical pairs will lead to a different set of predictions, for the same set of known parameters.

Table 2. Abbreviated table of Kaptein's rules for polarization of geminate cage products.*

Spin State of Radical Pair	$\Delta g > 0$	$\Delta g > 0$	$\Delta g < 0$	$\Delta g < 0$
	$a > 0$	$a < 0$	$a > 0$	$a < 0$
Singlet	Emission	Enhanced Absorption	Enhanced Absorption	Emission
Triplet	Enhanced Absorption	Emission	Emission	Enhanced Absorption

*The opposite polarization is expected for scavenged escape products of the radical pair. Free radicals which encounter to produce combination products behave qualitatively the same as triplet geminate pair with respect to the prediction.

17. Magnetic Effects on Chemical Reactions. External Magnetic Field Effect on the Reactivity of Radical Pairs.

The influence of magnetic effects in the radical pair may be classified in terms of the source of the coupling to the electron spins of the radical pair. These sources may be classified as internal and microscopic (spin-orbit, spin-spin and spin-lattice) or external and applied (static and oscillating). Of the internal couplings, the spin-spin hyperfine and exchange coupling are the easiest to manipulate experimentally and will serve as representative of the influence of external couplings on the measurable properties of radical pairs and the products of radical pairs. An applied magnetic field is the most important external coupling available for influencing the behavior of radical pairs. With the specific example of a ACO B radical pair, we shall present examples of how spin-spin couplings and applied magnetic static fields can dramatically influence the behavior of radical pairs.

In zero or very weak magnetic fields, the S and T states of a dynamic radical pair are degenerate when the pair is solvent separated (Region 3, Figure 32). Thus, interconversions of all three T states to S are energetically allowed. Under these circumstances we can consider the three triplet sublevels to be rapidly interconverting and that the ISC step occurs when a T_0 level undergoes rephasing to S or a $T_\pm$ undergoes a spin flip to S. The rephasing or spin flip may be due to any one of the usual couplings (spin orbit, hyperfine, spin lattice, etc.) if angular momentum is conserved. An external magnetic field lifts the degeneracy of the three triplet levels through the Zeeman interaction so that $T_\pm$ is separated from T_0 and S (Figure 33). If the $T_\pm$ pair is rendered completely incapable of ISC in a high field, we conclude that the rate of T-S interconversion of the triplet geminate pair will be reduced by $2/3$ compared to that at zero field! Conversely, if a singlet radical pair is the starting reagent (unusual, but known), the magnetic field will close off the $T_\pm$ channels for ISC of the pair and increase its reactivity. Translated into experimental terms, **the probability of the cage effect for a triplet geminate pair is reduced by an applied magnetic field and the probability of the cage effect for a singlet radical pair is enhanced by an applied magnetic field.**

In the presence of a magnetic field, H_Z, the details of T_0-S ISC are clearly distinct from those of $T_\pm$ ISC. In the case of T_0-S ISC, a rephasing of the electron spins is required to achieve ISC from T_0 to S (Figure 22). This rephasing does not induce ISC for $T_\pm$ because it does not induce a change of spin orientation which is required to convert the $T_\pm$ states to S or T_0 (Figure 21). Thus, another magnetic interaction is required to induce $T_\pm$ ISC in a strong magnetic field. Let us

suppose this interaction is due to the hyperfine coupling of the electron to the nucleus for our case history pair, ACO· ·B.

The **rate** of ISC from T_0 and $T_\pm$ is directly related to the magnitude of the matrix elements dervied from the spin Hamiltonian evaluated for the S and T wavefunctions. In a simplified version the matrix elements for the T_0-S and $T_\pm$-S ISC are given by Eqs. 42 and 43 (which are related to Eqs. 39 and 40 of the previous section).

$$\text{Rate } (T_0\text{-S}) \sim \Delta g \mu_e \mathbf{H} + a M_I \quad (42)$$

$$\text{Rate } (T_\pm\text{-S}) \sim a M_I \quad (43)$$

From Eq. 41 we note that the rate of ISC from the T_0 state is a function of the difference in g factors of the radical partners, the magnetic field strength, the magnitude of the hyperfine coupling and the orientation of the **nuclear** spin, precisely the factors that result in Kaptein's rules for CIDNP. Since hyperfine constants can be negative or positive, the rate also depends on the sign of the coupling constant. For the case history pair, $A^{13}CO\cdot\ \cdot B$, the coupling constant is positive. It follows from eq. 41 that in a strong magnetic field, the rate of T_0-S ISC, and consequently the probability of cage reaction of the geminate triplet pair, depends first on the difference in Zeeman energies of the pair ($\Delta g \mu_e \mathbf{H}$), second on the nuclear magnetic moments through the hyperfine coupling constant, a, and third on the orientation of nuclear spin orientation through the quantum number, M_I. The important difference between this discussion and that of CIDNP is that the observed effects are on isolated chemical product yields, not on a spectroscopic measurement pertaining only to pairs containing magnetic nuclei.

In actual examples hyperfine coupling will not be the only internal interaction which can induce ISC, and eqs. 41 and 42 must be modified to include contributions due to spin orbit coupling, spin lattice coupling, etc. However, the qualitative aspects of these couplings will be analogous to those introduced by the hyperfine couplings, i.e., they will modify the effect of the Zeeman coupling in eq. 41 and will induce $T_\pm$-S as in eq. 42.

Static Magnetic Field Effects on the Chemistry of the Case History Pair, ACOB.

Let us consider the influence of an applied magnetic field on the products of the photochemistry of ACOB. In this case we will consider the effect for a ketone containing ^{12}C at the carbonyl carbon (which is representative of natural abundance material). At zero field there will be a certain probability that the

triplet geminate radical pair produced by α-cleavage will undergo ISC and cage recombination. This process may be monitored chemically through the racemization of a chiral B group. Combination to regenerate (racemic) ACOB will compete with scavenging to form ACOX and BX. The mechanism of ISC at zero field can be envisioned as involving rapid internal interconversion of the triplet sublevels with one another and ISC from T_0 to S. The situation is analogous to the selection of one of several rapidly interconverting conformers, only one of which is chemical reactive.

At high field the T_- and T_+ levels are split so far from T_0 that they stop interconverting with this state and therefore stop undergoing ISC to S. However, the the T_- and T_+ levels can still separate and form free radicals that can be scavenged. Let the probability of geminate combination in zero field be a quantity, ϕ, so that the probability of the scavenging is (1 - ϕ). At high field, the probability ϕ will be reduced to ca. ϕ/3, since two of the three triplet states will become incapable of ISC as geminate pairs and undergo free radical formation and eventual scavenging.

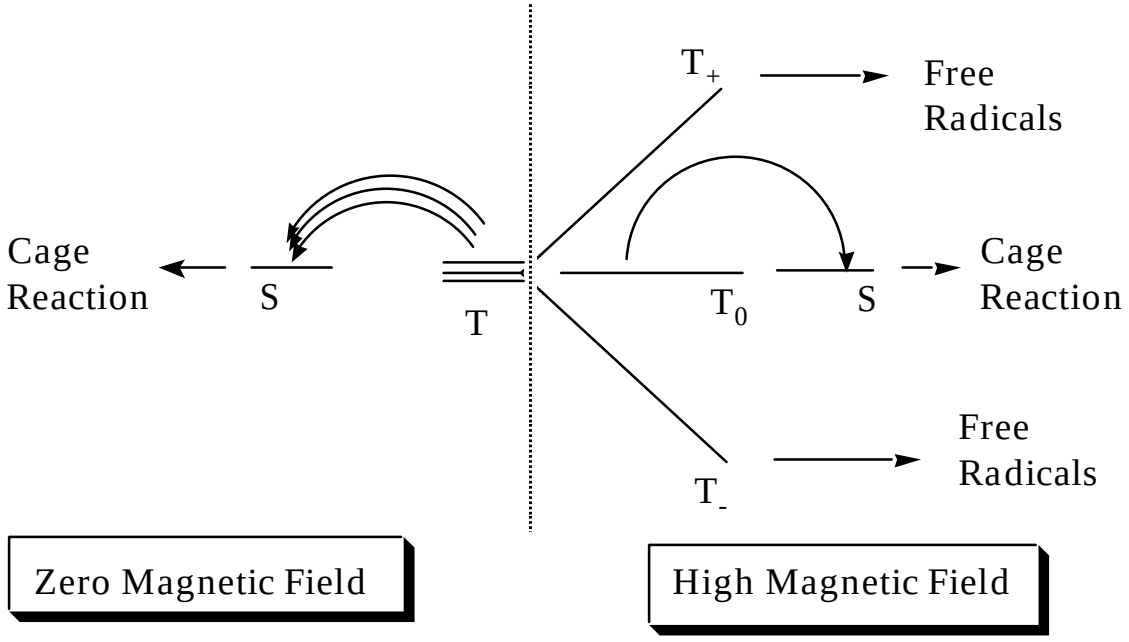

Figure 41. Basis for the magnetic field effect on the cage reaction of triplet geminate radical pairs.

These predictions of magnetic field effects have been difficult to verify in homogeneous non-viscous solutions because in these cases the probability of cage reaction is very small for triplet geminate pairs because rapid formation of free radicals (rapid pair separation in space) is much faster than ISC. However, when radical pairs are placed in restricted spaces that inhibit pair separation,

magnetic field effects on geminate pair reactions can be substantial. It is particularly interesting that only relatively weak fields are needed to effectively shut off ISC from T_- and T_+. This is because the magnetic coupling between these states and T_0 is relatively weak, so that the size of the applied field required to decouple T_- and T_+ from T_0 is often of the order of a few hundred gauss (the field provided by magnetic stirrer bars!).

Influence of Oscillating Magnetic Fields on the Dynamic Radical Pair. Reaction Yield Detected Magnetic Resonance.

Static magnetic fields cause the direct splitting of magnetic energy levels and the inhibition of T S ISC. Interestingly, this inhibition can be reversed by the application of the oscillating magnetic field of electromagnetic radiation. For example, the T_- and T_+ states that are split away from T_0 by an applied field can be converted to T_0 by the application of microwave radiation (which provides the oscillating magnetic field) of the correct frequency. Figure 42 schematically shows the basis of the use of microwaves to influence the behavior of dynamic radical pairs (throughout the discussion we shall assume J = 0, i.e., we are dealing mainly with interactions involving solvent separated pairs).

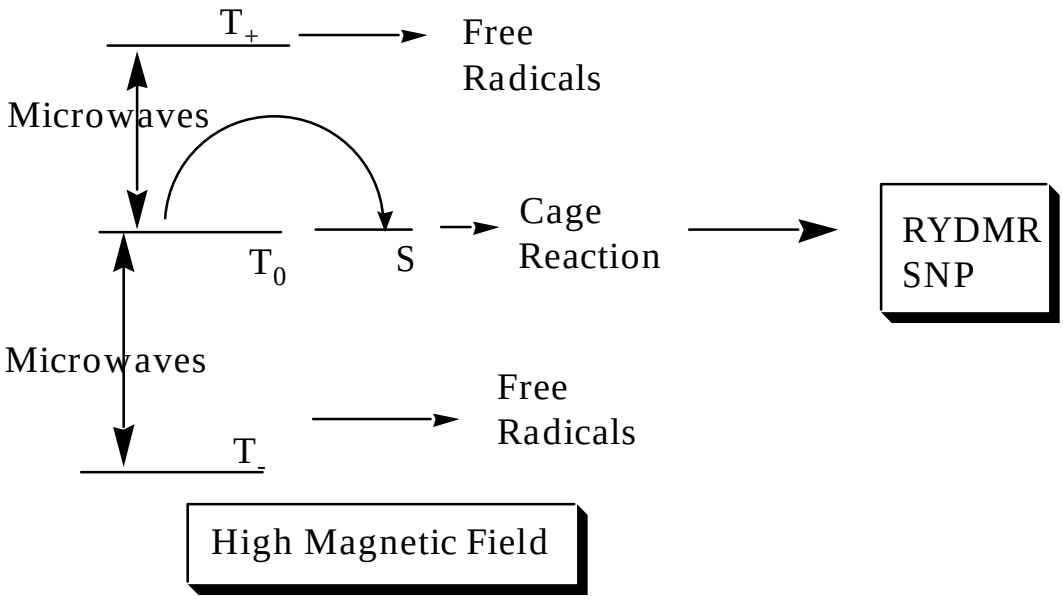

Figure 42. Energy diagram basis for the RYDMR and SNP phenomena. In both cases microwaves are employed to stimulate T $\varnothing$ T_0 transitions, which in turn lead to ISC to S. In one case the products of cage reaction are monitored (RYDMR) and in the other case nuclear polarization is monitored (SNP).

When microwaves corresponding to the resonance frequency that will interconvert T_- and T_+ with T_0 are applied to the dynamic geminate triplet radical pair, resonant transition to T_0 is stimulated by the electromagnetic field. If T_0 to S ISC is rapid, then the microwaves take the "inert" T_- and T_+ levels into the S state and effectively "catalyze" ISC of these states. The S state undergoes cage reaction. This enhancement of the cage reaction by applied microwaves may be detected experimentally. Varying the external field, H_Z allows the detection of the energy gap corresponding to the resonance condition. This is the same energy gap that is detected in the ESR spectroscopy of the triplet, but is detected by measuring chemical yields of products and is a form of "chemical spectroscopy"! Such measurements of ESR through the yields of products is termed "Reaction Yield Detected Magnetic Resonance" of RYDMR. In the case of the case history dynamic radical pair, the yield of geminate cage products would be monitored and would be increased by the application of resonant microwaves.

Influence of Oscillating Magnetic Fields on the Dynamic Radical Pair. Stimulated Nuclear Polarization (SNP).

We have seen that hyperfine interactions of the dynamic radical pair can lead to nuclear spin orientation dependent ISC of cage products and escape products which results in CIDNP. It is possible to use microwaves to selectively induce ISC of the nuclear spin states of a dynamic radical pair and thereby produce nuclear polarization. This phenomena is termed stimulated nuclear polarization (SNP).

The basis of the SNP phenomena may be understood for the concrete example of our case study dynamic radical pair, $A^{13}CO\cdot\ \cdot B$ through consideration of the ESR of the pair (Figures 37 and 39). The ESR line of the $A^{13}CO\cdot$ radical consists of a line at low frequency ($\omega_1\beta$) and a line at high frequency ($\omega_1\alpha$) separated by a frequency corresponding to the hyperfine coupling constant (ca 120 G). Irradiation of the dynamic radical pair at the frequency $\omega_1\beta$ will stimulate radiative transitions selectively to $T_0\beta$, which will in turn convert selectively to $S\beta$. **These singlet pairs will, in turn, produce cage combination products enriched in β nuclear spins**. Thus, if the NMR of the combination product is monitored as the microwaves are applied, at the resonance frequency corresponding to the $T_\pm \varnothing T_0$ transitions an emission corresponding to the selective formation of $A^{13}C_\beta OB$ will be observed. The reverse effect will be observed if the ω_α transition is irradiated with microwaves. The SNP experiment perhaps most elegantly shows the relationships of spin chemistry (spin selective formation of geminate cage products) and magnetic

resonance (ESR of precursor dynamic radical pair and NMR of geminate cage products). These relationships are shown schematically in Figure 43.

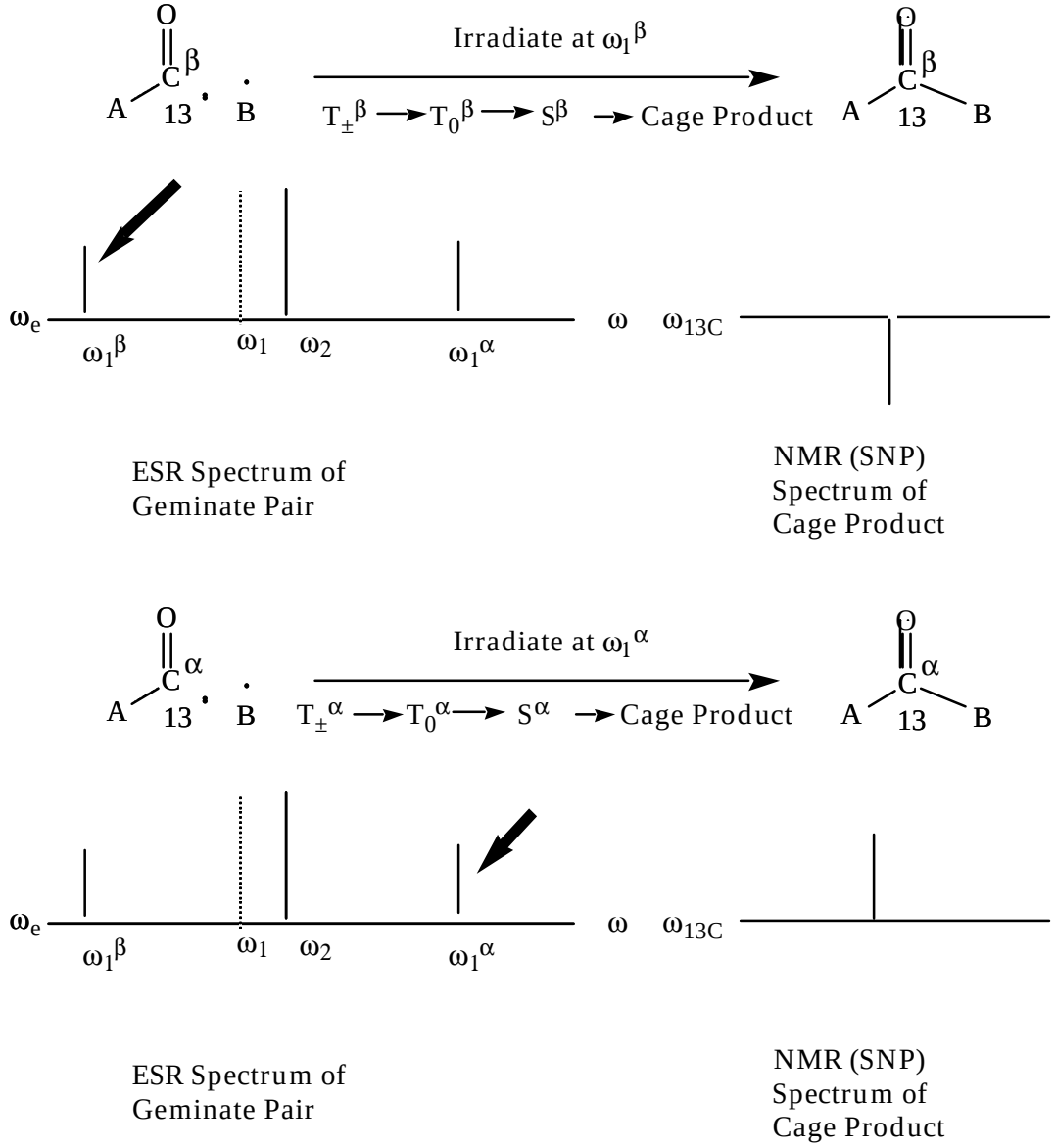

Figure 43. Schematic representation of the SNP phenomena. CIDNP emission results from selective irradiation at $\omega_1\beta$ and CIDNP enhance absorption results from selective irradiation at ω_1.

Summary

Magnetic interactions in correlated dynamice radical pairs control the spin dynamics and therefore the multiplicity of the radical pairs. Both applied static and dynamic magnetic fields can influence the rates of interconversions of various spinomers and therefore result in magnetic field effects on

photochemical processes involving radical pairs. These magnetic field effects are most pronounced when the geminate pair possesses a significant lifetime. Experimentally, the lifetime of the pair can be enhanced by a high solvent viscosity or by creating the pair in a small microhetergeneous confined space such as that provided by a micelle. The reactions and lifetimes of biradicals, which are contrained to remain geminate during their entire lifetime, are found to be significantly influenced by the application of applied magnetic fields.

18. The Magnetic Isotope Effect on Radical Pair Reactions

In the same manner that the orientation of a nuclear spin can influence the rate of ISC of two nuclear spinomers in the presence of a strong (spin orienting) magnetic field, the rate of ISC of two isotopomers will depend on the magnetic properties of isotopomers even in the absence of a magnetic field. Using the example of a ACO· ·B pair, we consider the geminate pair reactivity of $A^{12}CO\cdot\ \cdot B$ and $A^{13}CO\cdot\ \cdot B$ in the absence of an applied field. Under the usual assumption that the isotopomers pairs are produced as a triplet state, the dynamic radical pairs undergo similar diffusional trajectories in physical space, but different trajectories in spin space. The situation with respect to ISC of the isotopomeric pairs is analogous to that for nuclear spinomers in the case of CIDNP (Figure 38). In particular, the $A^{13}CO\cdot\ \cdot B$ pair is analogous to the $A^{13}C_\beta O\cdot\ \cdot B$ pair which undergoes rapid intersystem crossing and forms a cage combination product, and the $A^{12}CO\cdot\ \cdot B$ pair is analogous to the $A^{13}C_\beta O\cdot\ \cdot B$ pair, which undergoes escape from the cage and forms scavenged products. The net result is that the $A^{13}CO\cdot\ \cdot B$ pairs selectively form cage products, and the $A^{12}CO\cdot\ \cdot B$ pairs selectively form escape or scavenged products (Eq. 44 and 45).

$$A^{12}C\dot{O}\ \dot{B},\ A^{13}\dot{C}O\ \dot{B} \xrightarrow{^{13}C} A^{13}COB \quad \text{(Geminate combination, enriched in } ^{13}C) \qquad (44)$$

(Geminate pair)

$$A^{12}C\dot{O}\ \dot{B},\ A^{13}\dot{C}O\ \dot{B} \xrightarrow[RX]{^{12}C} A^{12}COX + BX \quad \text{(Products of Scavenging, enriched in } ^{12}C) \qquad (45)$$

The ketone that is regenerated by cage reactions is enriched in ^{13}C, and the escape product (or scavenging products) are enriched in ^{12}C compared to isotopic content of the starting ketone. The overall process serves to **separate the magnetic isotope (^{13}C) from the non-magnetic isotope (^{12}C), with the magnetic isotope directing the geminate triplet pair towards geminate combination reactions, and the non-magnetic isotope directing the pair toward free radical reactions.**

Since the fraction of geminate reactions is very small in non-viscous solutions because of the small fraction of reencounters, the magnetic isotope effect is not significant in ordinary solvents. Reencounters are strongly encouraged in constrained space provided by certain supramolecular systems

such as micelles. Under these conditions the magnetic isotope effect becomes quite efficient and readily measurable.

Some other remarkable expectations of the above model have been confirmed experimentally: (a) the quantum yield for disappearance of the magnetic isotope ^{13}C ketone is lower (because of the more efficient recombination of the magnetic pairs) than the quantum yield of disappearance of the non-magnetic isotope ^{12}C ketone; (b) the rate of disappearance of the magnetic isotope ^{13}C ketone is faster (because of the faster rate limiting ISC for recombination reactions) than the rate of disappeaance of the non-magnetic ^{12}C ketone. It has also been shown that the extend of ^{13}C enrichment at various positions starting from a natural abundance ketone is directly related to the magnitude of the hyperfine coupling at that position.

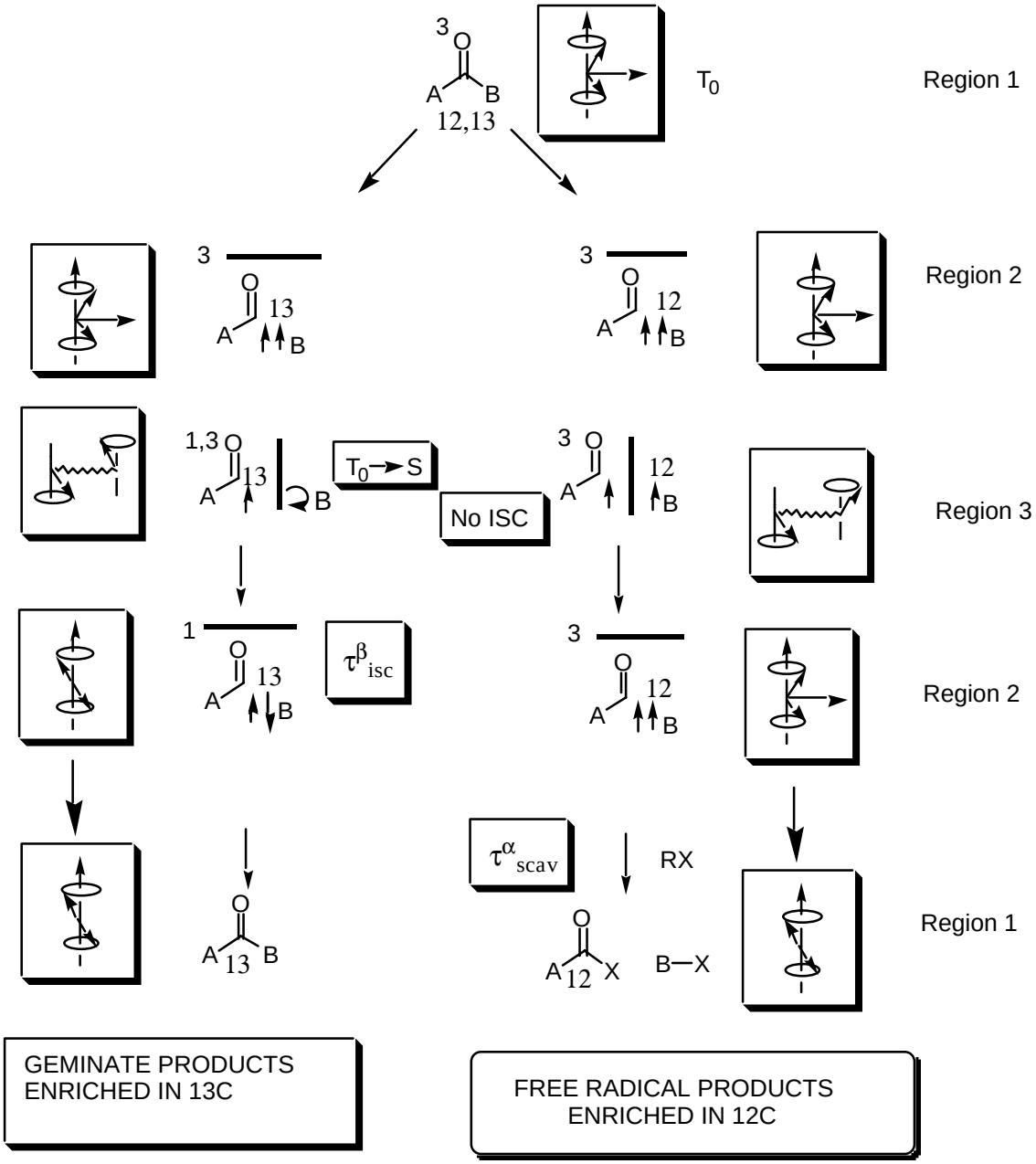

Figure 44. Vector model of the sorting of magnetic from non-magnetic nuclei that occurs in the dynamic radical pair. See text for discussion.